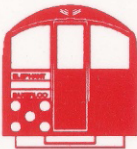


Series of Singularities and Their Topology

Rob Schrauwen



Series of Singularities and Their Topology

Series van Singulariteiten
en Hun Topologie

(Met een samenvatting in het Nederlands)

PROEFSCHRIFT

TER VERKRIJGING VAN DE GRAAD VAN DOCTOR AAN
DE RIJSUNIVERSITEIT TE UTRECHT OP GEZAG VAN DE
RECTOR MAGNIFICUS, PROF. DR. J.A. VAN GINKEL,
INGEVOLGE HET BESLUIT VAN HET COLLEGE VAN
DEKANEN IN HET OPENBAAR TE VERDEDIGEN OP MAAN-
DAG 11 FEBRUARI 1991 DES NAMIDDAGS TE 4:15 UUR

DOOR

ROBERT SCHRAUWEN

GEBOREN OP 20 MEI 1964 TE ROTTERDAM

PROMOTOR: PROF. DR. D. SIERSMA

FACULTEIT DER WISKUNDE EN INFORMATICA

Contents

| | |
|---|-----------|
| Introduction | 1 |
| 1 An introduction to the topology of plane curve singularities | 3 |
| 1.1 Fundamental preliminaries | 3 |
| 1.2 The EN-diagram of a plane curve singularity | 6 |
| 1.3 Splicing | 10 |
| 2 Computations around the EN-diagram | 14 |
| 2.1 Computing the linking number | 14 |
| 2.2 Multiplicities of dots and nodes | 14 |
| 2.3 Characteristic polynomials | 15 |
| 2.4 The zeta-function of the monodromy | 17 |
| 2.5 The multi-variable Alexander polynomial | 17 |
| 2.6 Zariski's numbers and the multiplicity sequence | 18 |
| 2.7 The EN-diagram vs. the resolution graph | 20 |
| 2.8 The polar ratios of a plane curve singularity | 21 |
| 3 Topological series of plane curve singularities | 23 |
| 3.1 Introduction | 23 |
| 3.2 The definition of topological series | 25 |
| 3.3 The case of a double component | 26 |
| 3.4 Higher multiplicities | 29 |
| 3.5 The zeta-function within a series | 31 |
| 3.6 Topological series and the resolution | 34 |
| 3.7 Curves in other spaces | 35 |
| 4 Splicing spectra | 38 |
| 4.1 Introduction | 38 |
| 4.2 Spectral pairs | 39 |

| | | |
|----------|---|------------|
| 4.3 | A formula for the spectral pairs | 40 |
| 4.4 | Spectral pairs and the real Seifert form | 43 |
| 4.5 | A splice formula for spectral pairs | 47 |
| 4.6 | The counterexample to the Spectrum Conjecture | 49 |
| 4.7 | The spectral pairs within a topological series | 50 |
| 5 | Deformations of plane curves singularities | 52 |
| 5.1 | Introduction | 52 |
| 5.2 | Invariants | 53 |
| 5.3 | Deformations | 56 |
| 5.4 | $D[p, q]$ -points and the Milnor number | 60 |
| 5.5 | Splicing of real morsifications | 68 |
| 6 | Series of hypersurface singularities | 73 |
| 6.1 | Introduction | 73 |
| 6.2 | Polar series | 74 |
| 6.3 | The polar filtration and the zeta-function | 82 |
| 6.4 | Another formula for the zeta-function of $f + \lambda\varphi$ | 84 |
| A | The EN-diagrams of the Arnol'd series | 92 |
| | References | 98 |
| | Index | 103 |
| | Dankwoord | 104 |
| | Samenvatting in het Nederlands | 105 |
| | Curriculum Vitae | 107 |

Introduction

All functions are in the series of the zero function.

—Jan Stevens / Duco van Straten.

Series of singularities have always been a source of inspiration for research in singularity theory. Although there is no definition of ‘series’, they “undoubtedly exist” (writes Arnol’d). The subject of this thesis is to look at the concept of series from a *topological* point of view.

We consider germs of holomorphic functions $f : (\mathbb{C}^{n+1}, 0) \rightarrow (\mathbb{C}, 0)$, i.e. functions with $f(0) = 0$ which are considered to be equal if they coincide on a small neighbourhood of the origin. The points where all partial derivatives vanish are called the singular points. If f is singular only at the origin, then f is said to have an isolated singularity.

In the largest part of this thesis we consider the case that $n = 1$, i.e. plane curve singularities. The function f defines an analytic set $X = f^{-1}(0)$, whose intersection with a small 3-sphere is a link. The components of this link correspond to the factors in the prime decomposition of f . Its complement is fibred (with the circle as base space) by the mapping $f/|f|$. This fibration, which is called the Milnor fibration, is one of the most important invariants of a singularity. In Chapter 1 we recall how to construct the link and we use EN-diagrams (defined by Eisenbud and Neumann) to denote a link. In Chapter 2, we show how to compute various topological invariants from the EN-diagram.

Except for some minor lemmas, these two Chapters contain known results. The remainder of this thesis is devoted to the following subjects:

- Our definition of topological series of plane curve singularities and the behaviour of topological invariants within such a series (Chapter 3);
- A splice formula for spectra and the relationship between the spectrum, the Seifert form and the signatures (Chapter 4);

- Deformation theory of plane curve singularities (Chapter 5);
- Results about series of hypersurface singularities (Chapter 6).

The contents of Chapter 3 were first published in [44], Chapter 4 is part of joint work with J. Steenbrink and J. Stevens [SSS] ([46]), and Chapter 5 is also to appear [45].

A simple example of a topological series consists of the functions $xy^2 + x^{p-1}$, called D_p by Arnol'd. It is intuitively clear that they fit into a series, and that the non-isolated singularity xy^2 is the 'head' of this series (it received the name D_∞). We show, that the Milnor fibration of a member of the series results from the Milnor fibration of D_∞ by removing a tubular neighbourhood of the singular locus and to glue something back in such a way that the result is the Milnor fibration of the isolated singularity. Using this idea, we define *topological series*. They satisfy all the familiar topological properties that we are used to from the Arnol'd examples, so the definition is very satisfactory. We also compute several invariants and investigate how they behave within the series. This may give in return information of the non-isolated singularity.

Many topological invariants arise from the monodromy on the Milnor fibre. A step further is the spectrum, defined by Arnol'd and Steenbrink. In Chapter 4 we study the spectrum within a series, but we need to prove some general results about the spectrum first. Interestingly, these theorems can be used to disprove former conjectures (as was done first in [46]).

A very beautiful paper in the theory of plane curve singularities is A'Campo's paper [1]. It gives a method to construct a Dynkin diagram of the intersection form on the Milnor fibre. Unfortunately, this method does not apply to the case of non-isolated singularities. In order to generalize, we need in any case deformation theory. In Chapter 5 the deformation theory of plane curve singularities is completely dealt with, using theory developed by R. Pellaan. At the end we indicate what we can do with it on the subject of Dynkin diagrams.

Finally, in Chapter 6 we look at series of hypersurfaces ($n \geq 1$), the non-isolated singularity still has to have a one-dimensional singular locus. A first test case is the generalization of the formula for the zeta-function. We give two methods. At present, the first results only in a formula on the level of the Euler characteristic. The second gives a good formula for the zeta-function, which is stronger than existing formulae. Still, we feel that if such a formula were to be used as basis for a concept of series of hypersurface singularities, even more functions should be part of the theory and the (uncompleted) first formula might be a good approach.

CHAPTER 1

An introduction to the topology of plane curve singularities

1.1 Fundamental preliminaries

(1.1.1) A *plane curve singularity* is for us a germ of an analytic space $(X, 0)$ in $(\mathbb{C}^2, 0)$ defined by the vanishing of a non-zero analytic function germ $f : (\mathbb{C}^2, 0) \rightarrow (\mathbb{C}, 0)$. In practice, we will not distinguish very carefully between a curve and its equation, and a germ and a representative. It will be clear from the context what is meant. We identify the ring \mathcal{O} of germs of analytic functions with $\mathbb{C}\{x, y\}$, the ring of convergent power series in the variables x and y . This ring is factorial, so we can decompose f into irreducible factors: $f = f_1^{m_1} \cdots f_s^{m_s}$. We write

$$X = m_1 X_1 \cup \cdots \cup m_s X_s,$$

where $X_i = f_i^{-1}(0)$. The curves X_i are called the *branches* of X .

A *singular point* is a point where all partial derivatives of f vanish. The germ f has an *isolated* singularity if the origin is its only singular point. Observe that it is the case if and only if f is reduced, i.e. $m_1 = \cdots = m_s = 1$.

Two singularities f, g are called *analytically equivalent* if the rings $\mathcal{O}/(f)$ and $\mathcal{O}/(g)$ are isomorphic. If f is smooth (which means that it has no singular points) then f is still called a singularity.

(1.1.2) From a topological viewpoint, the space $X = f^{-1}(0)$ is not very interesting (it is contractable). But if we look at the pair (B_ε, X) where $B_\varepsilon = \{z \in \mathbb{C}^2 \mid |z| \leq \varepsilon\}$ is a small ball, the situation is different and leads to a connection with knot theory. One can show that the pair (B_ε, X) is a cone over $(S_\varepsilon^3, X \cap S_\varepsilon^3)$, where the 3-sphere S_ε^3 is the boundary of B_ε . Since X is real

2-dimensional, the intersection $K_\varepsilon = X \cap S_\varepsilon^3$ is 1-dimensional. Therefore it is a *link* in S_ε^3 . Milnor [31] showed, that there is an $\varepsilon_0 > 0$ such that for $0 < \varepsilon < \varepsilon_0$ the topological type of $(S_\varepsilon^3, K_\varepsilon)$ is constant, and it is called the topological type of f . Topological equivalence is really weaker than analytical equivalence, see for instance the two remarkable examples in [8], pp. 590–591 (one of a topological type admitting only two analytical types, and one admitting an uncountable number of them).

If a link is the link of a plane curve singularity, it is called an *algebraic link*.

If $f = f_1^{m_1} \cdots f_s^{m_s}$, then $K = K_\varepsilon$ has s connected components $K_i = f_i^{-1}(0) \cap S_\varepsilon^3$. In particular, if f is irreducible, K is a *knot*. It is natural to assign to each component K_i the multiplicity m_i . In this way, K becomes a *multilink*, and we write: $K = m_1 K_1 + \cdots + m_s K_s$. These multiplicities become meaningful when we look at the exterior of the link K , as we will see later on.

(1.1.3) We now consider the *exterior* of a link, i.e. the complement of a small tubular open neighbourhood $N(L)$ of L in S_ε^3 . Contrary to the complement of the link, this is a compact 3-manifold with boundary. In knot theory, the link exterior is always a rich source of invariants, in particular if it is fibred. For algebraic links, this is always the case: in [31], Milnor showed that $f/|f| : S_\varepsilon^3 \rightarrow S^1$ is a C^∞ -fibration.

Often the following, equivalent, fibration is easier to work with. This time f itself is used instead of $f/|f|$. Choose a Milnor radius ε for f . Then there exists an η_0 such that for all positive $\eta < \eta_0$ the mapping $f : B_\varepsilon \cap f^{-1}(D_\eta) \rightarrow D_\eta$, where D_η is the disc of radius η , is a fibration above $D_\eta \setminus \{0\}$, equivalent to the previous fibration, see [31].

Both fibrations rejoice in the name of *Milnor fibration*, and a typical fibre of either fibration is called the *Milnor fibre*. Let F be the Milnor fibre of f . It is a surface consisting of $d = \gcd(m_1, \dots, m_s)$ connected components. The rank of $H_1(F)$ is $\mu(f)$, the *Milnor number* of f .

Looping once around the circle S^1 induces a diffeomorphism $h : F \rightarrow F$, which is called the (*geometric*) *monodromy* of the Milnor fibration; the induced action on the homology the *algebraic monodromy*.

If f is an isolated singularity, then the boundary of F is isotopic to K and F can be regarded as a Seifert surface for K . If f is non-isolated, then the boundary of F consists of cables around the components of K . It is here that the multilink structure of K becomes visible, K_i is approached from m_i directions. In order to be more precise, we first give the definition of a (p, q) -*cable* around a knot S . Choose standard longitude L and meridian M of $\partial N(S)$, the boundary of a small tubular neighbourhood of S . This

means that L and M are representatives of generators of $H_1(\partial N(S))$ satisfying $\text{Lk}(L, M) = 1$, $\text{Lk}(L, S) = 0$, $L \sim S$ in $H_1(N(S))$ and $M \sim 0$ in $H_1(N(S))$. Here Lk denotes linking number in S^3 . Now a (p, q) -cable consists of $\gcd(p, q)$ simply closed curves on $\partial N(S)$ whose sum is homologous to $pL + qM$. These definitions are up to isotopy. The following is proved in [14].

(1.1.4) Lemma *Let c_i ($1 \leq i \leq s$) be the linking number of K_i with the other components (counted with their multiplicities) i.e. $c_i = \sum_{j \neq i} m_j K_j$. Then $F \cap \partial N(K_i) \subset \partial F$ is an $(m_i, -c_i)$ -cable on K_i . \square*

(1.1.5) Remark

- (a) It is useful to recall that the linking number of two different components of K equals the algebraic intersection number of the corresponding branches of f , i.e. $\text{Lk}(K_i, K_j) = \dim_{\mathbb{C}} \mathcal{O}/(f_i, f_j)$.
- (b) In a multilink $K = m_1 K_1 + \cdots + m_s K_s$, we allow the possibility that one of the components, say K_1 , has multiplicity $m_1 = 0$. In that case, the Milnor fibre F is the Milnor fibre of $m_2 K_2 + \cdots + m_s K_s$ minus the intersection points of K_1 with F (K_1 intersects F transversally). Observe that this is consistent with lemma 1.1.4.

(1.1.6) Suppose that $f = f_1^{m_1} \cdots f_s^{m_s}$ is non-isolated, and that the singular locus is $\Sigma = \Sigma_1 \cup \cdots \cup \Sigma_r$, $r \leq s$. Let $1 \leq i \leq r$. In points of $\Sigma_i \setminus \{0\}$, the intersection with a transversal plane gives a well-defined transversal (zero-dimensional) singularity. It is clear that it can be described in local coordinates by $g(z) = z^{m_i}$, a singularity of type A_{m_i-1} . We can identify two monodromies, which will play a role later on. The first is called the *horizontal monodromy*, which is the Milnor monodromy of g . This is just a cyclic permutation of the m_i points that make up the transversal Milnor fibre F_i^b . The second monodromy, the *vertical monodromy*, results from the local system on $\Sigma_i \setminus \{0\}$: Looping once around $0 \in \Sigma_i$ induces another diffeomorphism of F_i^b . The names horizontal and vertical were first used by Steenbrink and will become more clear in 6.3.2. Denote the actions of the horizontal and vertical monodromies on $\widetilde{H}_0(F_i^b)$ by T_i and A_i , respectively. Then we have the following result, familiar from the cases of homogeneous singularities (cf. [56]) and quasi-homogeneous singularities (cf. [29]):

(1.1.7) Lemma *The horizontal and vertical monodromies A_i and T_i ($1 \leq i \leq r$) of a plane curve singularity X are related by $A_i = T_i^{-c_i}$, where $c_i = X_i \cdot (\cup_{j \neq i} m_j X_j)$.*

Proof. Regard F_i^b as situated on $F \cap \partial N(K_i)$, the connected components of the boundary of F near K_i . We can easily see that the complete trajectory of F_i^b which results from looping around 0 is isotopic to the complete link $F \cap \partial N(K_i)$, which is an $(m_i, -c_i)$ -cable by lemma 1.1.4. \square

1.2 The EN-diagram of a plane curve singularity

(1.2.1) If $f \in \mathcal{O} = \mathbf{C}\{x, y\}$ is irreducible, we can parametrize the curve $X = f^{-1}(0)$ by means of the famous *Puiseux expansions*:

$$x = t^n, \quad y = \sum_{i > n} c_i t^i,$$

with $n = \text{mult}(f)$ and $y(t) \in \mathbf{C}\{t\}$, provided that x and y are chosen in such a way that f is not tangent to the y -axis. Written in a more classical way:

$$y = \sum c_i x^{i/n},$$

expressing y as a fractional power series in x . This follows from Puiseux's Theorem, see [8] or [40]. These parametrizations can be found from the equation of f using Newton diagrams, which is explained in [8]. But it is also possible to resolve the singularities of f in order to find the parametrizations. We can rewrite the last expression in the following way:

$$y = x^{q_1/p_1}(a_1 + x^{q_2/p_1 p_2}(a_2 + \dots) \dots),$$

with $\text{gcd}(p_i, q_i) = 1$. The *characteristic pairs* or *Puiseux pairs* of f are the couples (p_i, q_i) with $p_i \neq 1$. It is well-known that only these characteristic pairs are important for the topology, cf. [8]. Observe that there is only a finite number g of p_i unequal to 1.

For the moment, we suppose that the Puiseux expansion contains only characteristic terms, hence $p_i > 1$ for all $i \leq g$. Then $p_1 p_2 \dots p_g = n$, the multiplicity of the curve at the origin. We can now describe the knot K of the branch X . A more detailed treatment can be found in [14], Appendix to Chapter I. For this purpose we can replace S_ε^3 by a "square sphere" $R = \{(x, y) \in \mathbf{C}^2 \mid (|x| = \varepsilon \text{ and } |y| \leq \varepsilon) \text{ or } (|x| \leq \varepsilon \text{ and } |y| = \varepsilon)\}$. By a suitable coordinate change, we can arrange that X intersects R only where $|x| = \varepsilon$ and $|y| < \varepsilon$. Let us consider the branch X with Puiseux pairs $(p_1, q_1), \dots, (p_g, q_g)$, i.e. with Puiseux expansion

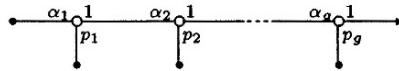
$$y = x^{q_1/p_1}(a_1 + x^{q_2/p_1 p_2}(a_2 + \dots + x^{q_{g-1}/p_1 \dots p_{g-1}}(a_{g-1} + a_g x^{q_g/p_1 \dots p_g}) \dots)).$$

Now $|x| = \varepsilon$ is small, so $y = a_1 x^{q_1/p_1}$ is even smaller. In “zeroth” approximation we can even think it vanishes completely (which results in the unknot K^0), but looking more closely we find that when x traverses the circle $\{x \mid |x| = \varepsilon\}$ p_1 times, y circles q_1 times around the origin. So the first approximation K^1 of K is a (p_1, q_1) -torus knot K^1 . It is not hard to imagine that the next stage, $y = x^{q_1/p_1}(a_1 + a_2 x^{q_1/p_1 p_2})$, is a cable K_2 around this (p_1, q_1) torus knot. In general, K^i is an (α_i, q_i) -cable around K^{i-1} , where α_i is defined by

$$\alpha_1 = p_1, \quad \alpha_{j+1} = q_{j+1} + p_j p_{j+1} \alpha_j, \tag{*}$$

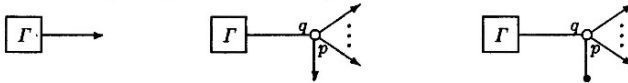
see [14], p. 51. The auxiliary knots K^0, \dots, K^{g-1} used in this approximation to find $K = K^g$, are intrinsic parts of the topology of K . They are called the *virtual components* of K . Incidentally, if we had non-characteristic terms in our original expansion, this would result in some extra “wobbling” of the knot, not in extra entangling.

We put this information together in a weighted graph that we will call the *EN-diagram* of K , after Eisenbud and Neumann who developed these graphs in [14]. In such a diagram, an arrow indicates a component of the link. The EN-diagram of the knot K above is:



The following proposition ([14], Proposition 9.1) may help understanding the EN-diagram.

(1.2.2) Proposition *Let p, q be positive integers with no common factor and let $d > 0$. Let Γ be the EN-diagram of a link L with distinguished component S (the arrow in the first picture below):*



Denote by $dS(p, q)$ the union of d (p, q) -cables around S (a (p, q) -cable was defined in 1.1.3). Then the links $L \cup dS(p, q)$ and $L \cup dS(p, q) \setminus S$ have EN-diagrams as in the second and third picture, respectively. In the second picture, the arrow pointing downwards now indicates the component S ; in the third picture, the dot signifies that S has been deleted and now belongs to the virtual components. \square

Special cases are the unknot 0_1 (the link of a smooth function), which gets EN-diagram $\bullet \longrightarrow$, and the link with two unknotted components with linking

number 1 (the link of an ordinary double point), which gets EN-diagram \longleftrightarrow . These definitions are consistent with Proposition 1.2.2.

(1.2.3) Until now, we have considered only the EN-diagram of an irreducible plane curve singularity. Let $X = m_1 X_1 \cup \dots \cup m_s X_s$ be the decomposition in irreducible components. Puiseux's Theorem asserts that we can parametrize all branches:

$$t \mapsto (t^{n_1}, \eta_1(t)), \dots, t \mapsto (t^{n_s}, \eta_s(t)),$$

where $\eta_i(t) \in \mathbb{C}\{t\}$ are smooth functions ($1 \leq i \leq s$). We can find parametrizations from an equation of X by applying the same techniques as mentioned for the irreducible case. The construction of the link of X follows the same procedure as before. But now some non-characteristic terms (only a finite number) could be important for the topology of f . For instance, consider an A_n singularity for n odd. One can take $y^2 - x^{n+1}$ as an equation. It has two smooth branches, each of which has no Puiseux pairs. Its link is a $(2, n + 1)$ -torus link, consisting of two linked unknotted components.

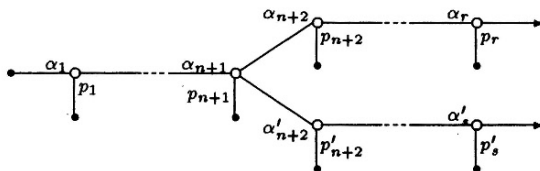
The definition of the EN-diagram of an algebraic link can now be completed (we refer again to [14], loc. cit., for details). Bearing in mind the result of proposition 1.2.2, we see that once we have done that, we have also found a method of construction of the link of X .

Suppose Y and Y' have Puiseux expansions

$$y = x^{q_1/p_1}(a_1 + x^{q_2/p_1 p_2}(a_2 + \dots + x^{q_{r-1}/p_1 \dots p_{r-1}}(a_{r-1} + a_r x^{q_r/p_1 \dots p_r} \dots)),$$

$$y = x^{q'_1/p'_1}(a'_1 + x^{q'_2/p'_1 p'_2}(a'_2 + \dots + x^{q'_{s-1}/p'_1 \dots p'_{s-1}}(a'_{s-1} + a'_s x^{q'_s/p'_1 \dots p'_s} \dots)),$$

where, for simplicity, r and s denote the respective numbers of relevant terms. In general, one should use the complete expansion and delete the terms with $p_i = 1$ afterwards. In [14] it seems that only the characteristic terms of the branches are meant, but that does not work, as we have just seen in our example A_n (n odd) above.

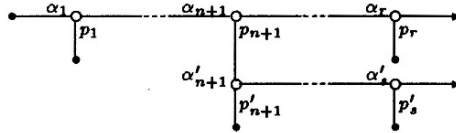


We look at the number of common terms: let n be such that $p_i = p'_i$, $q_i = q'_i$ and $a_i = a'_i$ for all $i \leq n$ but not for $i = n + 1$. We define α_i ($1 \leq i \leq r$) and

1.2 The EN-diagram of a plane curve singularity

α'_i ($1 \leq i \leq s$) by the recursive method (*). If $q_{n+1}/p_{n+1} = q'_{n+1}/p'_{n+1}$, we get the diagram above.

On each edge near a node (an open circle), there should be positioned a weight, but we usually omit weights equal to one. Otherwise we may assume that $r = n$ or $q_{n+1}/p_{n+1} < q'_{n+1}/p'_{n+1}$, and then the diagram is:



In order to treat the the case of more than 2 branches, we proceed inductively. Furthermore, if X_i carries the multiplicity m_i , we put ' (m_i) ' in front of the arrow of the corresponding link component.

Observe that there is something hidden in this construction that has still to be proved, namely that the link of X can indeed be constructed using the cabling operations described by the EN-diagram. Again, this is proved in [14], loc. cit..

(1.2.4) Definition We use the following terminology: The *nodes* are the open circles in the EN-diagram. From a node, at least 3 edges emerge, and to each edge there is attached a *weight*. The closed circles are called *dots*; they only have one incident edge.

Furthermore, if Γ is an EN-diagram, we put $A(\Gamma)$ for the set of arrow-heads of Γ , and $N(\Gamma)$ for the set of non-arrow-heads (dots and nodes).

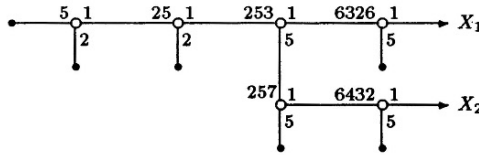
A diagram is called *minimal* if there are no dots attached to a weight 1. Our construction will give minimal diagrams, since we only look at characteristic terms.

(1.2.5) Example The EN-diagrams of $f(x, y) = (y^2 - x^3)^m$ and $g(x, y) = (y^2 - x^3)(y^3 - x^2)$ are:



The next example is a curve $X = X_1 \cup X_2$, with:

$$\begin{aligned} X_1 : x &= t^{100}, & y &= t^{250} + t^{375} + t^{390} + t^{391}; \\ X_2 : x &= t^{100}, & y &= t^{250} + t^{375} + t^{410} + t^{417}. \end{aligned}$$



Many more examples can be found in Appendix A, where the EN-diagrams of all Arnol'd series are presented.

(1.2.6) All constituents of an EN-diagram have a topological meaning, which we have already indicated for some of them. The arrow-heads correspond to the components of the link (and therefore the branches of the singularity). The dots correspond to the virtual components, resulting from the successive cabling operations.

The edges correspond to tori, separating S^3 . In our construction above, we can think of a torus somewhat smaller but parallel to the torus on which the cables are situated. In fact, the tori come from a more important structure, the *Waldhausen decomposition* of the link exterior. This is a decomposition of the link exterior into Seifert manifolds. Seifert manifolds are 3-dimensional compact circle bundles, with boundaries consisting of tori; they are completely classified. Results on these kinds of decompositions, obtained by Jaco, Shalen, Johannson, Thurston and others, were important for modern 3-manifold theory. Eisenbud and Neumann applied them to the theory of links [14]. Their EN-diagrams can be used in wider context than we have presented so far.

Each Seifert piece of the decomposition corresponds to a node with incident edges; the node itself will correspond to a regular fibre of the Seifert fibration on this piece. In section 2.8 we will find a relationship of the nodes with the polar curve of f .

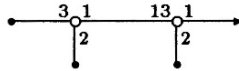
Furthermore, in 2.7 we will briefly discuss the relationship of the EN-diagram and the dual graph of the resolution of f .

1.3 Splicing

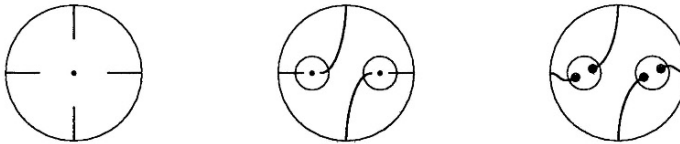
(1.3.1) In this section we describe the notion of *splicing*, due to Siebenmann and studied extensively in [14], to which we refer for a more detailed description. Splicing is a more general operation than cabling, that we have used before, but it is easier to use — certainly in connection with EN-diagrams, for which it is the basis. It will be of great use later on.

In the previous section, we looked at the construction of the knot K of a branch with g Puiseux pairs. Let us look more closely at this construction for

the singularity $f(x, y) = (y^2 - x^3)^2 - 4x^5y - x^7$, which is of type $W_{1,1}^\#$. It has Puiseux expansion $x = t^4, y = t^6 + t^7$, and therefore the following EN-diagram.



We argued that $K^0 = \{y = 0\} \cap R$ (where R denoted the polydisc $D_\epsilon^2 \times D_\epsilon^2$) was the zeroth approximation of K . Observe that this is not just the unknot, but the unknot traversed 4 times. It is more natural to consider the multilink $4K^0$ as zeroth approximation. The same applies to the first approximation K^1 , which is a $(2, 3)$ -torus knot around K^0 , traversed twice. Let N^i ($i \in \{0, 1, 2\}$) be a tubular neighbourhood of K^i . The pictures below show a cross-section of $\cup_{j \leq i} N^j$ together with a typical fibre of the Milnor fibration of $m_j K^j$.



This gives another reason why we should think of $4K^0$ and $2K^1$ as the approximating steps of K : The Milnor fibration on the exterior of K provides Milnor fibrations of $4K^0$ and $2K^1$ and not of K^0 and K^1 .

We can look at it in yet another way. Start with $4K^0$. This is a fibred multi-unknot, whose fibres consist of 4 copies of a disc. We can obtain $(S^3, 2K^1)$ by removing a tubular neighbourhood of K^0 and pasting in something else. This surgery approach will be the basis of the definition of splicing. For future use, it will be placed in the general setting of links in (integral) homology 3-spheres.

(1.3.2) Definition Let Σ' and Σ'' be homology spheres, and let two links (Σ', L') and (Σ'', L'') be given. Let S' and S'' be components of L' and L'' respectively and write $L' = m'S' + L'_0$ and $L'' = m''S'' + L''_0$ as multilinks (L'_0 and L''_0 may be empty). Let N' and N'' be tubular neighbourhoods of S' and S'' .

The *splice* of L' and L'' along S' and S'' is a link L in a certain homology sphere Σ , satisfying:

$$\begin{aligned} \Sigma &= (\Sigma' \setminus N') \cup_{\partial} (\Sigma'' \setminus N'') \\ &\quad \text{boundary tori glued meridian to longitude and vice versa,} \\ L &= L'_0 \cup L''_0. \end{aligned}$$

If L', L'' have EN-diagrams Γ', Γ'' then L has simply the EN-diagram Γ :



Observe that L has two components less than L' and L'' together.

(1.3.3) If L' and L'' are algebraic links in S^3 (links of plane curve singularities), we would like that L is again an algebraic link. This will in general not be the case unless we impose the following two conditions.

The first condition is a condition on the multiplicities m' and m'' . It demands that the Milnor fibrations of L' and L'' approach the splice torus exactly the same way, and links up well with our contemplations of 1.3.1.

Splice Condition

We can splice $L' = m'S' + L'_0$ and $L'' = m''S'' + L''_0$, if

$$m' = \text{Lk}(S'', L''_0), \text{ and } m'' = \text{Lk}(S', L'_0).$$

This indeed demands that the fibres of the Milnor fibration approach the splice torus from both sides in an (m', m'') -torus link, cf. lemma 1.1.4.

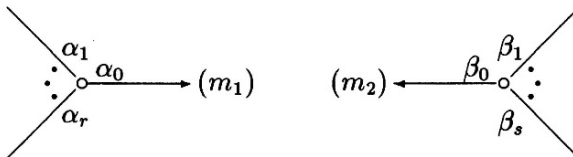
(1.3.4) The second condition is a condition on the weights in the EN-diagram. Recall the construction of the EN-diagram of a single branch. There we saw that we could not just use a Puiseux pair (p_i, q_i) as cabling direction but that we had to compute $\alpha_i = q_i + p_i p_{i-1} \alpha_{i-1}$ in order to get the right (p_i, α_i) -cable. If $\beta < \alpha_i$, (p_i, β) -cables of course also exist (even if β is negative), and the resulting links may well be fibred. But apparently, those links are not algebraic. This explains the

Algebraicity Condition

- (a) The link is obtained by repeated cabling, and
- (b) In each portion of the diagram of the following form, the inequality

$$\alpha_0 \beta_0 > \alpha_1 \cdots \alpha_r \beta_0 \cdots \beta_r$$

must hold.



The condition (a) requires that there are sufficiently many 1's around each node in the EN-diagram. If we omit (a), the splice and algebraicity conditions result in a link of a curve singularity, defined on a normal integral homology manifold.

(1.3.5) We get a *splice decomposition* of an EN-diagram (or of the exterior of the link) by performing the inverse operation of splicing. We say that we *break* the separating edges of the EN-diagram into pairs of arrows with the correct multiplicities of the splice condition. These multiplicities, being linking numbers, can be obtained very easily from the EN-diagram, see 2.1.

(1.3.6) **Example** The splice decomposition of $W_{1,1}^\#$ of the beginning of this section is given by:



Observe that the rightmost link has a component with multiplicity 0. The middle splice component is the link of the singularity $W_{1,\infty}^\#$, given by the equation $(y^2 - x^3)^2$. This illustrates the way we will introduce topological series of plane curve singularities in 3.2.3.

A'Campo's singularity, $g(x, y) = (y^2 - x^3)(y^3 - x^2)$, whose EN-diagram is redrawn below, decomposes into two isomorphic splice components given by the second EN-diagram. It is the EN-diagram of the non-isolated singularity with equation $x^2(y^2 - x^3)$.



Obviously, it is interesting to know how computational invariants behave under splicing. Then it remains to compute such invariants for our basic building blocks, the Seifert links (with only one node in their EN-diagram).

CHAPTER 2

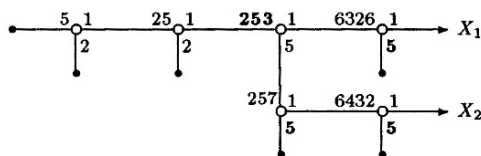
Computations around the EN-diagram

2.1 Computing the linking number

The linking number of two link components can be computed easily by walking from the first arrow to the second arrow and multiplying the edge weights *along*, but not *on* the path, see [14], section 10.

Since linking numbers are encountered so often (disguised as intersection numbers and various kinds of multiplicities), it is most useful to have such an easy algorithm at our disposal.

(2.1.1) Example Consider the third example of (1.2.5). X_1 and X_2 have intersection number $X_1 \cdot X_2 = 5 \cdot 253 \cdot 5 \cdot 5 = 31\,625$ (compare the elaborate computation in [8], p. 695).



It is an interesting exercise to verify that the topological type of a plane curve singularity is determined by the Puiseux pairs of the branches together with the intersection numbers of all pairs of branches.

2.2 Multiplicities of dots and nodes

The dots and nodes of an EN-diagram carry natural multiplicities, equal to the total number of the corresponding virtual components with the (multi)link K , see [14], section 10. In other words, let Γ be an EN-diagram and $j \in N(\Gamma)$.

Let K_j be the corresponding virtual component. Then

$$m_j = m(K_j) = \text{Lk}(K, K_j) = \sum_{i \in A(\Gamma)} m_i \text{Lk}(K_i, K_j).$$

The linking numbers can be computed exactly as in 2.1. In EN-diagrams, we put these multiplicities in parentheses.

(2.2.1) Example In the examples of 1.2.5 ($f(x, y) = (y^2 - x^3)^m$ and $g(x, y) = (y^2 - x^3)(y^3 - x^2)$), we obtain:



(2.2.2) Remark In general, the multiplicities do not determine the edge weights of an EN-diagram, as one can conclude from the following example:



where n is neither divisible by 2 nor by 3.

2.3 Characteristic polynomials

(2.3.1) Let $h : F \rightarrow F$ be the monodromy of the Milnor fibration. We can compute the characteristic polynomial of the induced action of h on several homology groups directly from the EN-diagram. We will always use integral homology, unless stated otherwise. We denote by $h_* : H_1(F) \rightarrow H_1(F)$ the algebraic monodromy on $H_1(F)$ and h_{*0} the algebraic monodromy on $H_0(F)$. Let N be a common multiple of the order of the eigenvalues of h_* (which are roots of unity). Define:

$$\begin{aligned} \Delta_0(t) &= \det(tI - h_{*0}), \\ \Delta_1(t) &= \det(tI - h_*), \\ \Delta_*(t) &= \Delta_1(t)/\Delta_0(t) \in \mathbf{Q}(t), \\ \Delta^1(t) &= \det(tI - h_* | \text{Ker}[I - h_*^N]), \\ \Delta'(t) &= \det(tI - h_* | \text{Im}[H_1(\partial F) \rightarrow H_1(F)]). \end{aligned}$$

Let Γ be the EN-diagram of the plane curve singularity f . For $j \in N(\Gamma)$ we denote the number of incident edges by δ_j .

(2.3.2) *The polynomials Δ_0 and Δ_1*

We have $\Delta_0 = t^d - 1$, where $d = \gcd\{m_i \mid i \in A(\Gamma)\}$, the number of connected components of F . The connected components are cyclically permuted by h .

For Δ_1 , [14] gives us the following formula:

$$\Delta_1(t) = (t^d - 1) \prod_{j \in N(\Gamma)} (t^{m_j} - 1)^{\delta_j - 2}.$$

Notice that this formula also gives us $\mu(f)$, the Milnor number of f , which is equal to the rank of $H_1(F)$ and hence to the degree of Δ_1 .

(2.3.3) *The polynomials Δ^1 and Δ'*

The polynomials Δ^1 and Δ' are less known. Since we know that Δ_1 has only Jordan blocks of sizes 1 and 2, we find that the roots of Δ^1 are precisely the roots of Δ_1 that occur in the 2×2 Jordan blocks. The monodromy can act non-trivially on the boundary of F , which is signalled by Δ' . Define:

- d = the number of connected components of F as before,
- d_E = the gcd of the two multiplicities that arise when edge E is broken as in 1.3.5 (E runs over the separating edges),
- d_v = the gcd of all link component multiplicities of the splice component with single central node v (v runs over the nodes),
- d_i = the number of components of $F \cap \partial N(K_i)$, where $N(K_i)$ is the boundary of a small tubular neighbourhood of component K_i ($i \in A(\Gamma)$).

Then, according to Neumann [35], we have:

$$\begin{aligned} \Delta^1(t) &= (t^d - 1) \cdot \frac{\prod_{E \text{ edge}} (t^{d_E} - 1)}{\prod_{v \text{ node}} (t^{d_v} - 1)}, \\ \Delta'(t) &= (t^d - 1)^{-1} \cdot \prod_{i \in A(\Gamma)} (t^{d_i} - 1). \end{aligned}$$

For the examples in 2.2 we obtain the following results:

- For $f(x, y) = (y^2 - x^3)^m$:

$$\Delta_0(t) = t^m - 1, \quad \Delta_1(t) = \frac{(t^m - 1)(t^{6m} - 1)}{(t^{2m} - 1)(t^{3m} - 1)}, \quad \Delta^1(t) = \Delta'(t) = 1.$$

– For A’Campo’s singularity $g(x, y) = (y^2 - x^3)(x^3 - y^2)$:

$$\Delta_0(t) = t - 1, \quad \Delta_1(t) = (t - 1)(t^5 + 1)^2, \quad \Delta^1(t) = t + 1, \quad \Delta'(t) = 1.$$

The polynomials Δ^1 and Δ' will become useful when we consider the Seifert form and the spectrum in section 4.4.

2.4 The zeta-function of the monodromy

Let F be the Milnor fibre of a singularity. In general, if $a_* \in \text{Aut}(H^*(F; \mathbf{Z}))$, we define the zeta-function $\zeta(a_*)$ of the operator a_* by:

$$\zeta(a_*)(t) = \prod_{q \geq 0} \det(I - ta_q)^{(-1)^{q+1}},$$

see [2] or [6]. Note, however, that in the latter reference the *inverse* of the usual zeta function is used. If h_* is the algebraic monodromy of a singularity f , we define $\zeta_f = \zeta(h_*)$, and call it the *zeta-function of (the monodromy of) f*.

In the case of plane curve singularities, the homology groups of dimensions greater than 1 vanish. The zeta-function is related to $\Delta_* = \Delta_1/\Delta_0$ by

$$\zeta_f(t) = t^{-\chi(F)} \Delta_*(t^{-1}).$$

The following formula holds:

$$\zeta_f(t) = \prod_{j \in N(F)} (1 - t^{m_j})^{\delta_j - 2},$$

so the zeta-function is also very easy to compute from the EN-diagram. This formula is due to A’Campo [2].

An important property shared by the zeta-function and the Δ_* is that they are multiplicative under splicing, see [14], Theorem 4.3. This is the basis for the proof of the corresponding formula for Δ_* (from which the formula for Δ_1 as in 2.3 is deduced).

2.5 The multi-variable Alexander polynomial

Another interesting invariant is the *multi-variable Alexander polynomial* of the link K , which is denoted by Δ_K . The number of variables of this polynomial,

s , is the same as the number of components of the link. The general definition can be found in [41]. According to [14], Theorem 12.1, we have:

$$\Delta_K(t_1, \dots, t_s) = \prod_{j \in N(\Gamma)} (t_1^{m_{1j}} \dots t_s^{m_{sj}} - 1)^{\delta_j - 2},$$

where $m_{ij} = \text{Lk}(m_i K_i, K_j)$. For the behaviour of Δ_K under splicing we refer to [14], Proposition 5.1. We can get Δ_* from Δ_K by putting all variables equal to t :

$$\Delta_*(t) = \Delta_K(t, \dots, t).$$

It follows that the multi-variable Alexander polynomial of a multilink $aL = a_1 L_1 + \dots + a_r L_r$ and the multi-variable Alexander polynomial of the reduced link $L = L_1 + \dots + L_r$ satisfy the following relationship:

$$\Delta_{aL}(t_1, \dots, t_r) = \Delta_L(t_1^{a_1}, \dots, t_r^{a_r}).$$

The multi-variable Alexander polynomial efficiently encodes linking and multiplicity information in such a way that the contribution of a certain arrow-head to that multiplicity can be retrieved. In 2.2.2 we saw an example of two EN-diagrams with the same sets of multiplicities. Their multi-variable Alexander polynomials are

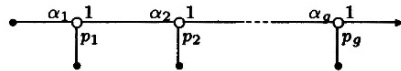
$$\frac{t_1^{2n} t_2^{3n} - 1}{t_1^2 t_2^3 - 1} \quad \text{and} \quad \frac{t_1^{4n} t_2^n - 1}{t_1^4 t_2 - 1}.$$

It is well-known that the one-variable Alexander polynomial is a complete invariant for the topological type of an irreducible isolated plane curve singularity. One can prove that the multi-variable Alexander polynomial is a complete invariant of the topological type of an arbitrary isolated plane curve singularity. This seems to be common knowledge, although we could not trace down a proof in the literature.

2.6 Zariski's numbers and the multiplicity sequence

For the sake of completeness, we show how to find Zariski's numbers $\bar{\beta}_0, \dots, \bar{\beta}_g$ and the multiplicity sequence directly from the EN-diagram. These results are easily established.

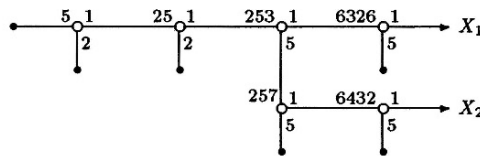
(2.6.1) Let X be a plane curve with Puiseux pairs $(p_1, q_1), \dots, (p_g, q_g)$ and hence with EN-diagram



(with all $p_i \geq 2$ and $\alpha_1 = q_1$, $\alpha_j = q_j + p_j p_{j-1} \alpha_{j-1}$). Let $\mathcal{O}_X = \mathbb{C}\{x, y\}/(f)$ — where f defines X — be the local ring of X . There exists a canonical valuation $v : \mathcal{O}_X \rightarrow \mathbb{N} \cup \{\infty\}$ (induced by a parametrization). It is well-known that $N = v(\mathcal{O}_X)$ is a semi-group. An easy translation of Zariski's result [64] to the language of EN-diagrams gives us that a minimal set of generators of N is $\{\bar{\beta}_0, \dots, \bar{\beta}_g\}$, where

$$\begin{aligned} \bar{\beta}_0 &= p_1 \cdots p_g, \\ \bar{\beta}_j &= \alpha_j p_{j+1} \cdots p_g \quad (1 \leq j \leq g). \end{aligned}$$

Consider the example of 1.2.5.



For X_1 we obtain $(\bar{\beta}_0, \dots, \bar{\beta}_g) = (100, 250, 625, 1265, 6326)$.

(2.6.2) The *multiplicity sequence* (Multiplizitätensequenz, [8], p. 673), describes the multiplicities in the blowing up sequence of the curve $X : f = 0$. This sequence is obtained by performing several Euclidean algorithms. The multiplicity sequences of all branches of a plane curve singularity determine together its topology.

We will describe how to find the multiplicity sequence of a branch from the EN-diagram. The method is best described by an example. We use the branch X_2 of the example above.

First algorithm: $(q_1, p_1) = (5, 2)$.

$$\begin{aligned} 5 &= 2 \cdot 2 + 1 && \text{gives } \mathbf{2, 2} \\ 2 &= 2 \cdot 1 && \text{gives } \mathbf{1, 1} \end{aligned}$$

Second algorithm: $(q_2, p_2) = (5, 2)$.

This algorithm is the same as the first one. Therefore we get again **2, 2, 1, 1**.

Third algorithm: $(q_3, p_3) = (7, 5)$.

$$\begin{aligned} 7 &= 1 \cdot 5 + 2 && \text{gives } \mathbf{5} \\ 5 &= 2 \cdot 2 + 1 && \text{gives } \mathbf{2, 2} \\ 2 &= 2 \cdot 1 && \text{gives } \mathbf{1, 1} \end{aligned}$$

g^{th} algorithm: $(q_g, p_g) = (7, 5)$.

The last algorithm is the same as the third.

Now we multiply the results of the i^{th} algorithm by $p_{i+1} \cdots p_g$, to obtain the multiplicity sequence:

$$(100, 100, 50, 50, 50, 50, 25, 25, 25, 10, 10, 5, 5, 5, 2, 2, 1, 1).$$

2.7 The EN-diagram vs. the resolution graph

Another well-known complete invariant of the topological type of a plane curve singularity is the dual graph of a good embedded resolution $\pi : Z \rightarrow \mathbb{C}^2$ which resolves the singularities of the plane curve singularity f . Let $E = \pi^{-1}(0)$ be the exceptional divisor and V the dual graph. $\pi^{-1}f^{-1}(0) = \cup_{\kappa \in AUUV} E_{\kappa}$ is a divisor with normal crossings on Z (the points of A are represented by arrow-heads). We assume that the reader is familiar with the resolution graph.

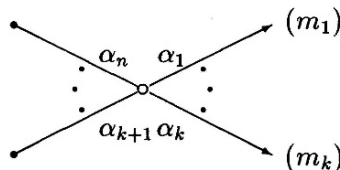
There are conversion algorithms from EN-diagram to resolution graph and back, see [14], Chapter V. We will not discuss these algorithms, but only mention some properties that are useful to remember.

As a graph, the EN-diagram is equal to the resolution graph from which all the vertices of valence 2 (i.e. with 2 incident edges) are removed. This leaves us with the vertices of valence 1, and the vertices of valence greater than 2 which are called *rupture points*. So the rupture points correspond to the nodes in the EN-diagram.

In a resolution graph, the vertices carry a multiplicity equal to the multiplicity of f on the corresponding branch of the total transform; i.e. for $\kappa \in AUUV$ we define m_{κ} by $\text{div}(f \circ \pi) = \sum_{\kappa \in AUUV} m_{\kappa} E_{\kappa}$. It happens to be the case that these multiplicities are equal to the multiplicities of the corresponding nodes and dots (and of course the arrows) in the EN-diagram.

In section 4.3, we will make use of the multiplicities of the neighbour vertices of a rupture point. It is possible to compute these multiplicities from the EN-diagram without having to build the complete resolution graph — which is not so easy.

(2.7.1) Lemma *Consider a (very general) splice component:*



Put $m_i = 0$ for $i \in \{k+1, \dots, n\}$; so $m = \sum_j \alpha_1 \cdots \hat{\alpha}_j \cdots \alpha_n m_j$ is the multiplicity of the central node.

Then, in the corresponding plumbing graph (in our application this will be a part of the resolution graph) the neighbour vertex on the edge marked with α_j has a multiplicity which is modulo m equal to s_j , where s_j can be found as follows. Choose integers β_j ($1 \leq j \leq n$), with $\beta_j \alpha_1 \cdots \hat{\alpha}_j \cdots \alpha_n \equiv 1 \pmod{\alpha_j}$. Then $s_j = (m_j - \beta_j m) / \alpha_j$. \square

See Neumann [35] for a proof. It should be possible to get this result in a completely number-theoretic manner.

2.8 The polar ratios of a plane curve singularity

For details of this section, consult [62], [26], or [57].

Let $f : (\mathbb{C}^2, 0) \rightarrow (\mathbb{C}, 0)$ be a plane curve singularity. Let $l : (\mathbb{C}^2, 0) \rightarrow (\mathbb{C}, 0)$ be a sufficiently general linear form with equation $l(x, y) = bx - ay$. We obtain a map germ $\Phi = (l, f) : (\mathbb{C}^2, 0) \rightarrow (\mathbb{C}^2, 0)$ whose critical locus is defined by

$$a \frac{\partial f}{\partial x} + b \frac{\partial f}{\partial y} = 0.$$

The *polar curve* of f with respect to the direction l is the union Γ of all irreducible components of the critical locus of Φ that are not contained in $X = f^{-1}(0)$; in other words:

$$\Gamma = \overline{\text{Sing}(\Phi) \setminus f^{-1}(0)}.$$

The image $\Delta = \Phi(\Gamma)$ is called the *Cerf diagram*. We use (u, v) as coordinates in the target space. Its branches $\Delta_1, \dots, \Delta_t$ have Puiseux expansions

$$v = a_i u^{\rho_i} + \text{higher order terms},$$

with $a_i \neq 0$ and $\rho_i > 1$. The rational numbers ρ_i are called the *polar ratios* of f . The set $\mathfrak{p}(f) = \{\rho_1, \dots, \rho_t\}$ is a topological invariant of f . Note, however, that the number of times that a certain polar ratio occurs in the t -tuple (ρ_1, \dots, ρ_t) is not a topological invariant (but it is an analytical one). One sometimes encounters the *inverses* of our polar ratios as polar ratios.

It is possible to view the set $\mathfrak{p}(f)$ topologically. Let R_1, \dots, R_p be the *intrinsic companions* of the link K of f , i.e. regular fibres of the Seifert pieces. They are represented by the nodes in the EN-diagram, and can be visualized by attaching an extra arrow with weight one to each node.

Define the following subset of \mathbf{Q} :

$$E(f) = \left\{ \frac{\text{Lk}(K, R_i)}{\text{mult}(R_i)} \mid R_i \text{ is an intrinsic companion} \right\}.$$

Here, $\text{mult}(R_i)$ denotes the multiplicity of R_i , i.e. the number $n = p_1 \cdots p_g$ in the EN-diagram of R_i . (It is, by the way, equal to the braid index of R_i , which is the minimal number of strings needed to get R_i as a closed braid.)

(2.8.1) Proposition *We have:*

- (a) $\mathfrak{p}(f) = E(f) \cup \{\text{mult}(f)\}$ if f has a tangent cone consisting of exactly two lines,
- (b) $\mathfrak{p}(f) = E(f)$ otherwise.

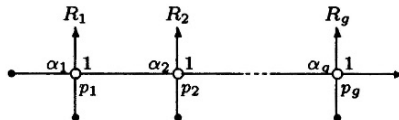
For the proof of this proposition, see [62] or [26]. □

It is not necessary for f to be reduced, as long as multiplicities are taken into account correctly and one does not forget that the zero-locus of f is subtracted from the critical space of Φ .

(2.8.2) Example Consider our standard examples $f(x, y) = (y^2 - x^3)^m$ and $g(x, y) = (y^2 - x^3)(y^3 - x^2)$:



We have drawn the unions of the links of f and g with the intrinsic companions. In the first example, there is one intrinsic companion R_1 . The polar ratio is $\rho = 6m/2 = 3m$. In the second example, there are two intrinsic companions R_1 and R_2 , giving ratios $\rho_1 = \rho_2 = (6 + 4)/2 = 5$. Moreover, the tangent cone consists of two lines (its equation is $x^2y^2 = 0$). Because $\text{mult}(f) = 4$, we get $\mathfrak{p}(g) = \{4, 5\}$.



Our third example is the general branch X with g Puiseux pairs. The EN-diagram shows $K + R_1 + \cdots + R_g$. We obtain:

$$\mathfrak{p}(X) = \left\{ \rho_i = \frac{\alpha_i p_i \cdots p_g}{p_1 \cdots p_i} \mid 1 \leq i \leq g \right\},$$

a set of g rational numbers.

CHAPTER 3

Topological series of plane curve singularities

3.1 Introduction

(3.1.1) As soon as one starts compiling lists of singularities of functions, one comes across *series* of singularities. The members of such series share various properties, but one finds that there are always some exceptions. Writing down an all-embracing definition of a series inevitably gives problems.

The first one who made lists of series was V.I. Arnold in [3], see also [5]. Some of these had already been given names, such as A_n , D_n , etc.. In hindsight it is not clear who was the first to use these names for singularities of functions. Hirzebruch [18] (1962/63) describes the dual graph of the resolution of the simple singularities, and observes that these graphs are the well-known A - D - E Dynkin diagrams. In Brieskorn [7] (1966) these names are used without further introduction. Later it was also proved that the monodromy groups of the A - D - E singularities (with an odd number of variables) are isomorphic to the Weyl groups of the Lie algebras with the same names.

In his lists, Arnol'd went further and introduced letters other than A , D and E when he encountered new classes. His lists are (partly) reproduced in Appendix A, where also the corresponding EN-diagrams are drawn. He wrote: "Series undoubtedly exist, although it is not at all clear what a series of singularities is" [5], p. 243. And another one of his statements — quoted by my predecessors as well — is: "It is only clear that the series are associated with singularities of infinite multiplicity [...], so that the hierarchy of series reflects the hierarchy of non-isolated singularities" [5], p. 244.

A series depends on one or more integral parameters. The simplest series is the A -series. An example of a function of type A_n is $y^2 + x^{n+1}$. Clearly, the

elements of A_n have to be classes of an equivalence relation; depending on the situation this could be right-equivalence, topological equivalence, etc.. It is clear that y^2 is a non-isolated singularity which could be called the *head* of the A -series. Siersma introduced the name A_∞ for this singularity (and likewise D_∞ , etc.) — obviously not modelled on the resolution graph or the Milnor lattice.

Series were an inspiration to many authors. We mention the work of Arnol'd (cited above), Wall (e.g. [61]) and Pellikaan [36].

(3.1.2) Remark We will not pursue the philosophical remarks behind series further. Our definition of topological series, presented in this Chapter, satisfies all the required properties. Yet one should note that there is an abuse of language: for example, below we will use Yomdin series to illustrate several points, but a Yomdin series is in fact a mere *sequence* of functions. The same applies to the ‘series’ in Chapter 6: perhaps it would be better to call them ‘sequences’, too, in order to stress the fact that we only consider very special *representatives* of members of a series.

Mind the Gap

(3.1.3) Yomdin Series

Let $f : (\mathbf{C}^{n+1}, 0) \rightarrow (\mathbf{C}, 0)$ be a germ of a non-zero holomorphic function with a one-dimensional critical locus Σ . Let x be a linear form satisfying $\Sigma \cap Z(x) = \{0\}$, where $Z(x) = \{x = 0\}$. For integers $k \geq 2$ we consider the functions

$$f_k = f + \varepsilon x^k,$$

where ε is a small non-zero complex parameter. We will call such a series a *Yomdin Series*, after I.N. Yomdin who first studied them, see [63] and Lê [25].

One of his results concerned the relationship between the Milnor numbers of f and f_k . He proved that for $k \gg 1$, $f + \varepsilon x^k$ has an isolated singularity, and that

$$\mu(f + \varepsilon x^k) = b_n(f) - b_{n-1}(f) + k(\Sigma \cdot Z(x)),$$

where $\Sigma \cdot Z(x)$ is the intersection number of Σ and $x = 0$ at the origin, and b_i denotes the i^{th} Betti number of the Milnor fibre of f . In fact, one can show that the formula holds for k greater than or equal to the largest polar ratio of f .

Siersma [52] generalized this formula by giving a relationship between the characteristic polynomials of f and f_k (cf. sections 3.5 and 6.2). Steenbrink [56]

conjectured a still stronger formula concerning the spectra of f and f_k . This conjecture was proved by M. Saito [42].

So a lot is known about Yomdin series, but the feeling remains that they are a poor reflection of the ‘original’ series of Arnol’d. Generally speaking, Yomdin series are extremely coarse. For example, a two parameter family such as $Y_{r,s} : x^2y^2 + x^{r+4} + y^{s+4}$, obviously cannot be obtained. Furthermore, if the multiplicity of Σ at the origin is greater than one, we do not get the full series. For instance, let $f(x, y) = (y^2 - x^3)^2$. Yomdin’s formula shows, that the Milnor number within the series increases with steps of 2. However, if we take

$$\begin{aligned} W_{1,2q-1}^\# &: (y^2 - x^3)^2 + x^{4+q}y \quad (q \geq 1) \\ W_{1,2q}^\# &: (y^2 - x^3)^2 + x^{3+q}y^2 \quad (q \geq 1), \end{aligned}$$

then we get the ‘full’ Arnol’d series $W_1^\#$, leaving no gaps.

It becomes even worse if we consider $f(x, y) = y^3$. Recalling Arnol’d’s statement that the hierarchy of the non-isolated singularities reflects the hierarchy of the series, we would like the non-isolated singularity with equation $y^3 + y^2x^k$ in its series. With Yomdin series this is of course impossible.

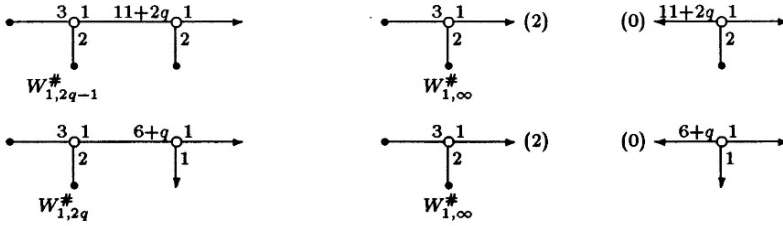
3.2 The definition of topological series

(3.2.1) In this section, we will give a definition of *topological series* of plane curve singularities. This definition was first published in [43], which appeared in revised form as [44]. The definition will be followed by the computation of various topological invariants and it will appear that they behave as expected within a series.

The motivation to look at topological series is, that many properties that hold a series together are of topological nature. We think of the Milnor number, the characteristic polynomial of the monodromy, the zeta-function — and indeed the spectrum. For plane curve singularities, this is more tractable than in a more general setting.

The definition will overcome many of the problems that we mentioned earlier with the Yomdin series. Our series will contain topological types.

(3.2.2) The standard example of our topological series has always been $W^\#$. Recall the splice decomposition of $W^\#$ (Example 1.3.6):



Also in the other Arnol'd series the phenomenon occurs that the non-isolated 'head' of the series is a splice component of each of the elements in the series. This means, that the Milnor fibration of a member of the series can be obtained from the Milnor fibration of the non-isolated singularity by removing tubular neighbourhoods of the multiple components and replacing them by something fibred in such a way, that the result is the Milnor fibration of a non-isolated singularity (or, more generally, a singularity with branches of 'lower' transversal types).

Unsurprisingly, the best way to state the definition is using EN-diagrams.

(3.2.3) Definition [Topological Series] Let $X = m_1X_1 \cup \dots \cup m_sX_s$ be a non-isolated plane curve singularity with $m_i > 1$ for $i \leq r$ and $m_i = 1$ otherwise. Let Γ be the EN-diagram of f , and denote by $\alpha_1, \dots, \alpha_r \in A(\Gamma)$ the arrow-heads belonging to m_1X_1, \dots, m_sX_r . Then the *topological series of f* consists of all topological types with EN-diagrams that arise from Γ by splicing something to each of the α_i — taking the splice and algebraicity conditions into consideration — in such a way that the multiplicities of the arrow-heads of the splice components attached to the α_i are smaller than m_i .

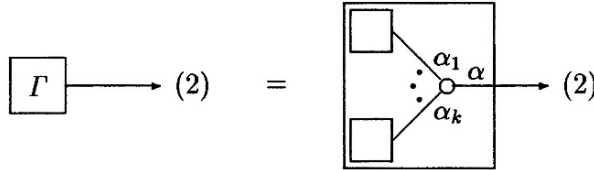
(3.2.4) Remark Our definition works equally well for certain other curve singularities (see section 3.7), but we think it is clearer to explain the situation for plane curve singularities first.

Now that we have this definition, we will investigate which possibilities there are to replace an arrow-head with an '(m)' in front of it by something with lower multiplicities. We start with the easiest case when we have an arrow-head of multiplicity 2, a *double component*.

3.3 The case of a double component

(3.3.1) Recall the notation $A(\Gamma)$ for the arrow-heads of an EN-diagram Γ and $N(\Gamma)$ for the other vertices (dots and nodes), introduced in 1.2.4.

Let X be a plane curve singularity with defining equation f , link K and EN-diagram Γ . Suppose there is a double component $\diamond \in A(\Gamma)$, i.e. $m_\diamond = 2$. Near the arrow-head \diamond , the EN-diagram looks like this:



where the boxes may denote any sub-EN-diagram and the arrow is $\diamond \in A(\Gamma)$. The second picture is only defined when $\Gamma \neq \bullet \rightarrow (2)$ and $\Gamma \neq (m) \leftrightarrow (2)$, since then there is no node.

Define the following numbers:

$$N_0 = \left[\frac{2\alpha_1 \cdots \alpha_k}{\alpha} \right],$$

$$c = \sum_{j \in A(\Gamma), j \neq \diamond} m_j \text{Lk}(K_\diamond, K_j),$$

where $[\cdot]$ denotes integral part. (In the two exceptional cases, $N_0 = 0$). We have encountered the number c already in lemma 1.1.4 and, more importantly, in the Splice Condition in 1.3.1.

We will now show which possibilities there are to replace the double component with. Recall the definition of the zeta-function in section 2.4.

(3.3.2) Theorem *The only two (classes of) possibilities to replace a double component with, are:*



with $N > N_0$ odd,

with $N > N_0$ even.

Furthermore, let ζ_∞ be the zeta-function of f and ζ_N the zeta-function of a singularity with the EN-diagram obtained by replacing the arrow-head \diamond by one of the possibilities above. Then we have

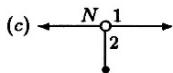
$$\zeta_N(t) = \zeta_\infty(t) \cdot (1 - (-1)^N t^{N+c}).$$

In particular, the Milnor number μ is linear in N with coefficient 1:

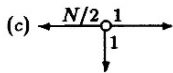
$$\mu_N = \mu_\infty + N + c + d - 1$$

where $d = \gcd(m_1, \dots, m_s)$, the number of connected components of the Milnor fibre of f .

Proof. The EN-diagrams of the theorem can be regarded as being the result of splicing the links K and the one given by the EN-diagram Γ'_N which is the left diagram below if N is odd and the right diagram if N is even.



with $N > N_0$ odd,



with $N > N_0$ even.

Splicing is done along the component K_\circ of K and the component K'_* with multiplicity $m_* = c$ (the arrow pointing leftwards), respectively. That the multiplicity of $*$ must be c follows from one half of the Splice Condition. The other half,

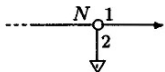
$$2 = \sum_{h \in A(\Gamma'_N), h \neq *} m_h \text{Lk}(K'_*, K'_h),$$

implies that these two diagrams are the only two essentially different EN-diagrams with the required property, for we want that $m_h = 1$ for each $h \in A(\Gamma'_N) \setminus \{*\}$, and that no dots are attached to a node with weight 1. For the first link (N odd) the splice condition reads ‘ $2 = 2 \cdot 1$ ’ and for the second ‘ $2 = 1 \cdot 1 + 1 \cdot 1$ ’; there are no more of this kind of partitions of the number 2.

The algebraicity condition gives $N > N_0$.

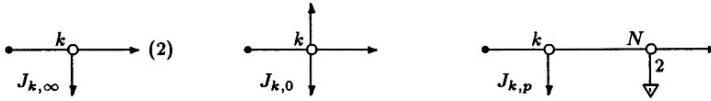
The formula for the zeta-function follows from the formula in 2.4 and the fact that the zeta-function is multiplicative under splicing. The statement about the Milnor number is an easy consequence of this. \square

(3.3.3) Definition We combine the two possibilities in one graph, where, depending on whether N is odd or even, the first or the second graph of the theorem must be substituted.



(3.3.4) Remark if $\alpha = 1$ or $\alpha = 2$ (see the figure at the beginning of this section) then the case $N = N_0$ is also allowed, although then the diagram has to be minimized by applying Theorem 8.1 of [14]. The formula for the zeta-function still holds. Yet, according to the definition of series, this element does not belong to the series, although it shares many properties with the other members. In section 4.6 we will meet a singularity whose spectrum behaves as in the series, but its spectral pairs do not.

(3.3.5) Example The singularity $f(x, y) = y^2(y + x^k)$ is of type $J_{k,\infty}$. We have $c = k$ and $N_0 = 2k$. The series is $J_{k,p} : y^3 + y^2x^k + x^{3k+p}$, $p \geq 0$. We have $N = 2k + p$. The case $p = 0$ is the special case with $N = N_0$.



We have $\mu(J_{k,\infty}) = 3k - 2$ and $\mu(J_{k,p}) = 3k - 2 + p$.

(3.3.6) Example If X has more than one branch with multiplicity two, we can treat each branch separately. For each arrow-head $\alpha \in A(\Gamma)$ with $m_\alpha = 2$, we obtain a c_α and an $N_{\alpha 0}$. The simplest example is the series of $f(x, y) = x^2y^2$, which is of type $Y_{\infty,\infty}$ (or of type $T_{\infty,\infty,2}$ if one wishes). Its EN-diagram is

$$(2) \longleftrightarrow (2).$$

We obtain the series $Y_{r,s} : x^2y^2 + x^{r+4} + y^{r+4}$ with $r, s \geq 1$, and $r = 0, s = 0$ give exceptional cases.

(3.3.7) The reader can verify in Appendix A that our topological series comprise of all Arnol'd's series of plane curve singularities. The cases missed by the Yomdin series, such as two-parameter families and series as $W^\#$, are part of our theory. But what is more: the series do not consist of anything *more* than they should. This is not obvious. For instance, Arnol'd [5], p. 243 gives an example of the relation of adjacency that could tie a series together, but then the A -series would belong to the D -series.

And we can do even better than this, as we will show in the next section.

3.4 Higher multiplicities

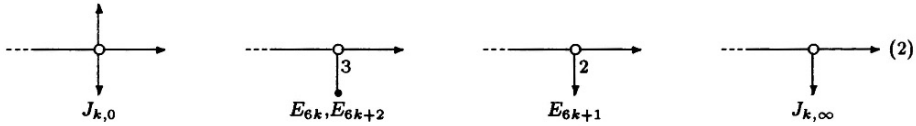
(3.4.1) When we have an arrow-head of multiplicity $m > 2$ in the EN-diagram of a plane curve singularity, exactly the same method can be used. The splice decomposition always gives us a finite number of essentially different graphs that can be spliced to a component of multiplicity m , and we can decide exactly which.

We enumerate the possibilities when $m = 3$ and $m = 4$. The names refer to the simplest case when $f(x, y) = y^m$.

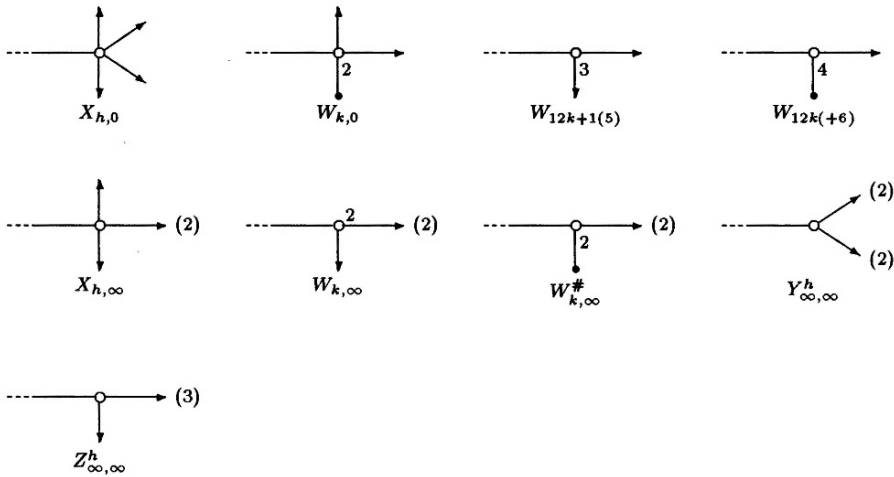
In the diagrams, the splice edges have variable weight N , N having no common factor with the other weights. The other omitted edge weights are

equal to 1. We only listed the diagrams with one node; some have an arrow of multiplicity greater than 1, which could be treated again.

The four possibilities for $m = 3$:



The nine possibilities for $m = 4$:



The following formula gives the number of essentially different diagrams with one node and only multiplicities less than m , that can be spliced to a component of multiplicity m .

(3.4.2) Proposition *The number is:*

$$\sum_{q|m} P(m/q) + \sum_{1 \leq p \leq m-1} \sum_{q|(m-p), q > 1} P((m-p)/q) - 1$$

where $P(n)$ is the number of integer partitions of n .

Proof. In such a diagram at most one dot appears, with at the node a weight ≥ 2 . The number of edges emerging from the node must be at least 3. There is at most one weight greater than 1. These are consequences of the algebraicity condition. The splice condition demands that the total linking number of the other components with the splice component equals m . The formula is now a matter of counting. \square

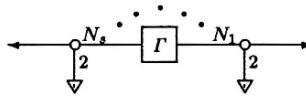
For $m < 15$ we obtain:

| | | | | | | | | | | | | | | |
|--------|---|---|---|---|----|----|----|----|----|----|----|-----|-----|-----|
| m | 1 | 2 | 3 | 4 | 5 | 6 | 7 | 8 | 9 | 10 | 11 | 12 | 13 | 14 |
| number | 0 | 2 | 4 | 9 | 12 | 22 | 27 | 42 | 54 | 76 | 91 | 134 | 159 | 211 |

This can be regarded as an upper bound on the number of symbols (such as A , $W^\#$, etc., with several parameters) needed to give names to all singularities of corank m .

3.5 The zeta-function within a series

Let $f = f_1^2 \cdots f_r^2 f_{r+1} \cdots f_s$ be a non-isolated plane curve singularity with double components only. Denote the singular locus of f by $\Sigma = \Sigma_1 \cup \cdots \cup \Sigma_r$. According to Theorem 3.3.2, a typical element f_N (with multi-index N) of the series has EN-diagram



where $N = (N_1, \dots, N_r) > (N_{01}, \dots, N_{0r})$ (we define N_{0i} and c_i as usual). This diagram represents the EN-diagram Γ of f , whose double components are replaced in order to get an isolated singularity.

The following corollary is immediate from Theorem 3.3.2. It is valid in a more general setting, see 3.7.

(3.5.1) Corollary *We have:*

$$\zeta_{f_N}(t) = \zeta_f(t) \cdot \prod_{i=1}^r (1 - (-1)^{N_i} t^{N_i + c_i}). \quad \square$$

Recall from 1.1.6 the definitions of the vertical and horizontal monodromies A_i and T_i ($1 \leq i \leq r$). We proved that $A_i = T_i^{-c_i}$. In the current application, T_i is equal to the 1×1 -matrix (-1) , since it describes the permutation of the two points in a transversal section along Σ_i on the reduced homology level. Let d_i be the multiplicity of Σ_i at the origin. According to 2.8, each of the r new nodes gives rise to a new polar ratio θ_i (the other polar ratios of f_N are the same as those of f). Observe that $d_i \theta_i = N_i + c_i$. Rewriting the corollary, we obtain:

$$\zeta_{f_N}(t) = \zeta_f(t) \cdot \prod_{i=1}^r \det(I - t^{d_i \theta_i} A_i T_i^{d_i \theta_i}).$$

This generalises a formula of Siersma [52], who proved that for the Yomdin series $f_k = f + \varepsilon x^k$, the following formula holds:

$$\zeta_{f_k}(t) = \zeta_f(t) \cdot \prod_{i=1}^r \det(I - t^{d_i k} A_i T_i^{d_i k}).$$

Observe that k is the only new polar ratio in a Yomdin series, hence $\theta_i = k$ for all $i \leq r$.

(3.5.2) We will now investigate the case when f does not only have branches of multiplicity two. The formula of 2.4 gives an easy way to compute the zeta-function of each member of the series. But one has to consider all cases separately as in section 3.4.

It is interesting to have also an expression involving A_i and T_i . We will now give some results in that direction. We consider only one irreducible component Σ_i at the time, and suppose that the transversal type is A_{m-1} . We drop the subscripts i accordingly. The branch Σ_i corresponds with an arrow with ‘ (m) ’ in front of it. Observe that, since we only look at splice components attached to this arrow-head of multiplicity m , we may suppose that $f(x, y) = x^c y^m$. The component x^c stands for all the other components of our original singularity. Observe also that, according to the method of 2.8 of calculating polar ratios, the product $d\theta$ remains the same under the operation of changing f into $x^c y^m$ (although d becomes 1). We are only interested in the factor ζ of the formula $\zeta_{f_N} = \zeta_f \cdot \zeta$.

We start with $f(x, y) = x^c y^3$. In the table given in section 3.4, we find 4 possibilities marked $J_{k,0}$, $E_{6k(+2)}$, E_{6k+1} and $J_{k,\infty}$. The first two are of Yomdin type. A’Campo’s method (see 2.4) gives a factor

$$\zeta(t) = (1 - t^{d\theta})^2 \quad \text{for ‘} J_{k,0}\text{’,}$$

and:

$$\zeta(t) = \frac{1 - t^{3d\theta}}{1 - t^{d\theta}} \quad \text{for ‘} E_{6k}\text{’ and ‘} E_{6k+2}\text{’}.$$

That Siersma’s formula gives the same answers, follows from the following lemma, whose proof is easy:

(3.5.3) Lemma *Let H_m be the reduced homology group of a discrete space consisting of m points. Let $T_m : H_m \rightarrow H_m$ be the automorphism induced by the cyclic permutation of these points. That is, T_m is the $(m-1) \times (m-1)$ matrix of order m , defined on the standard basis e_1, \dots, e_{m-1} by $T_m e_i = e_{i+1}$*

for $i \leq m-2$ and $T_m e_{m-1} = -(e_1 + \dots + e_{m-1})$. Let $k \in \mathbb{N}$ and $a = \gcd(k, m)$. Then the following holds:

$$\det(I - tT_m^k) = \frac{(1 - t^{m/a})^a}{1 - t}. \quad \square$$

The case ' E_{6k+1} ' is different. Here $d\theta = (6k + 3)/2 + c$ is not an integer. The method of 2.4 gives:

$$\zeta(t) = 1 - t^{2d\theta}.$$

We have to modify Siersma's result to obtain this answer. By reconstruction we get:

$$\zeta(t) = (\det(1 - t^{2d\theta} A^2 T^{2d\theta}))^{1/2},$$

since $A^2 T^{2d\theta}$ is the 2×2 identity matrix.

The case ' $J_{k,\infty}$ ' is of course special, too. Unfortunately, it is impossible to give a formula involving the horizontal and vertical monodromies this way. This would, however, be possible if we would use the multi-variable Alexander polynomial which shows clearly the contributions of each branch to the multiplicities (cf. 2.5). In general, we can obtain the following result:

(3.5.4) Proposition Write $d\theta = q/p$ with $\gcd(p, q) = 1$. If we splice to an arrow of multiplicity m something with exactly one node and arrows of multiplicity 1 only, then p is a divisor of $m - 1$, and:

$$\zeta(t) = (\det(I - t^{pd\theta} A^p T^{pd\theta}))^{1/p}.$$

If $p > 1$, $A^p T^{pd\theta}$ is the $(m - 1) \times (m - 1)$ identity matrix (cf. 3.5.5 for the reason of this notation).

Proof. [Our proof is a reconstruction from A'Campo's method. This proposition functions merely as an example of formula 6.3.3.] We consider the following two cases, which are the only ones satisfying the restrictions indicated above.



Let a be the number of arrows with edge weight 1 (pointing rightwards). In the first case we have $m = ap + 1$ and $\theta = q(ap + 1)/p + c$. A'Campo's method gives:

$$\zeta(t) = (1 - t^{q(ap+1)+pc})^a,$$

and our claim follows since T is now an $ap \times ap$ -matrix of order $ap + 1$.

In the second case we have $m = ap$ and $\theta = aq + c$. This time A'Campo's method gives:

$$\zeta(t) = \frac{(1 - t^{apq+pc})^a}{1 - t^{aq+c}},$$

and by applying the lemma we confirm the proposition in this case as well. \square

(3.5.5) Remark In the statements above, we wanted to use the vertical and horizontal monodromies only. That is why we had to use the p^{th} root of a polynomial. In fact we should consider $(m-1)/p \times (m-1)/p$ -matrices, giving a more natural formula. Please compare with 6.3.3.

3.6 Topological series and the resolution

In this section we give an outline of an alternative description of topological series, used by Jan Stevens who wanted to avoid EN-diagrams and stay in the familiar surroundings of the embedded resolution. From the relationship between EN-diagrams and the resolution (cf. 2.7) it will be clear that the resulting series are the same as with our definition.

Let X_∞ be a non-isolated plane curve singularity, given by an equation of the form $f = f_1^{m_1} \cdots f_r^{m_r}$ with $m_i \geq 1$ and not all m_i equal to one. Let $Z \rightarrow \mathbb{C}$ be the minimal good embedded resolution of X_∞ ; so the total transform of f is a divisor with normal crossings. Consider for each strict transform \widetilde{X}_i of a non-reduced irreducible components of X_∞ a deformation of \widetilde{X}_i into a (possibly singular) curve \widetilde{Y}_i , which still intersects the reduced exceptional divisor with multiplicity m_i . These local deformations blow down to a deformation Y of X_∞ . We define Y to be in the series of X_∞ .

Jan Stevens [58] proves that the series above depends only on the equisingularity class of the non-isolated singularity X_∞ . Furthermore, he proves that the curves Y that come out of the construction are deformations of X_∞ .

In the construction, Z becomes a partial resolution of Y . Because of the special role of the exceptional divisor, one needs to describe the singularities of \widetilde{Y}_i in terms of Arnol'd's boundary singularities [4]. In particular, consider the familiar case of a double line \widetilde{X}_i , which in local coordinates looks like $x^m y^2$. We allow deformations into B_k with $k \geq 0$, where B_k is given by $x^k + y^2$. Observe in particular that we allow $k = 0$, giving two lines (in local coordinates $x^m(1 + y^2)$). This corresponds to the exceptional case $N = N_0$ in definition 3.2.3 if such a case exists.

3.7 Curves in other spaces

(3.7.1) In this section we discuss the application of our definition of topological series to curves defined on other spaces than $(\mathbb{C}^2, 0)$. Let (W, w) be a germ of a normal surface with possibly a singularity at the point w . Suppose (W, w) is an *integral homology surface*, i.e. it has the same integral homology as a manifold. Then we can consider analytic functions $f : (W, w) \rightarrow (\mathbb{C}, 0)$. Such functions define curve singularities on W .

The surface W can be embedded in \mathbb{C}^m for some m . By intersecting $f^{-1}(0)$ with a small $2m - 1$ -sphere S we get a link K in the homology 3-sphere $\Sigma = W \cap S$. The EN-diagrams can also be used in this context, and they still correspond to the dual graph of the resolution of f as in the plane curve case. A more detailed account of such curve singularities is given in section 4.2.

If K has multiple components we use exactly the same methods to define the topological series of f as in the plane curve case. But the members of this series should all be defined on the same space (W, w) . In the case of topological series of plane curve singularities, this was enforced by the condition that the link was obtained by repeated cabling (which ensures that there are enough 1's around each node). An EN-diagram without arrow-heads represents a \mathbf{Z} -homology sphere (with an empty link, in fact). To see in which homology sphere a certain link is situated, one can replace the arrow-heads by dots. The resulting EN-diagram is in general highly non-minimal and all nodes attached with weight one should be discarded using [14], Theorem 8.1. For a link of a plane curve singularity, one ends up with nothing, since S^3 is represented by the empty EN-diagram (and minimal EN-diagrams are unique).

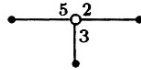
If one has a link with multiple components in a homology sphere other than S^3 , then the links of the members of its series should be in the same homology sphere. This means that the same operations as in the plane curve case are allowed — and nothing else. Summing up:

(3.7.2) **Theorem** *Let $f : (W, w) \rightarrow (\mathbb{C}, 0)$ be a curve singularity defined on a normal \mathbf{Z} -homology surface (W, w) which has at most an isolated singularity at the point w . Suppose that f has some multiple components in its EN-diagram. Then these multiple components can be replaced by, and only by, the same replacements as in the plane curve case. So for double components, Theorem 3.3.2 is still valid, and so are the cases of section 3.4. Furthermore, the formulae of the topological invariants we have seen, remain valid. \square*

(3.7.3) **Example** Let W be the Brieskorn singularity given by

$$W = \{(x, y, z) \in \mathbb{C}^3 \mid x^2 + y^3 + z^5 = 0\}.$$

Let P^3 be the intersection of W with a small 5-sphere. The homology sphere P^3 is known as the *Poincaré sphere*. Its fundamental group is the binary icosaeader group of order 120. The Poincaré sphere has EN-diagram:



Define $f : W \rightarrow \mathbb{C}$ by $f(x, y, z) = x^2$. Then f has EN-diagram as in the first picture below. Its Milnor number is 16. Its series consists of the functions with topological types indicated in the second EN-diagram, with $2N > 30$.



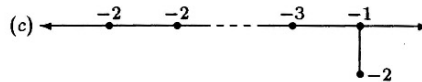
(3.7.4) Many examples of curve singularities are defined on *rational* normal surfaces, that have only the rational homology of a manifold.

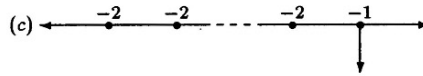
Some of the simplest examples are curves on the quadratic cone $z^2 = xy$, with links in the real projective space $\mathbb{R}P^3$. Dimca [11] gives an example of a series of curve singularities defined on this surface. EN-diagrams do not extend to the situation of rational homology spheres. Therefore we cannot apply exactly the methods of our definition.

Since the method of 3.6 still works, so we can use resolution graphs. However, it is not so easy to describe splicing or the algebraicity and splice conditions in these terms. This is because in the EN-diagrams all linear chains are contracted and we cannot easily predict, how the two linear chains leading to the splice arrows will survive the splice operation.

The members of the series should be defined on the same space as its non-isolated ‘head’. This is checked in a way analogous to the one above: remove all arrows from the resolution graph of the members as well as of the head of the series. The resulting graph is the resolution graph of the underlying surface. According to Neumann [33], there is a unique minimal resolution graph of this surface, and it can be obtained by successively blowing down (-1) -curves. In this way we get a kind of algebraicity condition.

In the case of a double component we had two possible EN-diagrams that we could splice onto it. The cases correspond to the singularities $x^c(y^2 - x^N)$. The resolution graph of such a singularity is the graph of A_{N-1} with an arrow of multiplicity c attached to the ‘long end’ of the diagram:



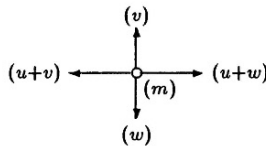


Therefore we can use this to extend Theorem 3.3.2 to this situation, since it is clear that these graphs are the only ones that satisfy the blowing down property mentioned above. Only the start of the series is not easy to see in advance.

(3.7.5) It would be nice to extend EN-diagrams to this more general situation of curves on a rational normal surface. The following idea can be tried to extend EN-diagrams to rational homology spheres. Eisenbud and Neumann put in a node a sign ‘+’ or ‘-’. The minus sign denotes reversal of orientation. In our context of algebraic links, the orientation is always +, and that is why we have omitted these signs. When computing linking numbers using the method of 2.1, one “officially” has to take these signs into consideration (see [14], section 10). Our idea is, to allow for an optional $1/n$ within each node, with $n \in \mathbf{N}$. For instance, in [46], Example 2.4, the curve singularity f on the quadratic cone $z^2 = xy$ in \mathbf{C}^3 , given by

$$f(x, y, z) = z^u(z - x)^v(z + y)^w,$$

is considered. We suggest the EN-diagram



for this singularity, where the edge weights are 1 and within the node should be thought a $\frac{1}{2}$. The resolution graph of f is exactly the same, and the central node has multiplicity $m = u + v + w$. This nicely fits with our $\frac{1}{2}$, because the rules of EN-diagrams now describe a multiplicity of $(v+w+(u+v)+(u+w))/2$.

Without the $\frac{1}{2}$ within the node, this would denote (as a set) a link in S^3 whose components have mutual linking number 1. This projects to \mathbf{RP}^2 under the usual $2 : 1$ covering map to the link of f . Observe that the linking number of two of the components is always $\frac{1}{2}$.

Neumann communicated to me that not all algebraic links in rational homology spheres could arise like this. A possibility is that one obtains the \mathbf{Q} -homology spheres that admit locally a \mathbf{Z} -homology sphere as a finite cover. It would be interesting to investigate this in the future.

CHAPTER 4

Splicing spectra

4.1 Introduction

The *spectrum* and the *spectral pairs* of a singularity f are very powerful invariants. They were introduced by Arnol'd and Steenbrink, see [54] and also [6]. The spectrum is a strong topological invariant; it determines for instance the characteristic polynomial. Also in other respects it is powerful: one can use it in connection with adjacencies of singularities, and it distinguishes large classes of singularities. For example, it distinguishes all isolated quasi-homogeneous singularities, and also all the examples found by Grima [17].

The spectral pairs are even stronger than the spectrum (later on we will give an example of two singularities with the same spectrum but different spectral pairs). When we spoke about “the spectrum” in earlier chapters, we usually meant the spectrum or the spectral pairs but in this chapter we will distinguish more carefully between the two.

In this chapter, we discuss several results that were jointly obtained by Steenbrink, Stevens and the author, published in [46] (better known as [SSS]). We will enter into detail only for the subjects that are related directly to the work of the earlier chapters. There used to be the following conjecture, raised by Steenbrink.

Conjecture [The Spectrum Conjecture] *The spectral pairs of a plane curve singularity form a complete invariant of the topological type.*

There also was another conjecture concerning the real Seifert form which appears to be equivalent to the Spectrum Conjecture. Neumann mentions this conjecture in [35], and he writes that the conjecture’s “originator now denies responsibility and will remain unnamed.”

Conjecture *The real Seifert form of a plane curve singularity is a complete invariant of the topological type.*

The answer to both conjectures — a negative one — arose from an example found by Steenbrink and Stevens in Hamburg. It is reproduced in section 4.6. It can be explained very well in terms of topological series. Furthermore, it comes with a splice formula for spectral pairs.

4.2 Spectral pairs

The setting will be as in [46]. There, the spectral pairs are introduced in a more general situation than was done before, cf. [6], p. 380. Let (X, x) be an isolated singularity of a complex space which is equidimensional of dimension $n + 1 > 0$. Let $f : (X, x) \rightarrow (\mathbf{C}, 0)$ be a germ of a holomorphic function vanishing at x .

A good representative for f is obtained as follows. Take an arbitrary representative X' , embedded into \mathbf{C}^m such that x corresponds to 0. Then choose ε, η with $0 < \eta \ll \varepsilon \ll 1$ and let $X = \{z \in X' \mid |z| < \varepsilon \text{ and } |f(z)| < \eta\}$. Put $\Delta = \{t \in \mathbf{C} \mid |t| < \eta\}$, $\Delta^* = \Delta \setminus \{0\}$ and $X^* = X \setminus f^{-1}(\Delta^*)$. Then $f : X^* \rightarrow \Delta^*$ is a C^∞ fibre bundle. Recall that a typical fibre is called the Milnor fibre of f , denoted for the moment by $X_{f,x}$.

Let $h : X_{f,x} \rightarrow X_{f,x}$ be the geometric monodromy of the Milnor fibration. The (algebraic, cohomological) monodromy of f is the induced action $T = h^{*-1}$ on the cohomology ring $H^*(X_{f,x})$.

The spectral pairs reflect the interplay between the action of T and the *mixed Hodge structure* on $H^*(X_{f,x})$. It consists of an increasing *weight filtration* W on $H^k(X_{f,x}; \mathbf{Q})$ and a decreasing *Hodge filtration* F on $H^k(X; \mathbf{C})$, cf. [54], [55]. If one writes $T = T_s T_u = T_u T_s$ with T_s semi-simple and T_u unipotent, then T_s preserves the filtrations W and F , whereas $N = \log T_u$ has $N(W_i) \subset W_{i-2}$ and $N(F^p) \subset F^{p-1}$. For each eigenvalue λ of T on $H^k(X_{f,x}; \mathbf{C})$ we define:

$$\begin{aligned} H_\lambda^{p,q}(k) &= \text{Ker}(T_s - \lambda I; \text{Gr}_{p+q}^W \text{Gr}_F^p \widetilde{H}^k(X_{f,x}; \mathbf{C})), \\ h_\lambda^{p,q}(k) &= \dim_{\mathbf{C}} H_\lambda^{p,q}(k). \end{aligned}$$

Here \widetilde{H}^k denotes reduced cohomology as usual, $\text{Gr}_i^W = W_i/W_{i-1}$ and $\text{Gr}_F^p = F^p/F^{p+1}$. Moreover, we let

$$h_\lambda^{p,q} = \sum_{k=0}^n (-1)^{n-k} h_\lambda^{p,q}(k).$$

For $\alpha \in \mathbf{Q}$ and $w \in \mathbf{Z}$ we define integers $m_{\alpha,w}$ as follows. Write $\alpha = n - p - \beta$ with $0 \leq \beta < 1$ and let $\lambda = \exp(-2\pi i\alpha)$. If $\lambda \neq 1$ then $m_{\alpha,w} = h_\lambda^{p,w-p}$, else $m_{\alpha,w} = h_1^{p,w+1-p}$. The *spectral pairs* are collected in the invariant

$$\text{Spp}(f) = \sum_{\alpha,w} m_{\alpha,w}(\alpha, w),$$

an element of the free abelian group on $\mathbf{Q} \times \mathbf{Z}$. By omitting the weights from the spectral pairs one obtains the *spectrum* $\text{Sp}(f)$ of f (cf. [56]):

$$\text{Sp}(f) = \sum_{\alpha} m_{\alpha}(\alpha), \text{ where } m_{\alpha} = \sum_w m_{\alpha,w}.$$

4.3 A formula for the spectral pairs

(4.3.1) In this section we state a formula for $\text{Spp}(f)$ where f is a holomorphic germ on a \mathbf{Z} -homology surface X . The proof can be found in [46].

Let $\pi : Z \rightarrow X$ be a good resolution with exceptional divisor E , and dual graph V . The cohomology group $H^1(M; \mathbf{Q})$ of the link M of x in X has a weight filtration $0 \subset W_0 \subset W_1 = H^1(M; \mathbf{Q})$, and $\dim W_0 = b_1(V)$, $\dim W_1/W_0 = \sum 2g(E_i)$ (where $g(E_i)$ is the genus of the component E_i of E). Hence X is a rational homology surface if and only if V is connected, $b_1(V) = 0$ — V is a tree — and $g(E_i) = 0$ for all i .

Let X be a normal integral homology surface and let $x \in X$. Let $f : (X, x) \rightarrow (\mathbf{C}, 0)$ be a holomorphic germ. We can choose a good resolution $\pi : Z \rightarrow X$ such that $\pi^{-1}f^{-1}(0) = \cup_{\nu \in A \cup V} E_{\nu}$ is a divisor with normal crossings on Z . Without loss of generality we assume $V \neq \emptyset$. Let Γ be the corresponding EN-diagram. In [46], the following is stated for rational homology surfaces; we restrict ourselves to integral homology surfaces in order to stay in the realm of EN-diagrams and splicing.

(4.3.2) **Remark** Let f be a curve singularity as above. Define $\text{Spp}_*(f) = \text{Spp}(f) - (0, 1)$. Suppose $\text{Spp}_*(f) = \sum_{\alpha,w} m_{\alpha,w}(\alpha, w)$. Then it follows from the definition that:

$$\Delta_*(t) = \prod_{\alpha,w} (t - \exp(-2\pi i\alpha))^{m_{\alpha,w}},$$

and, equivalently:

$$\zeta_f(t) = \prod_{\alpha,w} (1 - t \exp(-2\pi i\alpha))^{m_{\alpha,w}}.$$

One should always remember that in the definition of the spectrum reduced cohomology is used, whereas in the definition of the zeta-function we use non-reduced cohomology.

We see that the spectrum numbers α are logarithms of the eigenvalues λ . For $\lambda \neq 1$, there are two such logarithms possible (in the range $-1 < \alpha < 1$), and the Hodge filtration decides which branch of the logarithm to use.

(4.3.3) Recall that $A(\Gamma)$ denotes the set of arrow-heads of Γ and $N(\Gamma)$ the set of other vertices. We add the notations $R(\Gamma)$ for the nodes (they correspond to the rupture points in V) and $E(\Gamma)$ for the *separating edges*, that is, the edges between two nodes (or between two arrow-heads). If all such edges are broken (cf. 1.3.5) then we obtain the splice decomposition of Γ . Recall that breaking an edge gives two arrow-heads with multiplicities (one of which could be 0).

Furthermore, denote by $S_v(\Gamma)$ the set of nearest neighbours of the node $v \in R(\Gamma)$ when Γ is embedded in the resolution graph V . For such a neighbour $w \in S_v(\Gamma)$, we can compute its multiplicity m_w as the number s_j of lemma 2.7.1.

We also use the following notations, some of which are from sections 2.2 and 2.3:

- m_v = the multiplicity of the vertex $v \in N(\Gamma)$.
- d_e = the gcd of the two multiplicities that arise when edge e is broken ($e \in E(\Gamma)$).
- d_v = the gcd of all link component multiplicities of the splice component with single central node v ($v \in R(\Gamma)$),
- d_κ = the number of components of $F \cap \partial N(K_\kappa)$, where $N(K_\kappa)$ is the boundary of a small tubular neighbourhood of component K_κ ($\kappa \in A(\Gamma)$).

Finally, for a real number u we put $\{u\}$ for the fractional part of u (satisfying $0 \leq \{u\} < 1$).

Using these notations we get for $v \in R(\Gamma)$, $e \in E(\Gamma)$ and $\kappa \in A(\Gamma)$, the following elements of the free abelian group on $\mathbf{Q} \times \mathbf{Z}$:

$$\begin{aligned}
 a_v &= \sum_{0 < s < m_v, m_v \nmid s d_v} (-1 + \sum_{w \in S_v(\Gamma)} \{s m_w / m_v\}) \cdot \\
 &\quad \cdot [(s/m_v - 1, 1) + (1 - s/m_v, 1)], \\
 b_v &= \sum_{0 < s < d_v} [(-s/d_v, 2) + (s/d_v, 0)],
 \end{aligned}$$

$$c_e = \sum_{0 < s < d_e} [(-s/d_e, 2) + (s/d_e, 0)],$$

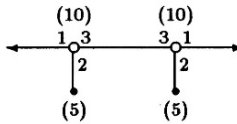
$$c'_\kappa = \sum_{0 < s < d_\kappa} (-s/d_\kappa, 2).$$

(4.3.4) Theorem *Let $f : (X, x) \rightarrow (\mathbb{C}, 0)$ be a curve singularity, defined on an integral homology normal surface. Then*

$$\text{Spp}(f) = \sum_{v \in R(\Gamma)} a_v - \sum_{v \in R(\Gamma)} b_v + \sum_{e \in E(\Gamma)} c_e + \sum_{\kappa \in A(\Gamma)} c'_\kappa + (\#A(\Gamma) - 1)(0, 1).$$

Proof. This is Theorem 2.1 of [46] written in terms of EN-diagrams instead of resolution graphs. □

(4.3.5) Example We compute the spectral pairs of A'Campo's singularity: $f(x, y) = (y^2 - x^3)(y^3 - x^2)$.



Call the left-hand node $*$ and the right-hand node \diamond . The resolution graph has only one more vertex, in between the two nodes. That vertex has multiplicity 4. We obtain:

$$a_* = a_\diamond = \left(-\frac{3}{10}, 1\right) + \left(-\frac{1}{10}, 1\right) + \left(\frac{1}{10}, 1\right) + \left(\frac{3}{10}, 1\right).$$

Since $d_* = d_\diamond = 1$, we obtain $b_* = b_\diamond = 0$; and because the only separating edge e has $d_e = 2$, we get

$$c_e = \left(-\frac{1}{2}, 2\right) + \left(\frac{1}{2}, 0\right).$$

This is an isolated singularity, hence $c' = 0$. Therefore

$$\text{Spp}(f) = \left(-\frac{1}{2}, 2\right) + 2\left(-\frac{3}{10}, 1\right) + 2\left(-\frac{1}{10}, 1\right) + (0, 1) + 2\left(\frac{1}{10}, 1\right) + 2\left(\frac{3}{10}, 1\right) + \left(\frac{1}{2}, 0\right).$$

Now consider $g(x, y) = x^p y^q$ (a $D[p, q]$ -point). Its EN-diagram has no node at all, only two arrow-heads (one of multiplicity p , the other of multiplicity q) connected by an edge e . Let $d = \text{gcd}(p, q)$. Then:

$$\text{Spp}(g) = \sum_{s=1}^{d-1} [(-s/d, 2) - (s/d, 0)] + (0, 1).$$

Compare this with $\zeta_g(t) = 1$.

4.4 Spectral pairs and the real Seifert form

(4.4.1) From now on, we will use the notation F again for the Milnor fibre $X_{f,x}$ of the curve singularity f . This will cause no confusion, since the Hodge filtration will no longer be used. Let $L : H_1(F; \mathbf{R}) \times H_1(F; \mathbf{R}) \rightarrow \mathbf{R}$ be the *real Seifert form* (its definition will become clear in a minute). In this section we will prove that the spectral pairs determine the Seifert form and vice versa. It is sufficient to prove this for the sesquilinearized Seifert form L on $H_1(F; \mathbf{C})$, and that is what we will do.

Neumann [34], [35] computed a normal form for the monodromy and L . If L is the Seifert form on $H_1(F; \mathbf{C})$, then $S = L - L^*$ is the skew hermitian intersection form on $H_1(F; \mathbf{C})$, so iS is an hermitian form. Let $H_1(F; \mathbf{C}) = \bigoplus_{\lambda} H_{\lambda}$ be the splitting of $H_1(F; \mathbf{C})$ according to the eigenvalues of the monodromy h_* . Define

$$\sigma_{\lambda}^{-} = \text{signature}(iS \mid H_{\lambda}),$$

the *equivariant signature* for the eigenvalue λ . It follows from [34] and [35] that the signatures and the Jordan normal form of the monodromy determine the Seifert form. We will show how to find the signatures from the weight 1 part of the spectral pairs. This enables us to prove that the Grima examples of singularities with the same rational monodromy [17] are distinguished by their signatures, as was conjectured by Neumann [35], §7.

In view of Theorem 4.3.4, we define the *a-part* of $\text{Spp}(f)$ to be the spectral pairs of the form $(\alpha, 1)$ — the weight one spectral pairs — with $\alpha \neq 0$.

(4.4.2) Proposition *The a-part of $\text{Spp}(f)$ determines the equivariant signatures. In fact, if we write*

$$a = \sum_{v \in R(\Gamma)} a_v = \sum n_{\alpha}(\alpha, 1),$$

then for $\lambda \neq 1$:

$$\sigma_{\lambda}^{-} = n_{\alpha} - n_{\alpha-1}$$

where α satisfies $\exp(+2\pi i\alpha) = \lambda$ and $0 < \alpha < 1$.

Observe that $\alpha - 1$ is the other logarithm of λ in the interval between -1 and 1 . One has $\sigma_{-1}^{-} = \sigma_1^{-} = 0$, see [34].

Proof. $H_1(F)$ has a weight filtration

$$W_{-2} \subset W_{-1} \subset W_0 = H_1(F),$$

dual to the weight filtration on $H^1(F)$:

$$\begin{aligned} W_{-2}H_1(F) &= W_1H^1(F)^\perp, \\ W_{-1}H_1(F) &= W_0H^1(F)^\perp. \end{aligned}$$

On $H_1(F)$ we have the monodromy operator $T = h_*$ and $N = \log T_u$. Furthermore, $W_{-2}H_1(F) = NH_1(F) \oplus \text{Ker}(j)$, where $j : H_1(F) \rightarrow H^1(F)$ induces the intersection pairing. The factor $\text{Ker}(j)$ clearly does not contribute to the equivariant signatures.

The factor $NH_1(F)$ corresponds to the 2×2 -Jordan blocks of T . Consider a 2×2 -Jordan block for the eigenvalue λ and choose a basis e_1, e_2 such that T and N are of the form

$$T = \begin{pmatrix} \lambda & 1 \\ 0 & \lambda \end{pmatrix} \text{ and } N = \begin{pmatrix} 0 & 1 \\ 0 & 0 \end{pmatrix}.$$

Then $W_{-2} = \mathbf{C}e_1$. Because N is an infinitesimal isometry, we have

$$S(e_1, e_1) = S(Ne_2, Ne_2) = -S(e_2, N^2e_2) = 0.$$

Hence on $\mathbf{C}e_1 \oplus \mathbf{C}e_2$, the matrix of iS is a 2×2 -hermitian matrix with non-zero determinant and top left entry equal to 0. So it has a positive and a negative eigenvalue. It follows that the contributions of the 2×2 -Jordan blocks are equal to 0.

Consequently, the signature of $iS | H_\lambda$ is equal to the signature of iS on $\text{Gr}_{-1}^W H_\lambda$, which by Poincaré duality will be identified with $\text{Gr}_1^W H^1(F)_\lambda$. Let ω be a holomorphic 1-form. Locally we can write $\omega = g(z)dz$ with $z = x + iy$. Then $i\omega \wedge \bar{\omega} = i|g(z)|^2 dz \wedge d\bar{z} = 2|g|^2 dx \wedge dy$. So

$$iS(\omega, \omega) = i \int_F \omega \wedge \bar{\omega} > 0.$$

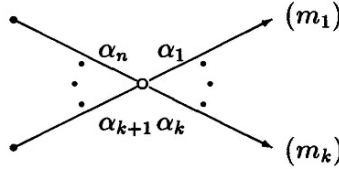
Similarly one proves that anti-holomorphic 1-forms give a negative contribution to the signature. Therefore:

$$\sigma_\lambda^- = \dim H_\lambda^{01} - \dim H_\lambda^{10},$$

which proves the proposition. \square

(4.4.3) Example We continue our previous example $f(x, y) = (y^2 - x^3)(y^3 - x^2)$. Clearly, if $\zeta = \exp(2\pi i/10)$, then $\sigma_\zeta^- = \sigma_{\zeta^3}^- = 2$ and $\sigma_{\zeta^7}^- = \sigma_{\zeta^9}^- = -2$, cf. [35], §7.

(4.4.4) **Example** Let $n \geq 3$ and let $\alpha_1, \dots, \alpha_n$ be pairwise relatively prime positive integers. Consider the EN-diagram



We encountered this EN-diagram already in lemma 2.7.1. It represents the function $f(z_1, \dots, z_n) = \prod_{i=1}^k z_i^{m_i}$, defined on the homology manifold

$$V(\alpha_1, \dots, \alpha_n) = \{z \in \mathbf{C}^n \mid \sum_{j=1}^n A_{ij} z_j^{\alpha_j} = 0 \text{ for } 1 \leq i \leq n-2\},$$

where A is a sufficiently general $(n-2) \times n$ -matrix. We can use Proposition 4.4.2 to compute the equivariant signatures of f . For a real number x , define

$$((x)) = \begin{cases} \frac{1}{2} - \{x\} & \text{if } x \notin \mathbf{Z}, \\ 0 & \text{if } x \in \mathbf{Z}. \end{cases}$$

Let $\lambda = e^{2\pi i \alpha}$ with $0 < \alpha < 1$. If α is not of the form p/m with m the multiplicity of the central node, then $\sigma_\lambda^- = 0$. So write $\alpha = p/m$ with m the multiplicity of the central node. Using lemma 2.7.1, we obtain:

$$\begin{aligned} n_{\alpha-1} &= -1 + \sum_{j=1}^n \{s_j p/m\}, \\ n_\alpha &= -1 + \sum_{j=1}^n \{s_j(m-p)/m\}. \end{aligned}$$

Observe that for $\beta \in]0, 1[$, we have $\{-\beta\} - \{\beta\} = 1 - 2\beta = 2((\beta))$. By Proposition 4.4.2, we obtain:

$$\sigma_\lambda^- = \sum_{j=1}^n \{-ps_j/m\} - \sum_{j=1}^n \{ps_j/m\} = 2 \sum_{j=1}^n ((ps_j/m)).$$

This gives an alternative proof of [35], Theorem 5.3.

We are now ready to state the main theorem of this section.

(4.4.5) **Theorem** *Giving the real Seifert form of a curve singularity defined on a homology manifold, is equivalent to giving the spectral pairs.*

Proof. In [35], Neumann showed how to compute the Seifert form from the equivariant signatures and the polynomials Δ_1 , Δ^1 and Δ' defined in section 2.3. It is also possible to retrieve these polynomials from the Seifert form, by analyzing the multiplicities of the eigenvalues.

We will show how to get the polynomials from the spectral pairs and conversely. Together with Neumann's result this proves the theorem. We use the notation $e(\alpha) = \exp(-2\pi i\alpha)$.

Let $\text{Spp}(f) = \sum_{\alpha,w} m_{\alpha,w}(\alpha, w)$ be the spectral pairs of some curve singularity f . The signatures have been computed in Proposition 4.4.2, so it suffices to give formulae for the characteristic polynomials. Let $\tilde{\Delta}_0$ be the characteristic polynomial of the monodromy on $\tilde{H}_0(F)$. Consider the rational function $\tilde{\Delta}_* = \Delta_1/\tilde{\Delta}_0$. We have seen that

$$\tilde{\Delta}_*(t) = \prod_{\alpha,w} (t - e(\alpha))^{m_{\alpha,w}}.$$

Observe that $r = m_{0,1} + 1$ is the number of branches of f . Write $m'_\alpha = m_{\alpha,2} - m_{-\alpha,0}$. Then $c' = \sum_{-1 < \alpha < 0} m'_\alpha(\alpha, 2)$ is the c' -part as in Theorem 4.3.4. Let P' be the polynomial

$$P'(t) = \prod_{-1 < \alpha < 0} (t - e(\alpha))^{m'_\alpha}.$$

There is a unique way to write P' in the following form:

$$P'(t) = \prod_{\kappa \in A} \frac{t^{d_\kappa} - 1}{t - 1}.$$

Now if $d = \gcd\{d_\kappa \mid \kappa \in A(\Gamma)\}$, then

$$\tilde{\Delta}_0(t) = \frac{t^d - 1}{t - 1},$$

and hence we obtain $\Delta_1 = \tilde{\Delta}_* \tilde{\Delta}_0$. Also, the c' -part gives us Δ' ; it is easy to check that

$$\Delta'(t) = (t^d - 1)^{-1} (t - 1)^2 \cdot \prod_{-1 < \alpha < 0} (t - e(\alpha))^{m'_\alpha}.$$

Since the roots of Δ^1 are precisely the eigenvalues of the monodromy that occur in the 2×2 -Jordan blocks, we have

$$\Delta^1(t) = \tilde{\Delta}_0(t) \prod_{0 < \alpha < 1} (t - e(\alpha))^{m_{\alpha,0}}.$$

Conversely, let the equivariant signatures σ_λ^- and the polynomials Δ_1 , Δ^1 and Δ' be given. We can obtain $\tilde{\Delta}_0$ from Δ' as we obtained it from P' above. Let b_λ , b_λ^1 , b'_λ and $b_{0,\lambda}$ be the multiplicities of λ as a root of Δ_1 , Δ^1 , Δ' and $\tilde{\Delta}_0$ respectively. It follows by straightforward computations, that

$$\text{Spp}(f) = \sum_{\alpha,w} m_{\alpha,w}(\alpha, w),$$

with

$$\begin{aligned} m_{\alpha,2} &= b'_{e(\alpha)} + b^1_{e(\alpha)} && \text{for } -1 < \alpha < 0, \\ m_{\alpha,1} &= (b_{e(\alpha)} - b'_{e(\alpha)} - 2b^1_{e(\alpha)} + \sigma_{e(\alpha)}^-)/2 && \text{for } -1 < \alpha < 0, \\ m_{0,1} &= b'_1 = r - 1 \\ m_{\alpha,1} &= (b_{e(\alpha)} - b'_{e(\alpha)} - 2b^1_{e(\alpha)} - \sigma_{e(\alpha)}^-)/2 && \text{for } 0 < \alpha < 1, \\ m_{\alpha,0} &= b^1_{e(\alpha)} - b_{0,e(\alpha)} && \text{for } 0 < \alpha < 1, \\ m_{\alpha,w} &= 0 && \text{otherwise.} \end{aligned}$$

(A similar formula for the spectrum was derived in [44].) This proves the theorem. \square

4.5 A splice formula for spectral pairs

(4.5.1) In this section we derive the splice formula for spectral pairs as presented in [46]. A splice formula for spectra has been given in [44]. We outline three of the sources of interest in this formula:

- It can be used to give a formula for the spectral pairs of a topological series of curve singularities.
- The splice formula can be used to define spectral pairs for certain non-algebraic links. This poses the question of how to interpret these spectral pairs. For instance, Proposition 4.4.2 still applies to compute the signatures.
- The counterexamples to the Spectrum and Seifert form Conjectures can be explained by the splice formula.

Before we state the theorem, we will give an illustrative example.

(4.5.2) Example In example 4.3.5, we computed the spectrum of the plane curve singularity $f(x, y) = (y^2 - x^3)(y^3 - x^2)$:

$$\text{Spp}(f) = (-\frac{1}{2}, 2) + 2(-\frac{3}{10}, 1) + 2(-\frac{1}{10}, 1) + (0, 1) + 2(\frac{1}{10}, 1) + 2(\frac{3}{10}, 1) + (\frac{1}{2}, 0).$$

In example 1.3.6, we saw that the splice decomposition of f consists of two pieces, each of which is isomorphic to the Seifert piece of the non-isolated singularity $g(x, y) = x^2(y^2 - x^3)$. We have

$$\text{Spp}(g) = \left(-\frac{1}{2}, 2\right) + \left(-\frac{3}{10}, 1\right) + \left(-\frac{1}{10}, 1\right) + (0, 1) + \left(\frac{1}{10}, 1\right) + \left(\frac{3}{10}, 1\right).$$

Notice that $\text{Spp}(g)$ contains the c' -part $\left(-\frac{1}{2}, 2\right)$. Splicing introduces a new edge, and both contributions to c' change into a contribution $\left(-\frac{1}{2}, 2\right) + \left(\frac{1}{2}, 0\right)$ to c (a new 2×2 Jordan block). This motivates our idea that $\text{Spp}_* = \text{Spp} - (0, 1)$ is *almost additive* (i.e. additive except for one small part which changes sides).

(4.5.3) Theorem [Splice formula for spectral pairs] *Let $f : (X, x) \rightarrow (\mathbb{C}, 0)$ be a curve singularity defined on a homology manifold, whose link is the result of splicing the links of the curve singularities $f_1 : (X_1, x_1) \rightarrow (\mathbb{C}, 0)$ and $f_2 : (X_2, x_2) \rightarrow (\mathbb{C}, 0)$ along components of multilink multiplicities m_1 and m_2 , in such a way that the splice and algebraicity conditions are respected. Let $\delta = \text{gcd}(m_1, m_2)$. Then*

$$\text{Spp}(f) = \text{Spp}(f_1) + \text{Spp}(f_2) - (0, 1) + \sum_{s=1}^{\delta-1} [(s/\delta, 0) - (-s/\delta, 2)].$$

Proof. Consider the EN-diagrams of f , f_1 and f_2 . By Theorem 4.3.4, it is clear that $\text{Spp}(f)$ is almost equal to $\text{Spp}(f_1) + \text{Spp}(f_2)$, except that we have to take into account that the EN-diagram of f has two arrow-heads less than the EN-diagrams of f_1 and f_2 together and one more edge instead.

Both arrow-heads κ_1 and κ_2 together give a total contribution of

$$2 \sum_{s=1}^{\delta-1} (-s/\delta, 2)$$

to $\text{Spp}(f_1) + \text{Spp}(f_2)$, whereas the new edge e contributes

$$\sum_{s=1}^{\delta-1} [(-s/\delta, 2) + (s/\delta, 0)]$$

to $\text{Spp}(f)$ — it follows directly from the definitions that $d_{\kappa_1} = d_{\kappa_2} = d_e = \text{gcd}(m_1, m_2) = \delta$.

This proves the splice formula. □

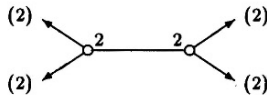
4.6 The counterexample to the Spectrum Conjecture

(4.6.1) In this section we present the counterexample to the Spectrum Conjecture. According to Theorem 4.4.5 this is also a counterexample to the conjecture about the real Seifert form. The example was found by Steenbrink and Stevens when the former visited the latter in Hamburg. In [46] it is presented alongside several other examples, each with its own special property.

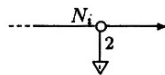
We will give the example in terms of topological series. Consider the plane curve singularity with equation

$$f(x, y) = (y^2 - x^4)^2(y^4 - x^2)^2.$$

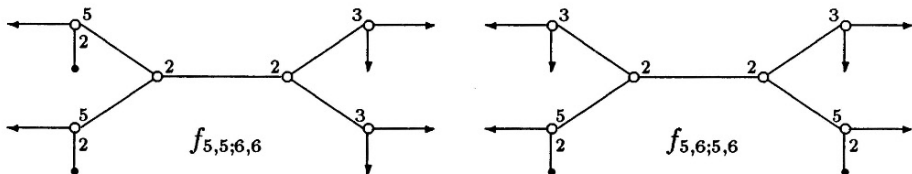
Its EN-diagram is



It has four double components. A typical element $f_{N_1, N_2; N_3, N_4}$ of its topological series has an EN-diagram which can be obtained by replacing each of the four arrows by



with $N_i > 4$ ($1 \leq i \leq 4$). Recall that such an extension has two arrows if N_i is even and one if N_i is odd; and that the multiplicity of the node is determined by $N_i + c_i$. But $c_i = 8$ for each $1 \leq i \leq 4$. From Theorem 4.3.4 or the splice formula, it is clear that the spectral pairs are the same for all permutations of $\{N_1, \dots, N_4\}$, but we can have more than one topological type. For instance, $f_{5,5,6,6}$ and $f_{5,6,5,6}$ have the same spectral pairs (and hence the same signatures) but different topological types.



(4.6.2) The same example also produces an example of functions with the same spectrum, but different spectral pairs. Observe that above also the special case $N_i = 4$ is allowed. This gives two arrows attached directly to one of the

nodes. The functions $f_{4,4;5,5}$ and $f_{4,5;4,5}$ clearly have the same spectrum but different spectral pairs: the first has pairs $(-\frac{1}{2}, 2)$ and $(\frac{1}{2}, 0)$ and the second has $(-\frac{1}{2}, 1)$ and $(\frac{1}{2}, 1)$ instead, cf. [46], Example 5.4.1.

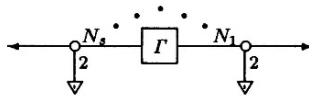
(4.6.3) Other examples of functions with the same spectral pairs but different topological type in [46] include functions with two branches and functions with the same integral monodromy. On the other hand, it is proved that the Grima examples [17] of plane curve singularities with the same rational monodromy are distinguished by their spectral pairs — in fact even by their signatures as was conjectured by Neumann [35].

Also the examples of Michel and Weber [30] of functions with the same integral monodromy are distinguished by their spectral pairs, since they are quasi-homogeneous (the spectrum of a quasi-homogeneous isolated singularity determines the weights, not only for curves, cf. [46]).

4.7 The spectral pairs within a topological series

(4.7.1) The splice formula allows us to give a formula for the spectral pairs within a topological series. We will do this in the case that we have only double components, since then we can be more explicit. As we have seen, the special case $N = N_0$ which does not formally belong to the series, but is often counted as such, causes trouble for the spectral pairs. The spectrum does not notice the difficulties.

Let f be a non-isolated singularity with only double components. Recall that according to Theorem 3.3.2, a typical element of its series has EN-diagram



where $N = (N_1, \dots, N_s) > (N_{01}, \dots, N_{0s})$ (we define N_{0i} and c_i as usual, cf. 3.5).

(4.7.2) Proposition Write for $i \leq s$: $\gamma_i = 0$ if c_i is even and $\gamma_i = \frac{1}{2}$ if c_i is odd. Let $\nu_i = N_i + c_i$. Then:

$$\text{Sp}(f_N) = \text{Sp}(f) + \sum_{i=1}^s \sum_{j=1}^{\nu_i-1} \left(\frac{1}{2} - \frac{\gamma_i + j}{\nu_i} \right).$$

Proof. One can work out the various cases using the splice formula. It is also possible to use the proof of [56], Theorem 4.5, which is valid in our situation.

□

(4.7.3) Remark The proposition is a generalization of Corollary 3.5.1. One can generalize further to spectral pairs. Almost all spectrum numbers that are added, have weight 1; only $(-\frac{1}{2})$ and $(\frac{1}{2})$, if present, have weight 2 and 0 respectively. The proposition as stated is also valid if $N_i = N_{0i}$ for some i .

CHAPTER 5

Deformations of plane curves singularities

5.1 Introduction

We consider non-zero holomorphic function germs $f : (\mathbb{C}^2, 0) \rightarrow (\mathbb{C}, 0)$ and certain deformations. The programme follows the established path laid by work of R. Pellikaan and T. de Jong. In his thesis [36], Pellikaan developed the deformation theory for application in the case of singularities of arbitrary dimensions with a one-dimensional singular locus and transversal type A_1 . De Jong [19] considered the case that the singular locus is a smooth curve but with more complicated transversal types. In later versions, Pellikaan stated his results more generally ([37], [38]), and we can obtain our key results by an easy and straightforward application of his theorems.

Our study is, however, in a sense transverse to that of Pellikaan, since we consider arbitrary transversal types but only in the plane curve case.

We start by defining the Jacobi number $j_I(f) = \dim_{\mathbb{C}} I/J_f$ (where I is the ideal defining the singular locus Σ and J_f the Jacobi ideal) and prove that finite Jacobi number is equivalent to finite I -codimension and to f having prescribed transversal singularities along the branches of the singular locus. For f with finite Jacobi number we consider deformations and count the number of special points in such a deformation. We prove that $j_I(f)$ in fact equals the Milnor number of the associated reduced singularity f_R .

We carry on by following Siersma [49], in order to express the Milnor number $\mu(f)$ in the number of special points. This generalizes results of Siersma and De Jong (in the plane curve case). The answer is the following: Let Σ^k be the reduced curve whose branches are the branches of the singular locus of f where f has transversal type A_{k-1} . Let $\#D[p, q]$ be the number of points in a deformation f_t of f which makes each Σ^k smooth, where, in local coordinates, the singularity of f_t is $x^p y^q$. Let d be the number of connected components of

the Milnor fibre. Then:

$$\mu(f) = \sum_{p < q} (p + q - 1) \cdot \#D[p, q] + \#D[1, 1] + \sum_k (k - 1)(\mu(\Sigma^k) - 1) + d - 1.$$

This work answers a question of Dirk Siersma, who asked how the Jacobi and Milnor numbers of an arbitrary plane curve singularity could be expressed in the number of “ p, q -points”, in other words: to get the plane curve case over and done with.

(5.1.1) Notation By $Z(I)$ we denote the analytic space defined by the vanishing of the elements of the ideal I of \mathcal{O} .

5.2 Invariants

(5.2.1) Recall the following notations: $\mathcal{O} = \mathbf{C}\{x, y\}$, \mathfrak{m} is its maximal ideal. We call the elements of \mathcal{O} (*plane*) *curve singularities*.

We denote by $\text{Sing}(f)$ the singular set of an analytic function germ $f \in \mathcal{O}$. If $C \subset \text{Sing}(f)$ is one-dimensional, then f is of *transversal type* A_{m-1} along C if for all $c \in C$ we can find local coordinates u, v in a neighbourhood of c such that $f(u, v) = v^m$. The name comes from the fact that on a transversal slice X the zero-dimensional singularity $f : (X, c) \rightarrow \mathbf{C}$ is of type A_{m-1} .

(5.2.2) Definition Let $p \geq 0, q \geq 1$ be integers. A germ of an analytic function $f : (\mathbf{C}^2, 0) \rightarrow (\mathbf{C}, 0)$ is said to be of *type* $D[p, q]$ if there are local coordinates x, y such that $f(x, y) = x^p y^q$. A function germ of type $D[p, p]$ is also called of type $A[p]$. We will also use Siersma’s notations, such as $A_\infty = D[0, 2]$ and $D_\infty = D[1, 2]$. Note that $D[p, q] = D[q, p]$.

(5.2.3) Let $I \subset \mathcal{O} = \mathbf{C}\{x, y\}$ be an ideal. Then we define the *primitive ideal* $fI = \{f \in \mathcal{O} \mid (f) + J_f \subset I\}$. Here J_f is the Jacobi ideal of f , generated by the partial derivatives. This definition is due to Pellikaan.

Suppose $I = (g')\mathcal{O}$ and let $g' = g_1^{m_1-1} \cdots g_r^{m_r-1}$, where $m_i \geq 2$, be the decomposition of g in irreducible factors. Then it is easy to see that $fI = (g_1^{m_1} \cdots g_r^{m_r})$, cf. [36] 1.7.

Let \mathcal{D} be the group of local analytic isomorphisms $\psi : (\mathbf{C}^2, 0) \rightarrow (\mathbf{C}^2, 0)$. For an ideal I we define: $\mathcal{D}_I = \{\psi \in \mathcal{D} \mid \psi^*(I) = I\}$.

(5.2.4) In the sequel we will always have the following situation:

- (a) $I = (g_1^{m_1-1} \cdots g_r^{m_r-1})\mathcal{O}$ with g_i irreducible, $m_i \geq 2$ ($1 \leq i \leq r$), and g_i and g_j having no common factor ($i \neq j$).

- (b) $fI = g\mathcal{O} = (g_1^{m_1} \cdots g_r^{m_r})\mathcal{O}$.
 (c) $\Sigma_i = Z(g_i)$, $\Sigma = \Sigma_1 \cup \cdots \cup \Sigma_r$.

If $f \in fI$ then $\Sigma \subset \text{Sing}(f)$. We are looking for conditions on f such that $\text{Sing}(f) = \Sigma$ and f has transversal type A_{m_i-1} along $\Sigma_i \setminus \{0\}$. It will prove useful to give $(\Sigma, 0)$ the (possibly non-reduced) analytic structure of I . Observe that in this case $\mathcal{D}_I = \mathcal{D}_{fI}$.

We have a right action of \mathcal{D}_I on fI and hence for all $f \in fI$ we have $\text{Orb}_I(f) \subset fI$. Consider the tangent space $T\mathcal{D}_I$ of \mathcal{D}_I at the identity. Observe that $T\mathcal{D}_I$ is a subset of $T\mathcal{D}$, the tangent space of \mathcal{D} at the identity. We identify $T\mathcal{D}$ with $\mathfrak{m}\Theta$, the germs of vector fields vanishing at the origin.

According to [36], p. 19 we have $T\mathcal{D}_I = \{\xi \in \mathfrak{m}\Theta \mid \xi(I) \subset I\}$.

(5.2.5) Definition Let $f \in fI$. Then we define $c_I(f) = \dim_{\mathbb{C}} fI/T\mathcal{D}_I(f)$, where $T\mathcal{D}_I(f) = \{\xi(f) \mid \xi \in T\mathcal{D}_I\}$. $c_I(f)$ is called the I -codimension of f .

Suppose $I = (y^{m-1})$. Then one easily sees that $c_I(f) = 0$ if and only if $fI = (f)$, i.e. f has transversal A_{m-1} singularities along $\text{Sing}(f)$; and $c_I(f) = 1$ if and only if f is of type $D[1, m]$.

We now state some standard finite determinacy results (cf. [48]). If \mathfrak{a} is an ideal in \mathcal{O} and $k \in \mathbb{N}$, then $f \in \mathfrak{a}$ is called k -determined in \mathfrak{a} if $f + \mathfrak{m}^k \mathfrak{a} \subset \text{Orb}_{\mathfrak{a}}(f)$.

(5.2.6) Theorem Let $f \in fI$. Then:

- (a) If f is k -determined in fI then $fI \cdot \mathfrak{m}^k \subset T\mathcal{D}_I(f) + fI \cdot \mathfrak{m}^{k+1}$.
 (b) If $fI \cdot \mathfrak{m}^k \subset \mathfrak{m}T\mathcal{D}_I(f)$, then f is k -determined in fI .

The proof is standard (cf. [48], [37]). □

(5.2.7) Corollary $c_I(f) < \infty$ if and only if f is k -determined for some $k \in \mathbb{N}$. Furthermore, if $c_I(f) < \infty$ then $\text{Sing}(f) = \Sigma$.

Proof. The first statement is obvious. Now suppose $c_I(f) < \infty$, so there is a k such that $fI \cdot \mathfrak{m}^k \subset T\mathcal{D}_I(f)$. Because $T\mathcal{D}_I(f) \subset \mathfrak{m}J_f \cap fI$, it follows that $Z(J_f) \cup \Sigma \subset \Sigma$, hence $\text{Sing}(f) = \Sigma$. □

(5.2.8) Definition Let I be as above. Then we define $j_I(f) = \dim_{\mathbb{C}} I/J_f$. We call $j_I(f)$ the *Jacobi number* of f .

The Jacobi number plays the same rôle as the Milnor number in the case of isolated singularities. Since $\dim_{\mathbb{C}} \mathcal{O}/J_f$ is infinite, we look at other quotients and it appears that I/J_f is the right choice.

(5.2.9) Example If $I = (y^{m-1})$ and $f(x, y) = y^m$ then $j_I(f) = 0$. If f is of type $D[p, q]$, then choose coordinates for which $f(x, y) = x^p y^q$. Let $I = (x^{p-1} y^{q-1})$. Then $j_I(f) = 1$.

Later we will show that the Jacobi number equals the Milnor number of the reduced singularity associated to f . This fact seems to have been unnoticed before and it is definitely false in higher dimensions.

(5.2.10) Proposition *Let $f \in fI$ and suppose $j_I(f) < \infty$ and $\text{depth}(\mathcal{O}/I) > 0$. Then:*

- (a) $T\mathcal{D}_I(f) = \mathfrak{m}J_f \cap fI$ ($\mathfrak{m}J_f = T\mathcal{D}(f)$),
- (b) $c_I(f) < \infty$.

Proof. This is Proposition 5.3 of [37]. The number $c_{I,e}(f) = \dim_{\mathbb{C}} fI/(J_f \cap fI)$ is also considered by Pellikaan. It is clear that $c_{I,e}(f) \leq c_I(f)$. In Proposition 5.3 of [37] it is in fact proved that $c_{I,e}(f) \leq j_I(f)$. But $c_I(f)$ is finite if $c_{I,e}(f)$ is finite, because the quotient $M = (J_f \cap fI)/(\mathfrak{m}J_f \cap fI)$ is a finitely generated \mathcal{O} -module and $\mathfrak{m}(J_f \cap fI) \subset T\mathcal{D}_I(f) = \mathfrak{m}J_f \cap fI$, so $\mathfrak{m}M = (0)$ and $\dim_{\mathbb{C}} M < \infty$. \square

This shows that $c_I(f)$ is an invariant of the right-equivalence class of f .

(5.2.11) Theorem *Let $f \in fI$. The following statements are equivalent:*

- (i) $j_I(f) < \infty$,
- (ii) $c_I(f) < \infty$,
- (iii) f is a singularity with singular locus $\Sigma = \Sigma_1 \cup \dots \cup \Sigma_r$ and transversal type A_{m_i-1} along $\Sigma_i \setminus \{0\}$ ($1 \leq i \leq r$).

Proof. (i) \Rightarrow (ii): Proposition 5.2.10.

(ii) \Rightarrow (iii): In Corollary 5.2.7 it has been observed that $\text{Sing}(f) = \Sigma$. We consider the sheaf \mathcal{O} of analytic functions on a small neighbourhood V of the origin (for $a \in V$ the stalk at a is \mathcal{O}_a). We have ideal sheaves \mathcal{I} , $f\mathcal{I}$ and \mathcal{J}_f with the obvious meanings. Let $\mathcal{F} = f\mathcal{I}/(\mathcal{J}_f \cap f\mathcal{I})$. Then \mathcal{F} is a coherent sheaf of \mathcal{O} -modules. Now because $c_I(f)$ is finite and $\dim_{\mathbb{C}} \mathcal{F}_0 = c_{I,e}(f)$, we can choose V such that $\dim_{\mathbb{C}} \mathcal{F}_a = 0$ for $a \in V \setminus \{0\}$ (\mathcal{F} is concentrated in a finite set of points). Look at a point $a \in \Sigma_i \setminus \{0\}$. (Σ_i, a) is defined by $(g_i^{m_i-1})$ and g_i can be used as one of the local coordinates near a . From the remark following definition 5.2.5 it follows that f has only transversal A_{m_i-1} singularities along $\Sigma_i \setminus \{0\}$ ($1 \leq i \leq r$).

(iii) \Rightarrow (i): According to example 5.2.9 the stalk of $\mathcal{I}/\mathcal{J}_f$ at $a \in V \setminus \{0\}$ is

(0) if we choose V sufficiently small. So $\mathcal{I}/\mathcal{J}_f$ is concentrated in a finite set of points and therefore we obtain that $j_I(f)$, the dimension of the stalk at the origin, is finite. \square

5.3 Deformations

(5.3.1) Deformations of isolated singularities are thoroughly studied. They are used to split up the complicated isolated singularity into a number of simple singularities which are better understood, and in this case it is well-known that it splits up into A_1 or *Morse* singularities (in our notation: $D[1, 1]$ singularities) and that their number is the Milnor number μ of the singularity.

In this section we will consider deformations of a non-isolated plane curve singularity f . In such a deformation, it is important to describe what happens to the singular set of f , because we want to recover various properties of f in the deformation (e.g. we would like that the Milnor fibrations of f and the deformed f_t are equivalent, cf. lemma 5.4.8). A theorem of Pellikaan is invoked to show that $j_I(f)$ is invariant under deformations.

We will consider two kinds of deformations in more detail and compute the number of special points (critical points) in such a deformation. In the next section we will use these two types to obtain two formulae for the Milnor number. The two special kinds are examples of deformations where the singularities of f split up into $D[p, q]$ singularities only. There are many other possible deformations, giving similar formulae for the Milnor number.

Our reference for this section is [38].

(5.3.2) Definition Let $I = (g_1^{m_1-1} \dots g_r^{m_r-1})$ define $(\Sigma, 0)$ as before.

- (a) We define $E_I = \{m_1, \dots, m_r\}$.
- (b) For $p \in E_I$, let Σ^p be the *reduced* curve defined by the product of all g_i such that $m_i = p$. We call Σ^p the *p-part* of Σ .
- (c) Let $f \in \mathcal{I}$ with $j_I(f) < \infty$. By Theorem 5.2.11 we can write

$$f = \prod_{p \in E_I \cup \{1\}} f_{(p)}^p.$$

For $p, q \in E_I \cup \{1\}$, $p \neq q$, we define $d_{p,q}(f) = \dim_{\mathbb{C}} \mathcal{O}/(f_{(p)}, f_{(q)})$, and for other p, q we put $d_{p,q}(f) = 0$.

It will appear in the next section that for $p \neq q$ the number $d_{p,q}$ is the number of $D[p, q]$ -points in a deformation. Notice that if $p, q > 1$, $d_{p,q} = \Sigma^p \cdot \Sigma^q$ (intersection number).

(5.3.3) The following definitions come from Pellikaan [38]. We think of Σ and I being as before, but for the definitions this is not important. Let $(\Sigma, 0)$ be a germ of an analytic space defined by the ideal I in \mathcal{O} . A *deformation* of $(\Sigma, 0)$ consists of a germ of a flat map $G : (\mathcal{X}, 0) \rightarrow (S, 0)$ of analytic spaces, together with an embedding $i : (\Sigma, 0) \rightarrow (\mathcal{X}, 0)$ such that $(i(\Sigma), 0) \cong (G^{-1}(0), 0)$ as analytic spaces. We can embed $(S, 0)$ in $(\mathbf{C}^\sigma, 0)$ and $(\mathcal{X}, 0)$ in $(\mathbf{C}^2 \times \mathbf{C}^\sigma, 0)$ such that the following diagram commutes:

$$\begin{array}{ccccc} (\Sigma, 0) & \xrightarrow{i} & (\mathcal{X}, 0) & \xrightarrow{G} & (S, 0) \\ \downarrow & & \downarrow & & \downarrow \\ (\mathbf{C}^2, 0) & \xrightarrow{j} & (\mathbf{C}^2 \times \mathbf{C}^\sigma, 0) & \xrightarrow{\pi} & (\mathbf{C}^\sigma, 0) \end{array}$$

where $j(z) = (z, 0)$ and π is the projection on the second factor. Let $\tilde{\mathcal{O}}$ be the local ring of germs of analytic functions on $(\mathbf{C}^2 \times S, 0)$. Let \tilde{I} be the ideal in $\tilde{\mathcal{O}}$ defining the germ $(\mathcal{X}, 0)$ considered as a subspace of $(\mathbf{C}^2 \times S, 0)$.

(5.3.4) **Definition** Let $(\Sigma, 0)$ be a germ of an analytic space in $(\mathbf{C}^2, 0)$ defined by I and $G : \mathcal{X} \rightarrow S$ a deformation of Σ . Let $f : (\mathbf{C}^2, 0) \rightarrow (\mathbf{C}, 0)$ be a germ of an analytic function such that $f \in fI$. Let $F : (\mathbf{C}^2 \times S, 0) \rightarrow (\mathbf{C}, 0)$ be a germ of an analytic map. Then (F, G) is called a *deformation* of $(f, \Sigma, 0)$ if $F(x, y, 0) = f(x, y)$ and

$$(F)\tilde{\mathcal{O}} + J_F \subset \tilde{I}$$

where $J_F = (\frac{\partial F}{\partial x}, \frac{\partial F}{\partial y})\tilde{\mathcal{O}}$ and x, y are local coordinates.

For example one could consider deformations of $(f, \Sigma, 0)$ with Σ fixed, as in [36] and [50]. We will not do this, because such a deformation only gives information about the $D[1, p]$ -points.

If the context is clear, then we say that F is a deformation of $(f, \Sigma, 0)$, or even that F is a deformation of f .

(5.3.5) Let $I = (g_1^{m_1-1} \dots g_r^{m_r-1})$, $fI = (g_1^{m_1} \dots g_r^{m_r})$ and $f \in fI$ as before. From now on we assume $j_I(f) < \infty$.

The first kind of deformation we consider, will be one with as much crossings as possible. It will be called a *network map* type of deformation¹.

Such a deformation arises as follows: First look at the *reduced* singularity f_R . This singularity can be deformed in such a way that it has only normal crossings and their number is δ , the virtual number of double points. An

¹We specifically think of the London Underground network map designed by Harry Beck in 1933.

explicit construction, involving small translations of the branches in the resolution, was first given by A'Campo [1] and by Gusein-Sade [6]. We now have a network map deformation $(f_R)_t$ of f_R , and get one for f by giving the branches of $(f_R)_t$ the correct multiplicities of f .

Write $f = g_1^{m_1} \cdots g_r^{m_r} h_{r+1} \cdots h_s$. Let the network map deformation of

$$f_R = g_1 \cdots g_r h_{r+1} \cdots h_s$$

be $F_R : (\mathbf{C}^2 \times \mathbf{C}^\sigma, 0) \rightarrow (\mathbf{C} \times \mathbf{C}^\sigma, 0)$. We may assume that we can write

$$F_R(z, t) = (G_1(z, t) \cdots G_r(z, t) H_{r+1}(z, t) \cdots H_s(z, t), t),$$

where the G_i and the H_i describe what happens to the branches of f_R (this is possible in the construction of A'Campo and Gusein-Sade), and $z = (x, y)$. Now let

$$F(z, t) = G_1(z, t)^{m_1} \cdots G_r(z, t)^{m_r} H_{r+1}(z, t) \cdots H_s(z, t)$$

and

$$G(z, t) = (G_1(z, t)^{m_1-1} \cdots G_r(z, t)^{m_r-1}, t).$$

Then (F, G) is a deformation of $(f, \Sigma, 0)$ and we say that (F, G) is a *network map type deformation* of f .

(5.3.6) The second type of deformation will be a deformation of $(f, \Sigma, 0)$ which makes each of the p -parts Σ^p of the singular locus Σ smooth. Recall that we consider $(\Sigma^p, 0)$ ($p \in E = E_I$) as a reduced curve. There exists a versal deformation $G_p : (\mathbf{C}^2 \times \mathbf{C}^{\sigma_p}, 0) \rightarrow (\mathbf{C} \times \mathbf{C}^{\sigma_p}, 0)$ of $(\Sigma^p, 0)$ with $G_p(z, t_p) = (G_{p1}(z, t_p), t_p)$. Let $\sigma = \sum_{p \in E} \sigma_p$. By $t = (t_p)_{p \in E}$ we denote local coordinates on \mathbf{C}^σ . Let

$$G(z, t) = \left(\prod_{p \in E_I} G_{p1}(z, t_p)^{p-1}, t \right);$$

then G defines a deformation of Σ . Furthermore, write $f = g_1^{m_1} \cdots g_r^{m_r} h$ and define $F : (\mathbf{C}^2 \times \mathbf{C}^\sigma \times \mathbf{C}^3, 0) \rightarrow (\mathbf{C}, 0)$ by

$$F(z, t, a, b, c) = \prod_{p \in E_I} G_{p1}(z, t)^p (h(z) + a + bx + cy).$$

Then (F, G) defines a deformation of $(f, \Sigma, 0)$, a *deformation which makes the p -parts smooth*.

The next theorem is an important result due to Pellikaan. In [38] it is proved as a part of a larger theorem.

(5.3.7) Theorem *Let $I, f \in \mathcal{I}$, and Σ be as before and $j_I(f) < \infty$. Let $G : (\mathcal{X}, 0) \rightarrow (S, 0)$ be a deformation of $(\Sigma, 0)$ with non-singular base $(S, 0)$ and let (F, G) be a deformation of $(f, \Sigma, 0)$. Let $\pi : (\mathbb{C}^2 \times S, 0) \rightarrow (S, 0)$ be the projection. Then there exist representatives for all considered germs such that for all $t \in S$*

$$j_I(f) = \sum_{a \in \pi^{-1}(t)} j(f_t, a).$$

So the Jacobi number is invariant under deformations. \square

The following theorems show that in our type of deformations, the number of special points is finite. We omit their straightforward but somewhat tedious proofs, which are analogous to the proofs of Propositions 7.18 and 7.20 of [36].

(5.3.8) Theorem *Let $I, f \in \mathcal{I}$, and Σ be as before and $j_I(f) < \infty$. Suppose $F : (\mathbb{C}^2 \times S, 0) \rightarrow (\mathbb{C}, 0)$ is a network map type deformation of $(f, \Sigma, 0)$, where $S = \mathbb{C}^\sigma$. Then there is a dense subset $V \subset S$ and an open neighbourhood U of $0 \in \mathbb{C}^2$ such that for all $t \in V$ sufficiently small:*

- (a) $f_t^{-1}(0)$ has only normal crossings, and their number equals $\delta(f_R)$, the virtual number of double points of the reduced germ f_R ,
- (b) f_t has only A_1 singularities in $U \setminus \Sigma_t$,
- (c) for $0 < p < q$, f_t has only $D[p, q]$ singularities on $\Sigma_t^q \cap U$, and their number is $d_{p,q}(f)$,
- (d) f_t has only $D[0, q]$ and a finite number of $D[q, q]$ singularities on the rest of $\Sigma_t^q \cap U$. \square

(5.3.9) Corollary $j_I(f) = \mu(f_R)$, i.e. the Jacobi number $j_I(f)$ equals the Milnor number $\mu(f_R)$ of the reduced singularity f_R .

Proof. A network map type deformation of f arises from a deformation of the same kind. It is well-known that $\mu(f_R)$ equals $\delta + \#A_1$, where δ is the number of crossing points and $\#A_1$ the number of A_1 singularities outside the zero-locus. By construction, the deformation of f has δ $D[p, q]$ crossing points. But it is also not difficult to see that there are as many A_1 -points outside the zero locus as there are outside the zero locus in the deformation of f_R .

By Theorem 5.3.7 it now follows that $j_I(f) = \mu(f_R)$, for we know that the Jacobi number of all $D[p, q]$ singularities is 1. \square

(5.3.10) Remark The Jacobi number being equal to the Milnor number of the reduced singularity gives interesting interpretations to several of the formulae to be found in Pellikaan's work. For instance, from [36], 5.14, it follows

that for an isolated plane curve singularity, the difference of the Milnor and Tjurina numbers $\mu(f) - \tau(f)$ equals the extended codimension $c_{I,e}(f^2)$.

(5.3.11) Theorem *We use the same notations, $j_I(f) < \infty$. Suppose F is a deformation of $(f, \Sigma, 0)$ which makes the p -parts smooth. Then there exists a dense subset $V \subset S$ and an open neighbourhood U of $0 \in \mathbf{C}^2$, such that for all $t \in V$ sufficiently small:*

- (a) Σ_t^p is smooth for each $p \in E_I$,
- (b) f_t has only A_1 singularities in $U \setminus \Sigma_t$,
- (c) for $0 < p < q$, f_t has only $D[p, q]$ singularities on $\Sigma_t^q \cap U$ and their number is $d_{p,q}(f)$,
- (d) f_t has only $D[0, q]$ singularities on the rest of $\Sigma_t^q \cap U$. □

5.4 $D[p, q]$ -points and the Milnor number

(5.4.1) From now on, we will write F for the Milnor fibre of f , whereas f_t will denote a deformation of $(f, \Sigma, 0)$, with $\Sigma = \text{Sing}(f)$, which is a network map deformation or a deformation which makes the p -parts smooth. The decomposition of f into irreducible factors is

$$f = f_1^{m_1} \cdots f_r^{m_r} f_{r+1} \cdots f_s,$$

where $r \geq 1$, $s \geq r$ and $m_i \geq 2$ ($1 \leq i \leq r$). We put $m_{r+1} = \cdots = m_s = 1$. F will denote the Milnor fibre of f .

A $D[p, q]$ -point of f_t is a point where f_t has a local singularity of type $D[p, q]$. We ignore $D[0, q]$ -points. Denote the number of $D[p, q]$ -points of f_t by $\#D[p, q]$, the number of $D[p, q]$ -points on $f_t^{-1}(0)$ by $\#D^0[p, q]$. We assume that for $(p, q) \neq (1, 1)$ all $D[p, q]$ -points are in fact situated on $f_t^{-1}(0)$.

We will express the Milnor number μ , which is the dimension of $H_1(F; \mathbf{Z})$, in the number of $D[p, q]$ -points of f_t . Put $d = \dim H_0(F; \mathbf{Z})$ (the number of connected components); d equals $\gcd(m_1, \dots, m_s)$. In this section, the singular locus has its *reduced* structure, i.e. it is defined by $(f_1 \cdots f_r)$. This is important, as $\mu(\Sigma)$, the Milnor number of Σ , will come in.

(5.4.2) Our formulae will generalize various known formulae for the Milnor number, which are, however, often valid for all dimensions. Some of them are outlined below.

- (i) In the case of *isolated singularities*, where $m_1 = \dots = m_s = 1$, we have the well-known

$$\mu = 2\delta - s + 1,$$

see [9]. The number δ is the virtual number of double points and equals the maximum of $\#D^0[1, 1]$ over all deformations of f . Another formula is

$$\mu = \#D[1, 1],$$

as used for instance in the method of A'Campo and Gusein-Sade [6].

- (ii) In the case of *transversal type* A_1 , where $m_1 = \dots = m_r = 2$ we have the formulae of Siersma:

$$\mu = 2\#D[1, 2] + \#D[1, 1] - \mu(\Sigma) + d - 2,$$

if Σ is deformed in such a way that it becomes *smooth*, see [49]; and:

$$\mu = 2\#D[1, 2] + \#D[1, 1] - 2\mu(\Sigma) - 1,$$

if $\#D[1, 2] > 0$ and Σ remains *fixed* under the deformation ([50]).

- (iii) In the case that Σ is a *non-singular curve and the transversal type is* A_{q-1} (e.g. $f = y^q f_2 \dots f_s$):

$$\mu = q\#D[1, q] + \#D[1, 1] - q + 1,$$

see De Jong [19].

Below, we state two formulae for the Milnor number of f , one for each of the special types of deformations that we consider. The first of them, which is known, we give for the sake of completeness. Then we give some examples of the computation of the Milnor number using our formulae. After that, we give the proofs. Recall that d is the number of connected components of the Milnor fibre F .

(5.4.3) Theorem (Formula 1) *Let f_t be a network type deformation of f . Then:*

$$\mu(f) = \sum (p + q) \cdot \#D^0[p, q] - S + d$$

where the sum runs over all $D[p, q]$ -points on $f_t^{-1}(0)$ with $p \leq q$, and $S = \sum_{i=1}^s m_i$, the number of branches counted with multiplicities.

(5.4.4) Theorem (Formula 2) Let f_t be a deformation which makes the p -parts Σ^p smooth. Then

$$\begin{aligned} \mu(f) = & \sum_{p < q} (p + q - 1) \cdot \#D[p, q] + \#D[1, 1] + \\ & + \sum_k (k - 1)(\mu(\Sigma^k) - 1) + d - 1, \end{aligned}$$

the first summation over the $D[p, q]$ -points with $p < q$, the second summation over all $k \in \{m_1, \dots, m_r\}$.

(5.4.5) Example We compute the Milnor number in four cases.

- (i) $f(x, y) = x^p y^q$. Then $d = \gcd(p, q)$, $\mu(\Sigma^p) = \mu(\Sigma^q) = 0$, and $\#D[p, q] = 1$. Both formulae give $\mu = d$.
- (ii) $f(x, y) = x^p y^q (x + y)$ with $1 \leq p < q$. Then $d = 1$, $\mu(\Sigma^p) = \mu(\Sigma^q) = 0$ and $\#D[p, q] = \#D[1, p] = \#D[1, q] = \#D[1, 1] = 1$. See figure 5.1. Both formulae give $\mu = p + q + 2$.

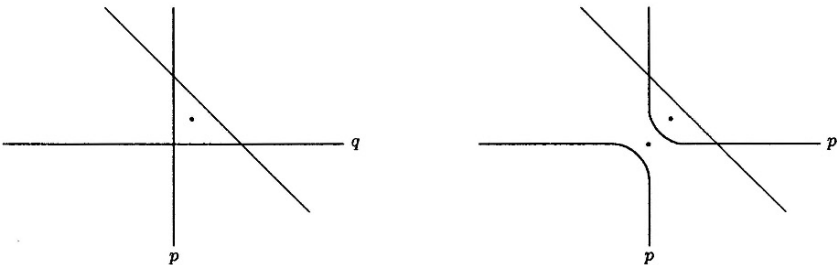


Figure 5.1: (ii), (iii) deformation 1; and (iii) deformation 2.

- (iii) $f(x, y) = x^p y^p (x + y)$ with $p > 1$. Then $d = 1$ and $\mu(\Sigma) = 1$. See figure 5.1.
 - Formula 1 only works with deformation 1 and gives: $\mu = 2p + 2$ (see (ii)).
 - Formula 2 only works with deformation 2 and gives the same result: $\mu = p\#D[1, p] + \#A_1 + (p - 1)(\mu(\Sigma) - 1) = 2p + 2$.
- (iv) $f(x, y) = (y^2 - x^3)^p (y^3 - x^2)^q$, with $p < q$. Then $d = \gcd(p, q)$, $\mu(\Sigma^p) = \mu(\Sigma^q) = 2$ and $\#D[p, q] = 4$. See figure 5.2.

- Formula 1 only works with deformation 1 and gives: $\mu = 5p + 5q + d$, because $\#D[p, p] = \#D[q, q] = 1$.
- Formula 2 only works with deformation 2 and gives: $\mu = 5p + 5q + d$, because $\#D[1, 1] = 7$.

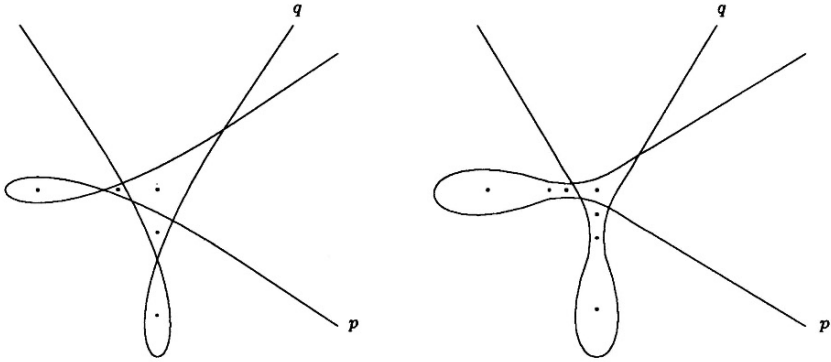


Figure 5.2: (iv) deformations 1 and 2.

(5.4.6) *Proof [of Theorem 5.4.3].* Near Σ_i the Milnor fibre is a m_i -sheeted covering of the zero locus $X = f_t^{-1}(0)$, except in the multiple points. So start with S copies of the disc D^2 , and cover the i^{th} branch with m_i copies. If for each $D[p, q]$ -point, we remove $p + q$ small discs and replace them by $\gcd(p, q)$ small annuli (the local Milnor fibre of type $D[p, q]$), we obtain the Milnor fibre F . So the Euler-Poincaré characteristic of F is clearly

$$\chi(F) = S - \sum_{p,q} (p + q) \cdot \#D^0[p, q].$$

Since F has d connected components, we obtain

$$\mu(f) = \sum_{p,q} (p + q) \cdot \#D^0[p, q] - S + d.$$

This proves the theorem. □

(5.4.7) The proof of Theorem 5.4.4 (Formula 2) requires more work; we will follow Siersma [49]. We have to start with some definitions and lemmas. In the following, f_t will be a deformation of $(f, \Sigma, 0)$ which makes the p -parts smooth and the notations are as in the theorem.

We write $X = f_t^{-1}(0)$. Let ε_0 be an admissible radius for the Milnor fibration, i.e. a positive number with the property that for all $\varepsilon \in [0, \varepsilon_0]$, $X \pitchfork \partial B_\varepsilon$ as stratified set. For each admissible $\varepsilon > 0$ there exists a $\delta_\varepsilon > 0$ such that $f^{-1}(u) \pitchfork \partial B_\varepsilon$ for all $|u| < \delta_\varepsilon$. Fix $\varepsilon \leq \varepsilon_0$ and $\delta \leq \delta_\varepsilon$, and let D be the disc of radius δ . Put $X_D = f^{-1}(D) \cap B_\varepsilon$ and $X_{D,t} = f_t^{-1}(D) \cap B_\varepsilon$. Consider $f : X_D \rightarrow D$ and $f_t : X_{D,t} \rightarrow D$.

(5.4.8) Lemma *For t and δ sufficiently small, we have:*

- (a) $f_t^{-1}(u) \pitchfork B_\varepsilon$ for all $u \in D$.
- (b) Over the boundary circle ∂D the fibrations induced by f and f_t are equivalent.
- (c) X_D and $X_{D,t}$ are homeomorphic.

The proof is analogous to the one presented in [49]. □

(5.4.9) We assume that $f_t : X_{D,t} \rightarrow D$ satisfies the conditions of the preceding lemma. Suppose $\text{Sing}(f_t) = \Sigma_t \cup \{c_1, \dots, c_\sigma\}$, where c_1, \dots, c_σ are the A_1 -points (that is, $D[1, 1]$ -points) of f_t , with critical values v_1, \dots, v_σ , respectively (so $\sigma = \#D[1, 1]$). Let 0 be the critical value of all non-isolated singularities. We may assume that all critical values are distinct.

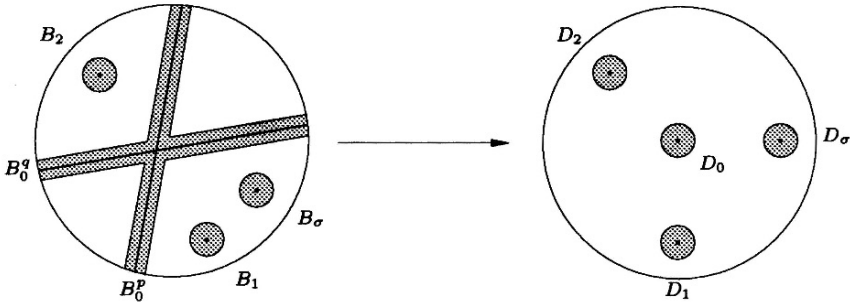


Figure 5.3: $f_t : B_\varepsilon \rightarrow D$

Now choose, as indicated in figure 5.3:

- (a) Small disjoint balls B_i around c_i ($1 \leq i \leq \sigma$);
- (b) Small tubes B_0^p around Σ_i^p ($p \in \{m_1, \dots, m_r\}$), all of the form $B_0^p = \Sigma_i^p \times D(\eta)$, where $D(\eta)$ is the disc of radius $\eta > 0$ (recall that Σ_i^p is smooth);

(c) Small disjoint discs $D_i \subset D$ around v_i ($1 \leq i \leq \sigma$), and $D_0 \subset D$ around $v_0 = 0$, such that $f^{-1}(u) \cap \partial B_i$ for all $u \in D_i$;

(d) Points $a_i \in \partial D_i$ and a point $a \in \partial D$.

Furthermore, (re)define:

$$\begin{aligned} B_0 &= \bigcup_{p \in \{m_1, \dots, m_r\}} B_0^p \\ \Sigma_i &= \Sigma_i \cap B_0 & \Sigma_i^p &= \Sigma_i^p \cap B_0 \\ E &= B \cap f^{-1}(D) & F &= B \cap f^{-1}(a) \\ E_i &= B_i \cap f^{-1}(D_i) & F_i &= B_i \cap f^{-1}(a_i) \quad (i \in \{0, \dots, \sigma\}) \\ E_0^p &= B_0^p \cap f^{-1}(D_0) & F_0^p &= B_0^p \cap f^{-1}(0) \quad (p \in \{m_1, \dots, m_r\}) \end{aligned}$$

E is called the *Milnor ball*, F is still called the *Milnor fibre* and (E, F) the *Milnor pair*.

(5.4.10) Proposition $\widetilde{H}_{*-1}(F) \cong H_*(E, F) \cong \bigoplus_{i=0}^{\sigma} H_*(E_i, F_i)$.

Proof. The first isomorphism follows from the homology sequence of the pair (E, F) , since E , being the Milnor ball, is contractible; for the second, see [49], (2.8). \square

Unlike F , the Milnor pair (E, F) has homology that splits into a direct sum, hence (E, F) is easier to work with. We start by computing the homology of the Milnor pair of our basic singularity, the $D[p, q]$ -point in the following easy lemma.

(5.4.11) Lemma *The Milnor fibre of a $D[p, q]$ -point is homeomorphic to $e = \gcd(p, q)$ annuli. Therefore, the Milnor pair of a $D[p, q]$ -point has homology as follows:*

$$H_j(E_{D[p,q]}, F_{D[p,q]}) = \begin{cases} \mathbf{Z}^{e-1} \\ \mathbf{Z}^e \\ 0 \end{cases} \quad \text{if } j \neq 1, 2 \quad \square$$

(5.4.12) Proposition

- (a) $H_1(E, F) = H_1(E_0, F_0) = \mathbf{Z}^{d-1}$,
- (b) $H_2(E, F) = H_2(E_0, F_0) \oplus \mathbf{Z}^{\sigma}$ ($\sigma = \#D[1, 1]$), and
- (c) $H_j(E, F) = 0$ if $j \neq 1, 2$.

Proof. The homology sequence of the pair (E, F) gives $H_1(E, F) \cong \widetilde{H}_0(F) = \mathbf{Z}^{d-1}$ (F has d connected components). For $i \leq \sigma$, $H_1(E_i, F_i) = 0$, since at c_i we have a $D[1, 1]$ singularity, see lemma 5.4.11. Hence the first statement follows by Proposition 5.4.10. The proof of the second statement is analogous to the first, the third is trivial. \square

(5.4.13) It remains to compute $H_2(E_0, F_0)$. By the preceding lemma it is sufficient to compute the Euler characteristic $\chi(E_0, F_0) = \dim H_2(E_0, F_0) - \dim H_1(E_0, F_0)$ of the pair (E_0, F_0) . Recall the following properties of the Euler characteristic:

- (i) if (X, A) is a pair of topological spaces, then $\chi(X, A) = \chi(X) - \chi(A)$ ([53], p. 205);
- (ii) if $\{X, Y\}$ is an excisive couple of spaces then $\chi(X \cup Y) = \chi(X) + \chi(Y) - \chi(X \cap Y)$ ([53], p. 205);
- (iii) if $\pi : (\widetilde{X}, \widetilde{A}) \rightarrow B$ is a fibre bundle pair with fibre the pair (X, A) , then $\chi(\widetilde{X}, \widetilde{A}) = \chi(X, A) \cdot \chi(B)$ ([53], p. 481).

Recall $E_0^p = B_0^p \cap f^{-1}(D)$, where $B_0^p = \Sigma_i^p \times D(\eta)$ is a small tube around the smooth curve Σ_i^p . Let π_p be the projection onto the first factor. If η is chosen sufficiently small, then $\pi_p : (E_0^p, F_0^p) \rightarrow \Sigma^p$ is a fibre bundle pair, locally trivial outside the $D[p, q]$ -points, and with general fibre equivalent to the Milnor pair $(\overline{E}^p, \overline{F}^p)$ of the transversal A_{p-1} singularity. Observe that \overline{F}^p consists of p points.

(5.4.14) **Definition** For $Y \subset \Sigma_i^p$, define $E_Y = \pi_p^{-1}(Y) \cap E_0^p$, and $F_Y = \pi_p^{-1}(Y) \cap F_0^p$. The definition is extended in the obvious way to subsets Y of Σ_i^p that are disjoint unions of real two dimensional manifolds with boundary, each of which is lying entirely in a Σ_i^p .

In each Σ_i^p ($p \in \{m_1, \dots, m_r\}$) choose small discs $W_{p,q,i}$, $q \neq p$, $i \in \{1, \dots, \#D[p, q]\}$ around the $D[p, q]$ -points that do not meet each other. We may assume that $E_{W_{p,q,i}} = E_{W_{q,p,i}}$ and $F_{W_{p,q,i}} = F_{W_{q,p,i}}$. Let $W_p = \cup_{q,i} W_{p,q,i}$ and $M_p = \overline{\Sigma_i^p} \setminus \overline{W_p}$.

(5.4.15) **Proposition** $\pi_p : (E_{M_p}, F_{M_p}) \rightarrow M_p$ is a trivial fibre bundle with fibres equivalent to the Milnor pair $(\overline{E}^p, \overline{F}^p)$ of the transversal A_{p-1} singularity.

Proof. Use [49] (4.7) in a somewhat more general setting. \square

Let $p \in \{m_1, \dots, m_r\}$. We have defined W_p as the (disjoint) union of all discs $W_{p,q,i}$ around the $D[p, q]$ -points in Σ_i^p . The space Σ_i^p is a Riemann surface with holes and has a wedge of circles as deformation retract. Let B_p be the union of this wedge with $\#D[p, q]$ non-intersecting paths connecting the wedge point with the discs $W_{p,q,i}$, as in figure 5.4. Observe that $W_p \cap B_p$ consists of a finite set of points.

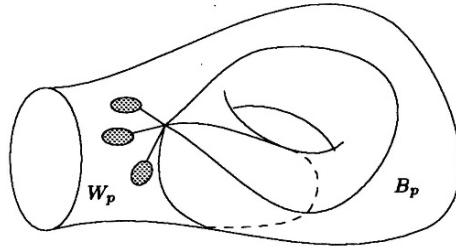


Figure 5.4: Σ_i^p

(5.4.16) Proposition *Let $W = \cup_p W_p$, $B = \cup_p B_p$. Then:*

$$\chi(E_0, F_0) = \chi(E_{W \cup B}, F_{W \cup B}) = \chi(E_W, F_W) + \chi(E_B, F_B) - \chi(E_{W \cap B}, F_{W \cap B}).$$

Proof. The first equality follows from the fact that $(E_{W \cup B}, F_{W \cup B})$ is homotopy equivalent to (E_0, F_0) . Indeed, for each p , $W^p \cup B^p$ is homotopy equivalent to Σ_i^p (rel. W_p), and therefore by the homotopy lifting property of the map $\pi_p : (E_{M_p}, F_{M_p}) \rightarrow M_p$ ($p \in \{m_1, \dots, m_r\}$), $(E_{W \cup B}, F_{W \cup B})$ is homotopy equivalent to (E_0, F_0) .

The fact that $(F_{W \cup B}; F_W, F_B) \subset (E_{W \cup B}; E_W, E_B)$ is an inclusion of excisive triads (by the properties of the Euler characteristic 5.4.13) implies the second equality. \square

(5.4.17) Lemma

- (a) $\chi(E_W, F_W) = \sum_{p < q} \#D[p, q]$.
- (b) $\chi(E_B, F_B) = \sum_p (p - 1)(\mu(\Sigma^p) - 1)$.
- (c) $\chi(E_{W \cap B}, F_{W \cap B}) = -\sum_{p < q} (p + q - 2) \cdot \#D[p, q]$.

Proof.

- (a) W is the disjoint union of the $W_{p,q,i}$, $p < q$, $i \in \{1, \dots, \#D[p, q]\}$. So $\chi(E_W, F_W)$ is the sum of the $\chi(E_{W_{p,q,i}}, F_{W_{p,q,i}})$ which are all equal to 1 (see lemma 5.4.11).
- (b) B is the disjoint union of the B_p , so $\chi(E_B, F_B) = \sum_p \chi(E_{B_p}, F_{B_p})$. B_p is a wedge of $\mu(\Sigma^p)$ circles (Σ_i^p and Σ^p have the same homotopy type), so its Euler characteristic is $1 - \mu(\Sigma^p)$. (E_{B_p}, F_{B_p}) is a trivial fibre bundle

pair over B_p with fibres $(\overline{E}^p, \overline{F}^p)$. Since \overline{E}^p is a topological disc and \overline{F}^p a set of p points, we have that $\chi(\overline{E}^p, \overline{F}^p) = 1 - p$. By 5.4.13 (iii) we obtain $\chi(E_{B_p}, F_{B_p}) = (p - 1)(\mu(\Sigma^p) - 1)$.

- (c) $W_p \cap B_p$ is a set of $\sum_{q \neq p} \#D[p, q]$ points. Above each point the fibre is equivalent to the Milnor pair of the transversal A_{p-1} singularity, which has Euler characteristic $1 - p$ as we have seen in (b). So $\chi(E_{W_p \cap B_p}, F_{W_p \cap B_p}) = \sum_{q \neq p} (1 - p) \#D[p, q]$. Hence $\chi(E_{W \cap B}, F_{W \cap B}) = \sum_p \sum_{q \neq p} (1 - p) \#D[p, q] = -\sum_{p < q} (p + q - 2) \#D[p, q]$.

□

(5.4.18) *Proof [of Theorem 5.4.4].* By combining all previous computations, we obtain the desired formula

$$\mu(f) = \sum_{p < q} (p + q - 1) \cdot \#D[p, q] + \#D[1, 1] + \sum (p - 1)(\mu(\Sigma^p) - 1) + d - 1. \quad \square$$

5.5 Splicing of real morsifications

In this section we consider polynomials $f = f_1^{m_1} \cdots f_r^{m_r}$ whose irreducible factors are polynomials with real coefficients. A deformation or morsification will be a *real* network map type deformation f_t of a function germ f with real coefficients, as in [1]. By considering parametrizations, one sees that such real deformations exist. The necessary data are contained in the intersection of \mathbf{R}^2 and the level $f_t^{-1}(0)$ (a ‘partage signé’), and we will even call this morsification diagram a morsification.

(5.5.1) In the preceding section we proved a formula which expresses the Milnor number of a plane curve singularity in the number of special points of a deformation. It is not comparably easy to obtain from deformations more topological details, in particular the Waldhausen decomposition of the exterior of the link of the singularity. On the other hand, that decomposition may give us some results on deformations.

One such result will now be described briefly, merely as an illustration: an algorithmic way to obtain formally a morsification of an isolated plane curve singularity. This can be used to obtain a Dynkin diagram of the intersection form by the A’Campo–Gusein-Sade method ([1], [6]). Such algorithms are not new, cf. Schulze-Röbbecke [47], who obtained a *Dynkindiagramm für jede Singularität*, where in that case “each singularity” meant “each irreducible isolated plane curve singularity.”

(5.5.2) Consider a plane curve singularity $(X, 0)$ with $X = m_1 X_1 \cup \dots \cup m_r X_r$, defined by a polynomial as above. Recall that the construction of the Waldhausen decomposition is by glueing Seifert pieces together, using the operation of splicing. If we follow the construction of the EN-diagram in Chapter 1, we can even assume that the Seifert pieces, our basic building blocks, are defined by functions $x^a y^b (y^p - x^q)^c$, where $a, b, c \geq 0$ and $p, q \geq 1$. For such an uncomplicated singularity, it is not difficult to find a real network map deformation (for example using the A'Campo–Gusein-Sade method).

If we can describe how to splice two morsification diagrams, we are able to produce morsification diagrams for all plane curve singularities, and Dynkin diagrams for all isolated plane curve singularities. Again, this should be seen primarily as a way of manipulating morsification diagrams.

Consider also $Y = n_1 Y_1 \cup \dots \cup n_s Y_s$, another plane curve singularity. It is perhaps slightly unusual that we allow n_1 to be zero without having in mind that we should ignore Y_1 . It means, that as a plane curve singularity, Y is just $n_2 Y_2 \cup \dots \cup n_s Y_s$, but its link will contain the component K_1 of multiplicity zero, defined by intersecting Y_1 with the Milnor sphere.

The splicing takes place “along” an m_i -fold branch X_i of the one part, X , and an n_j -fold branch Y_j of the other part, Y . By the splice condition, we have the following relationship: $n_j = X_i \cdot \cup_{k \neq i} m_k X_k$, the intersection number of X_i with the other branches counted with their multiplicities, and also $m_i = Y_j \cdot \cup_{l \neq j} n_l Y_l$.

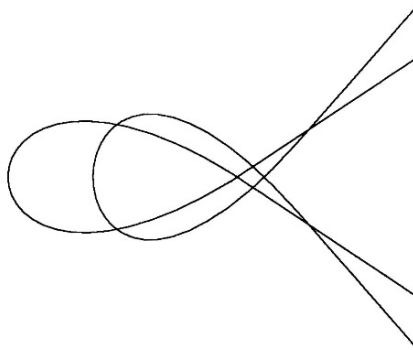


Figure 5.5: Doubling a morsification of $(y^2 - x^3)^2$

The first step consists of *multiplying* the branches X_i and Y_j by m_i and n_j , respectively. This means that one takes m_i resp. n_j parallel copies very near to

each other, which are deformed slightly to take care of intersections between each of the copies. In figure 5.5 a doubled morsification of the cusp is depicted. In the A'Campo–Gusein-Sade method, where the morsification is obtained by small modifications of the strict transform in the partial resolutions, this is accomplished as follows: In the resolution, the strict transform of $m_i X_i$ can in local coordinates (u, v) be written as v^{m_i} . Replace this by $v^{m_i} - 1$, and perform the usual steps to obtain a deformation.

We can take small common neighbourhoods M of the m_i new branches in the morsification diagram of X , and N of the n_j new branches in the morsification diagram of Y . Because of the splice condition we may assume that the intersection of M with the other branches of X consists of n_j segments, and the intersection of N with the other branches of Y consists of m_i segments. The splice operation is just patching those segments on the multiplied branches of the other.

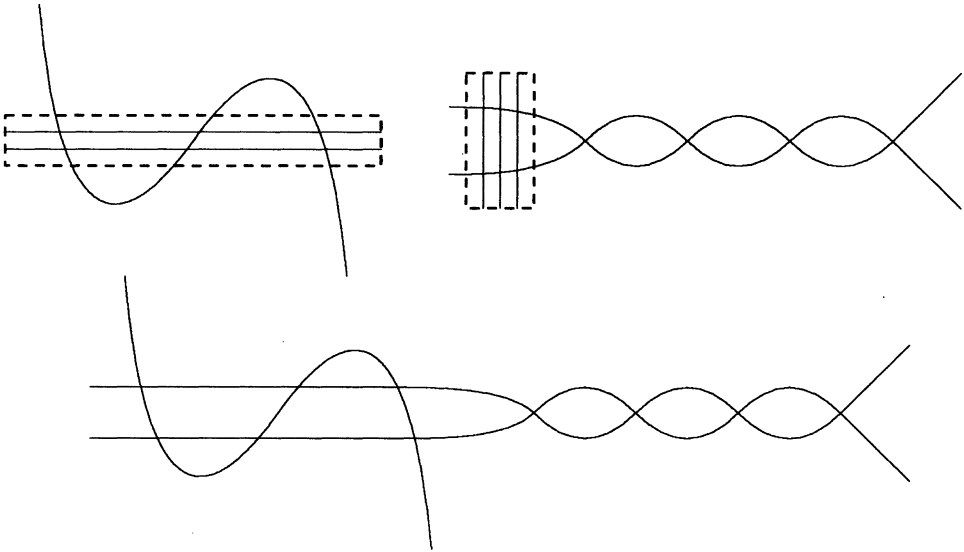
This procedure works by inspection of the proof of the A'Campo–Gusein-Sade method, bearing in mind that the splice components are related to partial resolutions of the singularity. This was shown to me by Jan Stevens, who communicated a proof of the case of “cabling” of morsifications.

(5.5.3) Example (See figure 5.6.) We apply our method in the simple case of $J_{3,2}$ (equation: $f(x, y) = (y^2 - x^8)(y - x^3)$). It has two splice components. The first is $J_{3,\infty}$ (equation $y^3 - x^3 y^2$). The second is isomorphic to $x^3(y^2 - x^{6+p})$. In figure 5.6 there are morsification diagrams for both, and we can identify the 2×3 lines along which the splicing takes place.

In the picture, we can identify the 18 cycles which form a distinguished basis for the homology of the Milnor fibre of $J_{3,2}$. The top right morsification is made up from the well-known morsification of A_7 . Analogously we obtain the morsification diagrams of $J_{3,p}$ ($p \geq 0$) by using A_{p+5} instead of A_7 . Interestingly, the morsification diagram does not reveal a reason for the algebraicity condition $p \geq 0$.

(5.5.4) The multiplication of branches is in practice sometimes confusing, a notation as in [47] is useful. As in [47] (for irreducible and isolated plane curve singularities) we have a way to construct a morsification for each topological type. For isolated singularities, we can use this to obtain a distinguished basis of vanishing cycles for the homology and a Dynkin diagram for the intersection form.

For non-isolated singularities, a basis and a Dynkin diagram could be constructed as well, but for distinguishedness (that we want for the relationship with the monodromy) the theory lacks. Compare [51], where the curve case

Figure 5.6: The splice decomposition of $J_{3,2}$

must be excluded. A basis can be obtained from the morsification diagram in the following way. We distinguish *A-cycles*, *D-cycles* and *tube-cycles*:

– *A-cycles*

For each A_1 point off the zero locus, we have a vanishing *A-cycle* defined analogous to the \oplus and \ominus cycles in A'Campo [1], which arise from the maxima and minima.

– *D-cycles*

For each $D[p, q]$ point on the zero locus we have $\gcd(p, q)$ vanishing *D-cycles*. They are defined analogous to the \bullet cycles in A'Campo [1], which arise from the saddle points.

– *Tube-cycles*

Let p be one of the m_i . Take the union of the p -fold branches in the deformation, and take a tube around it. In this tube, the Milnor fibre has a deformation retract consisting of the central circles of the annuli at $D[p, q]$ -points connected by p -tuples of segments. There is in general an enormous choice of cycles that we can pick for a basis of the homology. It would go too far to define these tube cycles in more detail.

It is not so easy to describe the intersections between the cycles. In the case of a line singularity (with singular set a smooth curve) this is still manageable, and following unfinished work of C. Cox we obtained some unsatisfactory results in this direction (unpublished). Goryunov [16] derived in a similar way the intersection form of a plane line singularity.

Perhaps more can be expected from the description of the Waldhausen decomposition in terms of the polar filtration and the Gabrielov-method for finding a distinguished base, see [13], Chapter 2 or [6].

The following result follows immediately from the preceding discussion.

(5.5.5) Proposition *Let f_N be a member of a topological series of a plane curve singularity f with only double components (i.e. only transversal A_1 -singularities). If we choose a basis for the homology of the Milnor fibre as in the A'Campo–Gusein-Sade method, departing from a deformation constructed with our splice operation, then the Dynkin diagram of the intersection form contains r tails of the form*



corresponding to each of the r branches of the singular locus. In terms of Theorem 3.3.2, the length of such a chain will be N_i .

Another application of deformations is the computation of intersection numbers. For example, consider the number c_i of lemma 1.1.7, which is used for the computation of the vertical monodromy on a fibre of the transversal singularity along $\Sigma_i \setminus \{0\}$. Suppose that we have transversal A_{p-1} singularities along $\Sigma \setminus \{0\}$, where Σ is a branch of the singular set. The number c_i can be computed as the sum of all $D[p, q]$ -points with $q \geq 1$ on Σ_i , each counted with multiplicity q .

CHAPTER 6

Series of hypersurface singularities

6.1 Introduction

In this chapter we discuss some possible ways to generalize the topological series of plane curve singularities to higher dimensional hypersurface singularities with a one-dimensional singular locus. We will not enter a full treatment of series of hypersurface singularities. Apart from the question whether it would be right or possible to give a ‘full’ treatment — series have always been a source of inspiration because the concept was deliberately held vague — this would embrace a vast area of topics that we do not yet understand in their totality. Jan Stevens and the author hope to give a good description of *Polar Series* in a future paper.

Instead, we consider some properties that we would like to have within our series. Most importantly, we would like to go beyond the Yomdin series barrier of one parameter series which go with large steps. At least in the case where we have only transversal A_1 singularities along the branches of the one-dimensional singular locus, we would like to have for instance Milnor numbers increasing with steps of 1. Of course the results should be applicable to the Arnol’d series still missing from the list of series that we have already seen, such as Q , S , T and U . Our main aim here will be a formula for the zeta-function, in line with the formula for Yomdin series, cf. section 3.5.

We start with an analytic function germ $f : (\mathbb{C}^{n+1}, 0) \rightarrow (\mathbb{C}, 0)$ with a one-dimensional singular locus Σ , whose decomposition in irreducible components is $\Sigma_1 \cup \dots \cup \Sigma_r$. Let $g : (\mathbb{C}^{n+1}, 0) \rightarrow (\mathbb{C}, 0)$ have an isolated singularity. We think of g as $g = f + \varphi$, and assume that there is a one parameter family $f(\cdot, \lambda)$ such that $f(\cdot, 0) = f$, $f(\cdot, 1) = g$, $f(\cdot, \lambda)$ has an isolated singularity for all $\lambda \neq 0$, and $\frac{\partial}{\partial \lambda} f(z, \lambda) \neq 0$. (We have in mind that $f(\cdot, \lambda) = f + \lambda\varphi$, but it might be useful to allow more general families).

We will have to put constraints on the family $f(\cdot, \lambda)$ in such a way that it seems natural for g to ‘belong’ to the series of f . So we think of f as fixed, whereas g runs through the ‘series’ of f .

We want to stress again that in this chapter, we will not enter a full discussion of series. Otherwise, one would object to the last sentence in the previous paragraph. Indeed, it will in general only be possible to let g be a *representative* of a member of the series of f which will ideally be indexed by a collection of positive integers (each associated to a branch of the singular locus of f). Such a member will therefore be an equivalence class of functions, but we are not going to specify details here. So in the following we consider rather special functions g .

Below, we present two ways to look at the relationship between f and g . This is by no means a complete account of what is possible with these methods.

Similar results have been obtained by A. Némethi [32].

6.2 Polar series

(6.2.1) In this section, we use the polar filtrations on the Milnor fibrations of f and g as our source of inspiration. Let $l : (\mathbf{C}^{n+1}, 0) \rightarrow (\mathbf{C}, 0)$ be a linear form such that

$$\Sigma \cap Z(l) = \{0\}$$

(recall that $Z(h) = \{z \in \mathbf{C}^{n+1} \mid h(z) = 0\}$). This condition was already considered by Pellikaan. We consider $\Phi_l = (l, f) : (\mathbf{C}^{n+1}, 0) \rightarrow (\mathbf{C}^2, 0)$. Let $C_l = \text{Sing}(\Phi_l)$ be the critical locus of Φ_l , which consists of the points where the matrix $D\Phi_l$ of partial derivatives does not have maximal rank.

(6.2.2) **Lemma** *Suppose l satisfies $\Sigma \cap Z(l) = \{0\}$. Then C_l is one-dimensional.*

Proof. This is proved by Pellikaan [39], Proposition 3.1. □

(6.2.3) **Definition** The *polar curve of f with respect to the direction l* is defined by

$$\Gamma_l = \overline{C_l \setminus Z(f)},$$

i.e., it consists of the components of C not contained in the zero locus of f . The image $\Delta_l = \Phi_l(\Gamma_l)$ is called the *Cerf diagram*. If no subscript l is given, we assume $l = x$, the first coordinate function on \mathbf{C}^{n+1} .

(6.2.4) Remark Lê considers *admissible* linear functions l . This means that $f|Z(l)$ has an isolated singularity. The condition we use, is weaker: take for instance

$$f(x, y, z) = x(y^2 + z^2) + y^2z^2 \quad \text{and} \quad l(x, y, z) = x.$$

Then $\Sigma = Z(y, z)$, so $\Sigma \cap Z(l) = \{0\}$ but $f(0, y, z) = y^2z^2$ has a non-isolated singularity. C consists of Σ , $\Gamma = Z(x + y^2, x + z^2)$ and $\Omega = Z(x, y) \cup Z(x, z)$. Observe that $\Phi(\Omega) = \{(0, 0)\}$ and that Γ is the polar curve of f . This example is due to Pellikaan, see [36], Example (8.7).

(6.2.5) From now on we assume that $l = x$, the first coordinate function, and we will omit the subscripts l . Notice that in this case C is defined by $\frac{\partial f}{\partial y} = 0$, if (x, y) are the coordinates on $\mathbf{C}^{n+1} = \mathbf{C} \times \mathbf{C}^n$.

The critical locus C of $\Phi = (x, f)$, which is one-dimensional as we have just seen, consists of three main parts:

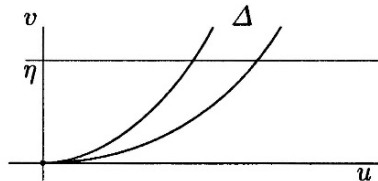
$$C = \Sigma \cup \Gamma \cup \Omega.$$

Here Σ is the critical locus of f , as usual, and Γ the polar curve as defined above. The third part, Ω , consists of the branches of C above the origin, i.e. $\Phi(\Omega) = \{(0, 0)\}$. If x is admissible, then $\Omega = \emptyset$.

Let $\Gamma = \Gamma_1 \cup \dots \cup \Gamma_s$ be the decomposition of Γ into irreducible components. The discriminant locus $\Delta = \Delta_1 \cup \dots \cup \Delta_s$, with $\Delta_i = \Phi(\Gamma_i)$, is the *Cerf diagram*. We will use coordinates (u, v) in the target- \mathbf{C}^2 .

(6.2.6) Lemma *The tangent cone of Δ is the u -axis.*

Proof. This is proved by Lê [21], Proposition (3.1). □



It follows from the lemma that each Δ_i has a Puiseux expansion

$$v = a_i u^{\rho_i} + \text{higher order terms},$$

with $a_i \neq 0$ and $\rho_i > 1$ a rational number. The number ρ_i is called a *polar ratio* of f . Observe that ρ_i may well be a non-characteristic Puiseux exponent: we

are not allowed to change coordinates in (u, v) -space. Therefore the topological type of Δ_i does not determine ρ_i . It is also possible to compute the polar ratios upstairs:

$$\rho_i = \frac{\Gamma_i \cdot Z(f)}{\Gamma_i \cdot Z(x)},$$

where \cdot denotes the intersection number at the origin. By $\mathfrak{p}(f)$ we denote the set of polar ratios of f .

(6.2.7) The assumptions

Let f be as above, and $g : (\mathbb{C}^{n+1}, 0) \rightarrow (\mathbb{C}, 0)$ be an isolated singularity, such that there is a family $f(\cdot, \lambda)$ with $f(\cdot, 0) = f$ and $f(\cdot, 1) = g$. Write $f_\lambda = f(\cdot, \lambda)$ and $\Phi_\lambda = (x, f_\lambda)$. Let C_λ be the critical locus of Φ_λ and let $D_\lambda = \Phi_\lambda(C_\lambda)$.

We will now formulate a number of assumptions in order that g ‘belongs’ to f . Possibly some of the assumptions can be weakened or deduced from the other assumptions. First of all, we assume that:

- (a) $\Sigma \cap Z(x) = 0$,
- (b) f_λ has an isolated singularity for all $\lambda \neq 0$.

In this case, the C_λ will form a family of curves. We have that $C_0 = \Sigma \cup \Gamma_0 \cup \Omega_0$, where Γ_0 is the polar curve of f and Ω_0 is the union of the branches whose Φ -image is the origin only (see 6.2.5). For $\lambda \neq 0$, we can view C_λ as a deformation of Σ , Γ_0 and Ω_0 separately, so

$$C_\lambda = \Sigma_\lambda \cup \Gamma_\lambda \cup \Omega_\lambda,$$

and as $\lambda \rightarrow 0$, each of the parts ends up as a part of the same name. The images in (u, v) -space are: $\Theta_\lambda = \Phi_\lambda(\Sigma_\lambda)$, $\Delta_\lambda = \Phi_\lambda(\Gamma_\lambda)$. We also assume:

- (c) For each λ , Θ_λ and Δ_λ are one-dimensional, whereas $\Phi_\lambda(\Omega_\lambda) = \{(0, 0)\}$. Hence $\Sigma_\lambda \cup \Gamma_\lambda$ is the polar curve of f_λ . Furthermore, we assume the following facts of the topology of Θ_λ and Δ_λ :
 - (d) The topological type and the first Puiseux exponents of all branches of Θ_λ are constant as $\lambda \neq 0$ varies.
 - (e) The topological type and the first Puiseux exponents of all branches of Δ_λ are constant as λ varies, including $\lambda = 0$.

In particular, the number of branches of the Cerf diagram of f_λ and the sets $\mathfrak{p}(f_\lambda)$ are constant for $\lambda \neq 0$. Furthermore, $\mathfrak{p}(f) \subset \mathfrak{p}(f_\lambda)$; the ‘new’ polar ratios come from the branches of Θ_λ . Recall $\Sigma = \Sigma_1 \cup \dots \cup \Sigma_r$ is the decomposition of Σ into irreducible components. We need a final assumption on the polar ratios arising from Θ_λ .

- (f) Suppose Σ_i deforms into the curve $\Sigma_{\lambda,i}$. Let $\Theta_{\lambda,i}$ be its image under Φ_λ . Then all branches of $\Theta_{\lambda,i}$ have the same first Puiseux exponent θ_i , and $\theta_i < \infty$.

Recall that if we replace condition (a) by the stronger condition

- (a') x is admissible, i.e. $f|Z(x)$ has an isolated singularity,

then the situation becomes easier since Ω_λ is empty.

(6.2.8) Remark Observe that $\mathfrak{p}(g) = \mathfrak{p}(f) \cup \{\theta_1, \dots, \theta_r\}$, but that we do *not* assume that all θ_j are larger or equal to the largest polar ratio in $\mathfrak{p}(f)$. We will return to this later.

(6.2.9) Remark If we assume that f has only transversal A_1 singularities, then the behaviour of the curves C_λ is much less complicated than with arbitrary transversal singularities.

(6.2.10) Example Let $\tilde{\mathfrak{p}}(f, g)$ be the set of first Puiseux exponents of $\Phi_1(\Sigma_i)$ ($1 \leq i \leq r$), i.e. the images of the branches of the singular locus of f under the mapping $\Phi_1 = (x, g)$. Our idea is that

$$\mathfrak{p}(g) = \mathfrak{p}(f) \cup \tilde{\mathfrak{p}}(f, g), \quad (*)$$

but also that that condition will imply a large part of the above. If that is the case, we would like to build a definition of *polar series* around condition (*) — or an improved version. In the following example, all assumptions (a) – (e) are satisfied. The example (d) is studied in [25] and [52]. In the other cases, note that the non-isolated singularity has only transversal A_1 singularities.

- (a) *The A-series*

Consider $f(x, y) = y^2$ and $g_N(x, y) = y^2 + x^N$; then f is of type A_∞ and g_N of type A_{N-1} . We have that $\mathfrak{p}(f)$ is the empty set and $\mathfrak{p}(g_N) = \tilde{\mathfrak{p}}(f, g_N) = \{N\}$.

Now we consider $g(x, y) = y^2 + 2x^k y + x^N$. It is easy to see that the function g is of type $A_{\min\{2k-1, N-1\}}$. $\mathfrak{p}(g) = \{N\}$, whereas $\tilde{\mathfrak{p}}(f, g) = \{\min\{2k, N\}\}$. This shows that for a definition of polar series, based on the behaviour of the polar ratios, we have to be very careful with the choice of equivalence relations and representatives thereof.

- (b) *The $W^\#$ -series*

Let $f(x, y) = (y^2 - x^3)^2$ ($W_{1,\infty}^\#$), and let $g_{2q-1}(x, y) = f(x, y) + x^{4+q}y$ and $g_{2q}(x, y) = f(x, y) + x^{3+q}y^2$. Then g_p is of type $W_{1,p}^\#$. We have $\mathfrak{p}(f) = \{6\}$, $\mathfrak{p}(g_p) = \{6, 6 + \frac{1}{2}p\}$ and $\tilde{\mathfrak{p}}(f, g_p) = \{6 + \frac{1}{2}p\}$.

(c) *The T-series*

Let $f(x, y, z) = xyz$ (type $T_{\infty, \infty, \infty}$, the ordinary triple point), and define $g_{p,q,r}(x, y, z) = xyz + x^p + y^q + z^r$ (type $T_{p,q,r}$) with $p, q, r \geq 3$. In this case we take e.g. $l(x, y, z) = x + y + z$ (or change coordinates accordingly). The singular set of f consists of the three coordinate axes. We have $\mathfrak{p}(f) = \{3\}$, $\mathfrak{p}(g) = \{3, p, q, r\}$ and $\tilde{\mathfrak{p}}(f, g) = \{p, q, r\}$. If one of p, q and r is less than 3, the condition is not satisfied, although, of course, one can define $T_{p,q,r}$ whenever $1/p + 1/q + 1/r < 1$. This shows that we miss some initial members of what one would call the series of $T_{\infty, \infty, \infty}$ — a problem that arises as soon as one starts looking for a property that is shared by all members.

(d) *The U-series*

Let $f(x, y, z) = y^3 + yz^2 - yx^{2k+1}$ (type $U_{k, \infty}$). Put $g_{2q-1}(x, y, z) = f(x, y, z) + z^2x^{k+q}$ and $g_{2q}(x, y, z) = f(x, y, z) + zx^{2k+q+1}$. Now g_p is of type $U_{k,p}$. Then $\Sigma = \{(t^2, 0, t^{2k+1}) \mid t \in \mathbb{C}\}$. We get: $\mathfrak{p}(f) = \{(6k+3)/2\}$, $\mathfrak{p}(g_p) = \{(6k+3)/2, (6k+3+p)/2\}$ and $\tilde{\mathfrak{p}}(f, g) = \{(6k+3+p)/2\}$.

(e) *Yomdin type series*

For Yomdin type series $f + x^N$, one computes for N not less than the largest polar ratio of f , that $\mathfrak{p}(f + x^N) = \mathfrak{p}(f) \cup \{N\}$ and $\tilde{\mathfrak{p}}(f, f + x^N) = \{N\}$. So within a Yomdin series, condition (*) is satisfied, but we can see the gaps: Firstly, if the singular locus of f consists of more than one branch, we would expect a multi-parameter series as in (c). Secondly, if a branch of Σ has a multiplicity greater than 1, we would expect a finer series, cf. (b) and (d).

(f) *Another motivating example*

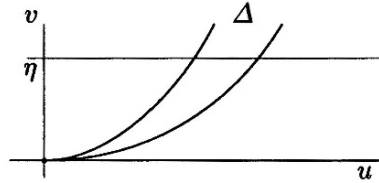
In Yomdin series, one usually assumes that N is at least as large as the maximal polar ratio. Otherwise the zeta-function formula (cf. [52]) is not valid. Here, we could demand that *all* θ_i be not less than the maximum of the polar ratios in $\mathfrak{p}(f)$. But take $T_{1000, \infty, \infty}$. Almost nothing changes from $T_{\infty, \infty, \infty}$, the polar ratios are now 3 and 1000. But it would be an enormous drawback to let q and r start from 1000 instead of 3.

(6.2.11) We recall the definition of the Milnor fibration and the polar decomposition from Lê's viewpoint, cf. [21], [22], [24] and [26].

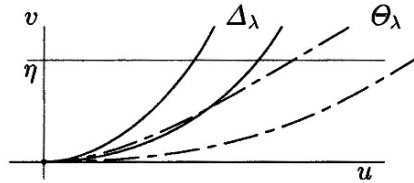
Let δ be a Milnor radius, and B_δ a $(2n+2)$ -ball in \mathbb{C}^{n+1} . There exists $\eta_0 > 0$ such that for $0 < \eta < \eta_0$, $f : B_\delta \cap f^{-1}(D_\eta^2) \rightarrow D_\eta^2$ is a C^∞ fibration over $D_\eta^2 \setminus \{0\}$. Consider $\Phi = (x, f)$. It will be convenient to have our target space coordinates (u, v) in a polydisc $D_\varepsilon^2 \times D_\eta^2$ where $\varepsilon > 0$ is appropriately chosen

and $\eta \ll \varepsilon$. Let $B = B_\delta \cap \{(x, y_1, \dots, y_n) \mid |x| \leq \varepsilon\}$. Then $\Phi : B \rightarrow D_\varepsilon^2 \times D_\eta^2$ is also a fibration. Observe that $\Phi^{-1}(D_\varepsilon^2 \times \{\eta\})$ is the Milnor fibre of f .

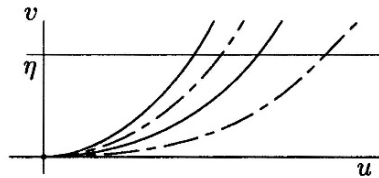
$\lambda = 0$



$0 < \lambda \ll 1$



$\lambda = 1$



We can choose δ, ε and η such that they can be used for both f and g . Not for all intermediate λ we have that $F_\lambda = \Phi_\lambda^{-1}(D_\varepsilon^2 \times \{\eta\})$ is the Milnor fibre of f_λ . However, it remains true that F_λ can be constructed from the Milnor fibre of $f_\lambda \mid Z(x)$ by attaching n -cells as in L e's work, e.g. [22] (using the real valued function $|x|^2$ on F_λ , which is singular in the intersection points with C_λ). For $\lambda \neq 0$ very small, the curves Θ_λ do not yet intersect the line $v = \eta$ within the polydisc. This is illustrated in the pictures above.

(6.2.12) Let $\mathfrak{p}(f) = \{\rho_{01}, \dots, \rho_{0p}\}$ be the set of polar ratios of f and likewise $\mathfrak{p}(f_\lambda) = \{\rho_{11}, \dots, \rho_{1q}\}$ be the set of polar ratios of f_λ (equal to the set of polar ratios of $g = f_1$), and assume that $\rho_{01} < \dots < \rho_{0p}$ and $\rho_{11} < \dots < \rho_{1s}$. The sequence $(\rho_{01}, \dots, \rho_{0p})$ is a subsequence of $(\rho_{11}, \dots, \rho_{1q})$. This holds because

of the conditions (a)–(f).

Recall the definition of θ_i ($1 \leq i \leq r$). The θ_i are those ρ_{1j} that arise from branches of Θ_i . Those branches have Puiseux expansions of the form

$$v = a_i(\lambda)u^{\theta_i} + \text{higher order terms.}$$

But since those branches tend to the u -axis as $\lambda \rightarrow 0$, the coefficients $a_i(\lambda)$ will become extremely small — so small in fact that they dominate the picture. The absolute value of the x -coordinates of the intersection points of these branches with the line $v = \eta$ will tend to infinity and therefore leave the ‘visible’ part where $|x| \leq \varepsilon$.

Recall, that on $\Sigma_i \setminus \{0\}$, we have a local system of transversal singularities: Take at any $w \in \Sigma_i \setminus \{0\}$ the germ of a generic transversal section. This gives an isolated $n - 1$ dimensional singularity, whose μ -constant class is well-defined. We denote a typical Milnor fibre of this transversal singularity by F_i^b . The Milnor number of this singularity (the rank of $\widetilde{H}_{n-1}(F_i^b)$, the reduced homology group) is denoted by μ_i^b .

(6.2.13) Lemma *Let $i \in \{1, \dots, r\}$. Define $d_i = \Sigma_i^{\text{red}} \cdot Z(x)$. Then $d_i \mu_i^b \theta_i$ is an integer.*

Proof. Observe that $d_i \mu_i^b = \Sigma_i \cdot Z(x)$. Choose a small λ , then $\Sigma_{\lambda,i}$ is a small perturbation of Σ_i and $d_i \mu_i^b = \Sigma_{\lambda,i} \cdot Z(x)$.

Let $\Sigma_{\lambda,i}$ be the curve into which Σ_i is deformed. Write $\Phi(\Sigma_{\lambda,i}) = \Theta_{\lambda,i} = \Theta_{\lambda,i,1} \cup \dots \cup \Theta_{\lambda,i,k_i}$ and let $\Sigma_{\lambda,i,j} = \Phi^{-1}(\Theta_{\lambda,i,j})$. All branches of $\Theta_{\lambda,i}$ ($\lambda \neq 0$) have first Puiseux exponent θ_i . Since $\Sigma_{\lambda,i}$ is small perturbation of Σ_i , we have

$$d_i \mu_i^b = \Sigma_i \cdot Z(x) = \Sigma_{\lambda,i} \cdot Z(x) = \sum_{j=1}^{k_i} (\Sigma_{\lambda,i,j} \cdot Z(x)).$$

So if $\sigma_{ij} = \Sigma_{\lambda,i,j} \cdot Z(x)$ then $d_i \mu_i^b = \sum_j \sigma_{ij}$.

Write $\theta_i = q_i/p_i$ with $\gcd(p_i, q_i) = 1$. By definition (and condition (f)) we have that

$$\theta_i = \frac{\Theta_{\lambda,i,j} \cdot Z(v)}{\Theta_{\lambda,i,j} \cdot Z(u)}$$

for all $j \in \{1, \dots, k_i\}$, and if we compute this upstairs we get

$$\theta_i = \frac{\Sigma_{\lambda,i,j} \cdot Z(f)}{\Sigma_{\lambda,i,j} \cdot Z(x)} = \frac{\tau_{ij}}{\sigma_{ij}}.$$

It follows that $q_i \sigma_{ij} = p_i \tau_{ij}$, and summation over j gives $p_i \mid q_i d_i \mu_i^b$. This proves the statement, since p_i and q_i are relatively prime. \square

(6.2.14) Proposition *The Euler characteristics of F_0 and F_1 are related by*

$$\chi(F_1) = \chi(F) + (-1)^n \left(\sum_{i=1}^r d_i \mu_i^b \theta_i \right).$$

Proof. We first establish that the Milnor fibres of the singularities

$$\Phi_\lambda = (x, f_\lambda) : (\mathbf{C}^{n+1}, 0) \rightarrow (\mathbf{C}^2, 0)$$

are homeomorphic. Note that these singularities are often identical or isomorphic. We choose a small ξ such that (ξ, η) is a regular value of all Φ_λ and therefore $\Phi_\lambda^{-1}(\xi, \eta)$ is the Milnor fibre of Φ_λ . This is possible since the map $(x, f_\lambda) : \mathbf{C}^{n+1} \times \mathbf{C} \rightarrow \mathbf{C}^2$ which depends also on λ has Jacobi matrix

$$\begin{pmatrix} \frac{\partial f}{\partial x} + \lambda \frac{\partial \varphi}{\partial x} & \frac{\partial f}{\partial y} + \lambda \frac{\partial \varphi}{\partial y} & \varphi \\ 1 & 0 & 0 \end{pmatrix},$$

(where we took $f_\lambda = f + \lambda\varphi$ for simplicity). It follows that the vectorfield $\partial/\partial\lambda$ can be lifted when started from $\Phi_0^{-1}(\xi, \eta)$, and we conclude that all $\Phi_\lambda^{-1}(\xi, \eta)$ are homeomorphic.

The Milnor fibre of f_λ arises from the Milnor fibre of (x, f_λ) by attaching n -cells for each intersection point of $F_\lambda = \Phi^{-1}(D_x^2 \times \{\eta\})$ with the polar curve, counted with multiplicities. The number of intersection points depends on the polar ratios.

For the Euler characteristic, it suffices to count cells for $\lambda = 1$ and $\lambda = 0$. The cells are attached in the preimages of the intersection points of the line $v = \eta$ with the Cerf diagram. Since Δ_0 and Δ_1 are connected by a topological trivial family Δ_λ and $\Gamma_\lambda \rightarrow \Delta_\lambda$ is a branched covering, we see that $\chi(F_1)$ is the sum of $\chi(F)$ and a part which comes from the intersection points of the Θ_i . That this gives rise to a total number of $\sum d_i \mu_i^b \theta_i$ n -cells to be attached, can be seen by closer inspection of the proof of lemma 6.2.13. \square

(6.2.15) Example We give some applications of the preceding formula, which show, that it is really stronger than existing formulae.

– *Yomdin series*

For Yomdin series $f + \lambda x^N$ we have that $\theta_i = N$ for all i . We obtain the Lê attaching formula

$$\chi(F_1) = \chi(F) + (-1)^n (\Sigma \cdot Z(x)).$$

– The $W_1^\#$ -series

See Example 6.2.10 (b) for the definition of $W_{1,p}$ and its polar ratios. We have $\mu^b = 1$, $d = 2$, $\theta = 6 + \frac{1}{2}p$. Furthermore $\chi(F) = 2 - \mu(F) = 2 - 4 = -2$ (see Appendix A). So

$$\chi(F_1) = -2 - 12 - p = 14 - p.$$

This can be confirmed in Appendix A.

– The singularities E_{6k+1}

Let $f_\lambda(x, y) = y^3 + \lambda y x^{2k+1}$. The singularity $g = f_1$ is of type E_{6k+1} . The polar curve of f_λ consists only of $\Sigma_\lambda = Z(3y^2 + \lambda x^{2k+1})$. It gives rise to the polar ratio $\theta = (6k + 3)/2$. Observe that $d = 1$ and that $d\theta$ is not an integer. Of course $\mu^b = 2$. We obtain

$$\chi(F_1) = 3 - (6k + 3) = -6k,$$

hence $\mu(g) = 6k + 1$. Note that other methods, such as the one presented in section 6.4 do not include this example.

6.3 The polar filtration and the zeta-function

(6.3.1) We use the same notations as in the previous section. For $\lambda = 0$ and $\lambda = 1$ we can do the following, which is familiar from Lê's work. Choose in D_ε^2 concentric discs of increasing radii

$$\{0\} = D_{00} \subset D_{01} \subset \cdots \subset D_{0p} = D_\varepsilon^2$$

such that the intersection of all branches of the Cerf diagram Δ with first Puiseux exponent ρ_{0i} intersect $D_\varepsilon^2 \times \{\eta\}$ precisely in $(D_{0i} \setminus D_{0,i-1}) \times \{\eta\}$. Analogously, there are discs

$$\{0\} = D_{10} \subset D_{11} \subset \cdots \subset D_{1q} = D_\varepsilon^2$$

for g instead of f . The reason that this is possible — after adjusting η if necessary — is that the ρ_{ij} are increasing. However, the pictures above show that the level $v = \eta$ is not good enough for smaller values of λ . This is because the coefficients $a(\lambda)$ will dominate the situation (of course for *very* small η' it looks just as the level η in the case $\lambda = 1$).

Lifting these filtrations to the Milnor fibres F_0 and F_1 gives filtrations

$$F_{00} \subset F_{01} \subset \cdots \subset F_{0p} = F_0,$$

with $F_{0i} = \Phi^{-1}(D_{0i})$, and, analogously

$$F_{10} \subset F_{11} \subset \cdots \subset F_{1q} = F_1,$$

which are called the *polar filtrations* of f and g , respectively.

(6.3.2) The following definitions and notations are taken from [52]. Consider $\widetilde{H}_{n-1}(F_i^b)$. In 1.1.6 we already encountered the *vertical* and *horizontal* monodromies on $\widetilde{H}_{n-1}(F_i^b)$:

- (a) The *vertical* monodromy $A_i : \widetilde{H}_{n-1}(F_i^b) \rightarrow \widetilde{H}_{n-1}(F_i^b)$, which is the characteristic mapping of the local system over the punctured disc $\Sigma_i \setminus \{0\}$.
- (b) The *horizontal* monodromy $T_i : \widetilde{H}_{n-1}(F_i^b) \rightarrow \widetilde{H}_{n-1}(F_i^b)$, which is the monodromy of the Milnor fibration of the isolated singularity of f restricted to the transversal slice.

The names horizontal and vertical arise from the Cerf diagram. Observe that A_i and T_i commute, since they are defined on $(\Sigma_i \setminus \{0\}) \times S_\eta^1$, which is homotopy equivalent to a torus.

In Proposition 3.5.4, we encountered a formula for the zeta-function for topological series of plane curve singularities in terms of polar ratios. Our idea is, that this formula is valid in a much wider context. This leads to the following problem:

(6.3.3) Problem *Determine conditions for f and g as in the previous section (probably involving the conditions (a)-(f)), such that the following holds: Suppose $d_i\theta_i$ is an integer for all $i \leq r$, then*

$$\zeta_g(t) = \zeta_f(t) \cdot \left(\prod_{i=1}^r \det(I - t^{d_i\theta_i} A_i T_i^{d_i\theta_i}) \right)^{(-1)^{n+1}}.$$

(where $d_i = \Sigma^{\text{red}} \cdot Z(x)$).

There are three stages of increasing difficulty in giving a full answer to the problem.

The first stage is to restrict ourselves to functions f with only transversal A_1 singularities. That makes everything easier, since we can then assume that the number of branches of C_λ remains constant.

The second stage is to remove the restriction of transversal A_1 -singularities. This immediately leads to various difficulties. For example, at present it is not

clear to us which conditions we have to impose in order that the curves C_λ evolve with time in a reasonable fashion.

The third stage goes even beyond the statement of the problem: remove the condition that the $d_i\theta_i$ must be integers. For example, the E_{6k+1} case mentioned earlier is in this category, and we would like this case within our theory. Examples show, that in this case the transversal singularities split into singularities of lower Milnor number, and that *powers* of the local vertical monodromies come in.

A strategy in attacking the problem is first to find out under which conditions the following holds:

(6.3.4) *There is an embedding $e : F_0 \rightarrow F_1$ from the Milnor fibration of f to the Milnor fibration of g , in such a way that e_* is a monomorphism which maps each $H_n(F_{0i}, F_{0,i-1})$ to the corresponding pair $H_n(F_{1j}, F_{1,j-1})$ belonging to the same polar ratio. Furthermore, the monodromy of f on $H_n(F_{0i}, F_{0,i-1})$ equals the monodromy of g on $H_n(F_{1j}, F_{1,j-1})$.*

The polar filtrations and the embedding e will not ‘commute’; in general, we will have only a relationship of the homology groups of consecutive pairs.

If we look closely at the definition of the topological series of 3.2.3 using the alternative description of the Waldhausen decomposition of [26], which arises from the polar filtration, one sees that 6.3.4 is true for $n = 1$.

If one finds the right context where 6.3.4 is true, then 6.3.3 will follow without much effort. The conditions (a)–(f) are expected to fulfil a central role. The interest in these problems lies entirely in the promising prospects for a starting point for *polar series*. Indeed, as soon as 6.3.3 holds for a certain class of functions, one will have the possibility of introducing a particularly fine concept of series.

6.4 Another formula for the zeta-function of $f + \lambda\varphi$

(6.4.1) The basic idea of the previous section started from the polar ratios within the series (but they alone are not enough). For Yomdin series $f + \lambda x^N$ a central fact is that — in the notation of the last section — C_λ remains fixed for all λ , and the Cerf diagram of f can be mapped diffeomorphically onto the Cerf diagram of $f + \lambda x^N$ using $(u, v) \mapsto (u, v + \lambda u^N)$ (cf. [52]).

If we look at our case $g = f + \lambda\varphi$, we can get the same two properties if we look at the pair $Q = (\varphi, f)$. In this pair, f is regarded as a fixed function with a one dimensional singular locus, whereas φ varies. Although this may be

further away from the series concept, we can prove a strong formula, analogous to 6.3.3.

Observe that $Q = (\varphi, f)$ defines the same space as $Q_\lambda = (\varphi, f + \lambda\varphi)$ and also the same critical space C . The space C will in general not be a particularly nice space. Of course we will have to put some constraints on Q .

We do not assume that Q is an isolated complete intersection singularity. As always, the Yomdin series should be incorporated within our theory. For a Yomdin series, $Q = (x^N, f)$ and the critical space C consists of the polar curve and the singular locus of f , as well as of the space $Z(x^{N-1})$, a non-reduced hyperplane.

The methods are closely related to work of Siersma [52] and Némethi [32].

(6.4.2) The map germ $Q : (\mathbb{C}^{n+1}, 0) \rightarrow (\mathbb{C}^2, 0)$ is assumed to be surjective. In the target space we use (u, v) as coordinates. We denote by $D = Q(C)$ the discriminant space, which is one-dimensional with a possible 0-dimensional embedded component at the origin. Let $D = D_1 \cup \dots \cup D_s$ be its decomposition in irreducible components. It is always possible to stratify Q such that Q satisfies the Thom conditions on the strata. In particular, between the strata upstairs and downstairs, Q is submersive. We may assume that we have chosen a representative of Q such that the strata downstairs are $\{0\}$, $\cup_{i=1}^s (D_i \setminus \{0\})$ and $\mathbb{C}^2 \setminus D$, cf. [23].

(6.4.3) Let $\Sigma = \Sigma_1 \cup \dots \cup \Sigma_r$ be the (one-dimensional) singular locus of f . In the sequel, we assume that $\varphi : (\mathbb{C}^{n+1}, 0) \rightarrow (\mathbb{C}, 0)$ satisfies:

- (a) $\Sigma \cap Z(\varphi) = \{0\}$;
- (b) $f + \lambda\varphi$ has an isolated singularity for all $\lambda \neq 0$;
- (c) $Q = (\varphi, f)$ is surjective;
- (d) the branches of D are either equal to the u -axis, the v -axis or tangent to the v -axis.

It is possible that these conditions are too strong. In [52], the same conditions appear with φ linear, although they are not presented in their utmost detail.

In the critical set C , one can distinguish four kinds of subspaces: $C_{\varphi=0} = C \cap Q^{-1}(Z(u))$, $C_0 = C \cap Q^{-1}(0, 0)$, $C_{f=0} = \overline{Q^{-1}(Z(v))} \setminus C_0$ and Γ , the preimage of the branches of D tangent but unequal to the v -axis. The conditions imply

$$C = C_{f=0} \cup C_0 \cup C_{\varphi=0} \cup \Gamma$$

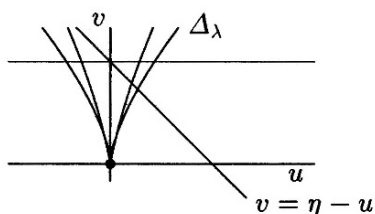
(this is not the decomposition of C into irreducible components).

(6.4.4) Lemma Q maps each branch of Σ onto the u -axis, and no other parts of C lie above it. I.e. $C_{f=0} = \Sigma$.

Proof. Observe that φ cannot be constant because of the first condition. A straightforward computation shows, that a curve in C with limit point in $f^{-1}(0) \cap \varphi^{-1}(0)$ lying above the u -axis but not in Σ must be contained in C_0 . \square

In many examples (see the end of this section) Γ is one-dimensional, whereas $C_{\varphi=0}$ is high dimensional (e.g. codimension 1). However, we do not demand anything of these dimensions (except of course of the dimension of Σ).

The general picture of the discriminant space is the following:



Observe that the preimage of $v = \eta$ is the Milnor fibre of f . The preimage of $v = \eta - \lambda u$ is the Milnor fibre of $f + \lambda\varphi$: in fact, if we consider both Q and $Q_\lambda = (\varphi, f + \lambda\varphi)$, then their discriminant spaces are diffeomorphic by an ambient linear diffeomorphism

$$h_\lambda : (u, v) \mapsto (u, v + \lambda u)$$

which satisfies $h_\lambda Q = Q_\lambda$; and therefore it is indeed possible to view the Milnor fibre of $f + \lambda\varphi$, the set $Q_\lambda^{-1}(\{v = \eta\})$, as $Q^{-1}(\{v = \eta - \lambda u\})$.

Although, for instance, over the v -axis, Q is in general very singular, the general idea of [52] can be applied: using “rotation” of $v = \eta$ we can compare the Milnor fibres of f and g by looking at the preimages of the intersection points of $v = \eta - \lambda u$ with the u -axis (which lie on the singular locus of f , Σ).

(6.4.5) Lemma *There is an embedding $e : F_0 \rightarrow F_1$ from the Milnor fibre $F = F_0$ of f into the Milnor fibre F_1 of g . We have the exact sequence*

$$0 \rightarrow H_n(e(F)) \rightarrow H_n(F_1) \rightarrow H_n(F_1, e(F)) \rightarrow H_{n-1}(e(F)) \rightarrow 0.$$

$H_n(e(F))$ is isomorphic to $H_n(F)$ and, moreover, the geometric monodromy $h_f : H_n(F) \rightarrow H_n(F)$ of f is equal to the restriction of the monodromy h_g to $H_n(e(F))$.

Proof. The proof of [52] extends to this case.

As usual, our (u, v) coordinates are in a polydisc $D_\varepsilon^2 \times D_\eta^2$. Let $\Delta = Q(\Gamma)$ be the irreducible components of the discriminant D tangent but not equal to the v -axis. Choose a disc $W \subset \{v = 0\}$ such that the intersection point $(0, \eta)$ of $v = \eta - \lambda u$ and the u -axis is outside W , but all the intersections of Δ with $v = \eta$ are within $W \times \{\eta\}$. This is possible since the branches of Δ can be written as $v = au^\alpha +$ higher order terms, with $a \neq 0$ and $\alpha < 1$ because of the fourth condition. (The proofs work also if $\alpha = 1$.)

With the help of the second isotopy lemma, we can lift the isotopy

$$\{v = \eta\} \cap (W \times D_\eta^2) \rightarrow \{v = \eta - \lambda u\} \cap (W \times D_\eta^2)$$

where we regard λ as a parameter, to obtain an embedding $e : F_0 \rightarrow F_1$.

The mapping Q is a stratified submersion. Therefore we need not be concerned about the behaviour of Q above the v -axis and the origin, and we can use the isotopy to obtain a geometric monodromy on $e(F_0)$. \square

(6.4.6) We still have to cope with the remainder $F_1 \setminus e(F_0)$. Let W_1 be a slightly larger disc (centred at the origin) than W . On $D_\varepsilon^2 \setminus W_1$, we may assume that the monodromy of f we used in the proof above, has the identity as u -component. Indeed, the intersections of the discriminant with $v = \eta$ are all inside $W \times \{\eta\}$. We use $W_1 \setminus W$ to glue them together.

This geometric monodromy extends from $(D_\varepsilon^2 \setminus W_1) \times S_\eta^1$ to $(D_\varepsilon^2 \setminus W_1) \times D_\eta^2$. This gives a monodromy T of Q .

For g , however, we have to take care of the intersection of $\{v = \eta\}$ and the extra line in the discriminant of $Q_1 = (\varphi, f + \varphi)$; translated in terms of Q : the u -axis has exactly one intersection point with the line $\{v = \eta - u\}$, which is the image of F_1 under Q . So the u component of the monodromy of g is induced by a full rotation around the origin. Let S be the diffeomorphism $F \setminus e(F_0) \rightarrow F \setminus e(F_0)$ which integrates a lift of this rotation vector field.

Now we can proceed exactly as in [52], p. 190, where it is proved that TS is the monodromy of g on $F_1 \setminus e(F_0)$. Again just as in [52] (p. 191), one proves:

(6.4.7) Lemma *Let a_i be the topological covering degree of the branched covering $Q : \Sigma_i \rightarrow \{v = 0\}$. Then*

$$H_n(F_1, e(F_0)) = \bigoplus_{i=1}^p \bigoplus_{j=1}^{a_i} H_{n-1}(F_{i,j}^b),$$

where $F_{i,j}^b$ are the Milnor fibres of the local singularities of Q in the a_i intersection points of Σ_i with the Milnor fibre of $g = f + \varphi$. These Milnor fibres $F_{i,j}^b$

($1 \leq j \leq a_i$) can be identified with the typical Milnor fibre F_i^b of the transversal singularity along $\Sigma_i \setminus \{0\}$. \square

Observe that $a_i = Z(\varphi) \cdot \Sigma_i^{\text{red}}$.

Now consider the exact sequence of the pair $(F_1, e(F))$:

$$0 \longrightarrow H_n(e(F)) \longrightarrow H_n(F_1) \longrightarrow H_n(F_1, e(F)) \longrightarrow H_{n-1}(e(F)) \longrightarrow 0$$

As in Siersma [52] and Némethi [32], we establish that the characteristic polynomial of h_{rel} , the monodromy on $H_n(F_1, e(F))$, is:

$$\prod_{i=1}^r \det(t^{a_i} I - A_i T_i^{a_i}),$$

where A_i and T_i are the vertical and horizontal monodromies, respectively. A consequence of this is the following formula for the zeta-function:

(6.4.8) Theorem *Suppose f and $g = f + \lambda\varphi$ satisfy the conditions of this section, A_i and T_i are the vertical and horizontal monodromies of f along the branch Σ_i of the one-dimensional singular locus of f , and $a_i = Z(\varphi) \cdot \Sigma_i^{\text{red}}$. Then*

$$\zeta_g(t) = \zeta_f(t) \cdot \left(\prod_{i=1}^r \det(I - t^{a_i} A_i T_i^{a_i}) \right)^{(-1)^{n+1}}$$

For the Euler characteristics of the Milnor fibres of f and g , this formula reads:

$$\chi(F_g) = \chi(F_f) + (-1)^n \sum_{i=1}^r a_i \mu_i^b.$$

(6.4.9) Remark We observed earlier that Yomdin series $f + x^N$ left gaps, i.e. we could not always obtain Milnor numbers increasing with steps of 1. When we now vary φ in the pair (φ, f) , the steps are smaller, but can still be 'large'. For instance, if f has only transversal A_2 singularities, Theorem 6.4.8 shows that the Milnor numbers of $f + \lambda\varphi$ can only increase by even numbers. Therefore it is no surprise that the case E_{6k+1} , where $f(x, y) = y^3$ and $\varphi(x, y) = x^{2k+1}y$ is left out. Indeed, the pair (f, φ) does not satisfy the conditions. Yet the number of functions satisfying the conditions is considerable.

(6.4.10) Example We finish by giving some examples.

- *The Yomdin series again*

We have $\varphi = x^N$. The critical space of $Q = (x^N, f)$ consists of $Z(x^{N-1})$, Σ and the polar curve Γ with respect to the direction x . The condition that Δ be tangent to the v -axis implies that $N > \theta_i$ for all i . We retrieve the meanwhile very familiar formula.

– The T -series

Let $f(x, y, z) = xyz$ and $\varphi = x^p/p + y^q/q + z^r/r$. Then the critical space of $Q = (\varphi, f)$ consists of Σ (the three coordinate axes) and Γ , a curve which can be parametrized by

$$(x, y, z) = (t^{qr}, t^{pr}, t^{pq}).$$

So Δ has parametrization

$$\begin{aligned} u &= (1/p + 1/q + 1/r)t^{pqr} \\ v &= t^{pq+pr+qr} \end{aligned}$$

hence the formula for the zeta-function holds whenever $1/p + 1/q + 1/r < 1$ (even ≤ 1). Since A_i is the identity and $T = (-1)$, we obtain

$$\zeta_{T,p,q,r}(t) = ((1 - t^p)(1 - t^q)(1 - t^r))^{-1},$$

since $T_{\infty,\infty,\infty}$ has trivial ζ -function.

(6.4.11) Quasi-homogeneous singularities

Let f be quasi-homogeneous of type $(w_0, \dots, w_n; d)$ with a one-dimensional singular locus $\Sigma = \Sigma_1 \cup \dots \cup \Sigma_r$. Suppose that the weights are normalized such that $\gcd(w_0, \dots, w_n) = 1$. For $\sigma \in \{1, \dots, r\}$, we define

$$\begin{aligned} I_\sigma &= \{i \mid x_i \equiv 0 \text{ on } \Sigma_\sigma\}, \\ J_\sigma &= \{i \mid x_i \not\equiv 0 \text{ on } \Sigma_\sigma\}, \\ k_\sigma &= \gcd\{w_j \mid j \in J_\sigma\}. \end{aligned}$$

The following proposition was proved by Dimca [12], Proposition 3.19(i).

(6.4.12) Proposition *Suppose there exists a $\varphi \in \mathcal{O}_{n+1}$ such that $f + \varepsilon\varphi$ is isolated for some $\varepsilon \neq 0$ and which is quasi-homogeneous of the same quasi-homogeneous type $(w; d)$. Suppose that (f, φ) satisfies the conditions of this section, cf. 6.4.3. Then*

$$b_n(f) - b_{n-1}(f) = \prod_{i=0}^n \frac{d - w_i}{w_i} - d \sum_{\sigma=1}^r \frac{\mu_\sigma^b}{k_\sigma},$$

where $b_q(f)$ is the rank of $\widetilde{H}_q(F_f)$.

Proof. It is well-known that if there exists an isolated quasi-homogeneous singularity of type $(w; d)$, it belongs to a unique μ -class. Let $g = f_{w,d}^{\text{reg}}$ denote a typical element of this class. According to 6.4.8, we have for g :

$$\mu_*(g) = \mu_*(f) + \sum_{\sigma=1}^r a_\sigma \mu_\sigma^b,$$

where $a_\sigma = \Sigma_\sigma^{\text{red}} \cdot Z(\varphi)$. Now φ consists of monomials $\alpha_m x^m$ (written in multi-index notation: $m = (m_0, \dots, m_n)$). Not all of these monomials vanish entirely on Σ_σ . Choose such a monomial $\alpha_m x^m$. Observe that for $j \in J_\sigma$ we have that $\Sigma_\sigma^{\text{red}} \cdot x_j = w_j/k_\sigma$. So

$$a_\sigma = \sum_{j \in J_\sigma} m_j (\Sigma_\sigma^{\text{red}} \cdot x_j) = (1/k_\sigma) \sum_{j \in J_\sigma} m_j w_j = d/k_\sigma.$$

Since $\mu_*(f_{w,d}^{\text{reg}}) = \prod_{i=0}^n (d - w_i)/w_i$ (cf. [5]), this proves the formula. \square

Theorem 6.4.8 also gives the zeta-function, so we can generalise the above Proposition. It is known that the spectrum of $g = f_{w,d}^{\text{reg}}$ is

$$\text{Spp}(g) = \sum_{\alpha \in \mathbf{Q}} c_\alpha (\alpha - 1, n),$$

where c_α is found by writing out

$$\prod_{i=0}^n \frac{t - t^{w_i/d}}{t^{w_i/d} - 1} = \sum_{\alpha \in \mathbf{Q}} c_\alpha t^\alpha,$$

see [46], Example 5.2. We can therefore compute the zeta-function of $f_{w,d}^{\text{reg}}$ as in Remark 4.3.2. We know that $a_\sigma = d/k_\sigma$, and according to a personal note by Dimca, we have

$$A_\sigma T_\sigma^{a_\sigma} = \text{Is}_\sigma,$$

where Is_σ is the *isotropy action*, whose order is k_σ , which is the action on $\widetilde{H}_{n-1}(F_\sigma^b)$ induced by multiplication by $\exp(2\pi i/k_\sigma)$. If this action is known, then $\zeta_f(t)$ can be computed explicitly. We have proved:

(6.4.13) Proposition

$$\zeta_f(t) = \zeta_{f_{w,d}^{\text{reg}}}(t) \cdot \prod_{\sigma=1}^r \det(I - t^{a_\sigma} \text{Is}_\sigma)^{(-1)^n} \quad \square$$

(6.4.14) Example Take $f(x, y) = y^4 + y^2x^3$. Then $w_0 = 2$, $w_1 = 3$ and $d = 12$. We get that

$$\zeta_{f_{w,d}^{\text{reg}}}(t) = \frac{(1 - t^{12})^2}{(1 - t^6)(1 - t^4)}.$$

Furthermore $k = 2$, $\mu^b = 1$ (transversal type A_1) and $a = 6$. Therefore $\det(I - t^a \text{Is}) = 1 + t^6$. Hence

$$\zeta_f(t) = (1 - t^{12})/(1 - t^4).$$

This can be confirmed in Appendix A ($W_{1,\infty}$).

APPENDIX A

The EN-diagrams of the Arnol'd series

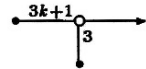
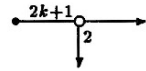
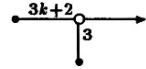
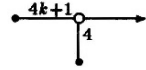
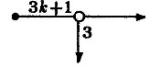
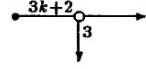
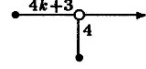
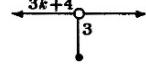
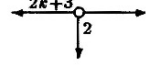
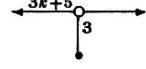
In this appendix the EN-diagrams of the series of plane curve singularities listed in [5] are drawn.

The first part consists of the *exceptional families* E ., W . and Z .. We also give the Milnor number and the set of polar ratios. These examples belong to the topological series of y^3 , xy^3 or y^4 . They are interesting, because some of them are not part of other descriptions of 'series'.

The second part contains the *infinite series* A , D , J , W , $W^\#$, X , Y and Z . All variants are given. In the tables, we have that:

- (a) μ = the Milnor number;
- (b) N_0 and the graph constant c are as in Theorem 3.3.2;
- (c) ζ_∞ is the zeta-function of the non-isolated head; the zeta-function of a member of the series can be obtained by multiplying with $1 - t^{N+c}(-1)^N$.
- (d) \mathfrak{p}_∞ is the set of polar ratios of the non-isolated head; the polar ratios of a member of the series can be computed using the formula in section 2.8, each branch of the singular locus gives a new polar ratio.

In order to save space, we sometimes write '—' in the equations. This means that one has to prepend the equation with the equation of the corresponding head of the series.

| Name | Formula | μ | EN-diagram | $\mathfrak{p}(f)$ |
|-------------|---------------------------------|-----------|---|------------------------|
| E_{6k} | $y^3 + x^{3k+1}$ | $6k$ |  | $3k + 1$ |
| E_{6k+1} | $y^3 + x^{2k+1}y$ | $6k + 1$ |  | $3k + \frac{3}{2}$ |
| E_{6k+2} | $y^3 + x^{3k+2}$ | $6k + 2$ |  | $3k + 2$ |
| W_{12k} | $y^4 + x^{4k+1}$ | $12k$ |  | $4k + 1$ |
| W_{12k+1} | $y^4 + yx^{3k+2}$ | $12k + 1$ |  | $4k + \frac{4}{3}$ |
| W_{12k+5} | $y^4 + yx^{3k+2}$ | $12k + 5$ |  | $4k + \frac{8}{3}$ |
| W_{12k+6} | $y^4 + yx^{3k+3}$ | $12k + 6$ |  | $4k + 3$ |
| Z_{6k+11} | $x(y^3 + yx^{2k+3} + x^{3k+4})$ | $6k + 11$ |  | $4, 3k + 5$ |
| Z_{6k+12} | $x(y^3 + yx^{2k+3} + x^{3k+5})$ | $6k + 12$ |  | $4, 3k + \frac{11}{2}$ |
| Z_{6k+13} | $x(y^3 + yx^{2k+4} + x^{3k+5})$ | $6k + 13$ |  | $4, 3k + 6$ |

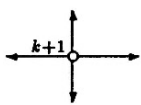
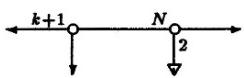
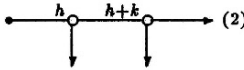
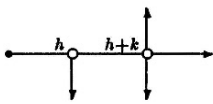
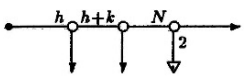
| Name | Formula | μ | EN-diagram | |
|----------------|----------------------------|----------|------------|---|
| A_∞ | y^2 | 0 | | $\zeta_\infty = \frac{1}{1-t^2}$ |
| A_0 | y | 0 | | $p \geq 2, N = p + 1,$ |
| A_1 | $y^2 + x^2$ | 1 | | $N_0 = 1, c = 0$ |
| A_p | $y^2 + x^{p+1}$ | p | | $\mathfrak{p}_\infty = \emptyset$ |
| D_∞ | xy^2 | 1 | | $\zeta_\infty = 1$ |
| D_4 | $xy^2 + x^3$ | 4 | | $p \geq 5, N = p - 2,$ $N_0 = 2, c = 1$ |
| D_p | $xy^3 + x^{p-1}$ | p | | $\mathfrak{p}_\infty = \{3\}$ |
| $J_{k,\infty}$ | $y^3 + x^k y^2$ | $3k-2$ | | $\zeta_\infty = \frac{1-t^{3k}}{1-t^3}$ |
| $J_{k,0}$ | $y^3 + x^k y + x^{3k}$ | $6k-2$ | | $k \geq 2, p \geq 1, c = k$ $N = p+2k, N_0 = 2k$ |
| $J_{k,p}$ | $y^3 + x^k y^2 + x^{3k+p}$ | $6k-2+p$ | | $\mathfrak{p}_\infty = \{3k\}$ |

| Name | Formula | μ | EN-diagram | |
|-------------------|----------------------|------------|------------|--|
| $W_{k,\infty}$ | $y^4 + y^2 x^{2k+1}$ | $8k+1$ | | $\zeta_\infty = \frac{1-t^{8k+4}}{1-t^4}$ |
| $W_{k,0}$ | $- + x^{4k+2}$ | $12k+3$ | | $k \geq 1, p \geq 1,$ $N = p + 2k + 1;$ $\mathfrak{p}_\infty = \{4k + 2\}$ |
| $W_{k,p}$ | $- + x^{4k+2+p}$ | $12k+3+p$ | | $N_0 = 2k + 1,$ $c = 2k + 1$ |
| $W_{k,\infty}^\#$ | $(y^2 + x^{2k+1})^2$ | $4k$ | | $\zeta_\infty = \frac{1-t^{4k+2}}{1-t^4}$ |
| $W_{k,2q-1}^\#$ | $- + yx^{3k+1+q}$ | $12k+2q+2$ | | $k \geq 1, q \geq 1,$ $c = 0$ |
| $W_{k,2q}^\#$ | $- + y^2 x^{2k+1+q}$ | $12k+2q+3$ | | $N = 8k + 2q + 3$ $N' = 8k + 2q + 4$ |
| X_∞ | $y^4 + x^2 y^2$ | 5 | | $\zeta_\infty = 1 - t^4$ |
| X_9 | $- + x^4$ | 9 | | $p \geq 10, N = p - 7,$ $N_0 = 2, c = 2$ |
| X_p | $- + x^{4+p-9}$ | p | | $\mathfrak{p}_\infty = \{4\}$ |

"—" means: include equation of non-isolated head of the series.

| Name | Formula | μ | EN-diagram | |
|-----------------------|-------------------------------|----------------------|------------|--|
| $X_{h,\infty}$ | $y^4 + x^h y^3 + x^{2h} y^2$ | $8h-3$ | | $\zeta_\infty = \frac{(1-t^{4h})^2}{1-t^4}$ |
| $X_{h,0}$ | $- + x^{3h} y$ | $12h-3$ | | $h \geq 2, p \geq 1,$ $N = p + 2h,$ $N_0 = 2h, c = 2h$ |
| $X_{h,p}$ | $- + x^{4h+p}$ | $12h-3+p$ | | $\mathfrak{p}_\infty = \{4h\}$ |
| $Y_{\infty,\infty}$ | $x^2 y^2$ | 4 | | $\zeta_{\infty,\infty} = 1$ |
| $Y_{r,\infty}$ | $y^{4+r} + x^2 y^2$ | $r+5$ | | $r, s \geq 1,$ $c_1 = c_2 = 2$ |
| $Y_{r,s}$ | $y^{4+r} + x^2 y^2 + x^{4+s}$ | $9+r+s$ | | $\mathfrak{p}_\infty = \{4\}$ |
| $Y_{\infty,\infty}^h$ | | $4h-2$ | | $h \geq 2; r, s \geq 1$ |
| $Y_{r,s}^h$ | See [5], p. 248 | $12h-3$ $+ r + s$ | | $\mathfrak{p}_\infty = \{4h\}$ |

"—" means: include equation of non-isolated head of the series.

| Name | Formula | μ | EN-diagram | |
|------------------|---------------------|--------------|---|--|
| $Z_{k,\infty}$ | $xy^3 + x^{k+2}y^2$ | $3k+5$ |  | $\zeta_\infty = 1 - t^{3k+4}$ |
| $Z_{k,0}$ | $- + x^{3k+4}$ | $6k+9$ |  | $k, p \geq 1, c = k + 2$ $N = p + 2k + 2,$ $N_0 = 2k + 2$ |
| $Z_{k,p}$ | $- + x^{3k+4+p}$ | $6k+9+p$ |  | $\mathfrak{p}_\infty = \{4, 3k + 4\}$ |
| $Z_{k,\infty}^h$ | | $8h+3k-3$ |  | $\zeta_\infty = \frac{(1-t^{4h})(1-t^{4h+3k})}{1-t^4}$ |
| $Z_{k,0}^h$ | See [5], p. 249 | $12h+6k-3$ |  | $h \geq 2, k, p \geq 1,$ $N = p + 2h + 2k,$ $N_0 = 2h + 2k,$ $c = 2h + k$ |
| $Z_{k,p}^h$ | See [5], p. 249 | $12h+6k-3+p$ |  | $\mathfrak{p}_\infty = \{4h, 4h + 3p\}$ |

“—” means: include equation of non-isolated head of the series.

References

- [1] N. A'Campo, Le groupe de monodromie du déploiement des singularités isolées de courbes planes I, *Math. Annalen*, **213** (1975), pp. 1–32.
- [2] N. A'Campo: La fonction zêta d'une monodromie, *Comm. Math. Helv.* **50** (2) (1975), pp. 233–248.
- [3] V.I. Arnol'd: Local normal forms of functions, *Invent. Math.* **35** (1976), pp. 87–109. Also in Russian in *Uspekhi Math. Nauk*, tome XXX (5) (1975), pp. 3–65.
- [4] V.I. Arnol'd: Critical Points of Functions on a Manifold with Boundary, the Simple Lie Groups B_k , C_k , F_4 and Singularities of Evolutes, *Uspekhi Mat. Nauk* **33** (5) (1978) pp. 91–105.
- [5] V.I. Arnol'd, S.M. Gusein-Sade, and A.N. Varchenko: *Singularities of Differentiable Maps I*, Birkhäuser, 1985.
- [6] V.I. Arnol'd, S.M. Gusein-Sade, and A.N. Varchenko: *Singularities of Differentiable Maps II*, Birkhäuser, 1988.
- [7] E. Brieskorn: *Über die Auflösung gewisser Singularitäten von holomorphen Abbildungen*, *Math. Annalen* **166** (1966), pp. 76–102.
- [8] E. Brieskorn and H. Knörrer: *Ebene Algebraische Kurven*, Birkhäuser, 1981.
- [9] R.-O. Buchweitz and G.-M. Greuel: The Milnor Number and Deformations of Complex Curve Singularities, *Invent. Math.*, **58** (1980), pp. 241–281.
- [10] P. Deligne: *Le formalisme des cycles évanescents*, SGA VII², Springer LNM **340** (1973), pp. 82–115.
- [11] A. Dimca: Function germs defined on isolated hypersurface singularities, *Compositio* **53** (1984), pp. 245–258.

- [12] A. Dimca: On the Milnor Fibration of Weighted Homogeneous Polynomials, *Compositio* **76** (1990), pp. 19–47.
- [13] W. Ebeling: *The Monodromy Groups of Isolated Singularities of Complete Intersections*, Springer LNM **1293**, 1987.
- [14] D. Eisenbud and W.D. Neumann: *Three-Dimensional Link Theory and Invariants of Plane Curve Singularities*, Annals of Mathematics Study 110, Princeton U.P., 1985.
- [15] C.G. Gibson, K. Wirthmüller, A.A. du Plessis and E.J.N. Looijenga: *Topological Stability of Smooth Mappings*, Springer LNM **552**, 1976.
- [16] V.V. Goryunov: *An Intersection Form of a Plane Isolated Line Singularity*, July 1989, to appear in the Proceedings of the Warwick Symposium on Singularities, 1989.
- [17] M.-C. Grima: La monodromie ne détermine pas la topologie d'une hypersurface complexe, *Fonctions de plusieurs variables complexes*, Springer LNM **409**, pp. 580–602, 1974.
- [18] F. Hirzebruch: The Topology of Normal Singularities of an Algebraic Surface, *Séminaire Bourbaki*, 15e année 1962–1963, Fasc. 2, exposé 250.
- [19] Th. de Jong: Some Classes of Line Singularities, *Math. Zeit.* **198** (1988), pp. 493–517.
- [20] Lê D.T.: Sur un critère d'équisingularité, *Comptes Rendus* **272** (1971), pp. 138–140.
- [21] Lê D.T.: Calcul du nombre de cycles évanouissants d'une hypersurface complexe, *Ann. Inst. Fourier*, Grenoble, **23** (4) (1973), pp. 261–270.
- [22] Lê D.T.: La monodromie n'a pas de points fixes, *J. Fac. Sci. Univ. Tokyo*, Sec. 1A, **22** (1975), pp. 409–427.
- [23] Lê D.T.: Some Remarks on Relative Monodromy, *Real and Complex Singularities* ed. P. Holm, Sijthoff-Noordhoff, Alphen aan den Rijn, 1977, pp. 397–403 ('Oslo').
- [24] Lê D.T.: The geometry of the monodromy theorem, *C.P. Ramanujam—A Tribute*, Studies in Mathematics **8**, Tata Institute of Fundamental Research, 1978, pp. 157–173.
- [25] Lê D.T.: Ensembles analytiques complexes avec lieu singulier de dimension un (d'après I.N. Yomdin), *Séminaire sur les singularités*, Publ. Math. Univ. Paris VII, 1980, pp. 87–95.

- [26] Lê D.T., F. Michel, C. Weber: *Courbes polaires et topologie des courbes planes*, Preprint July 1988; to appear in *Ann. de l'Ec. Norm. Sup.*.
- [27] Le Van Tanh and J.H.M. Steenbrink: *Le spectre d'une singularité d'un germe de courbe plane*, preprint Max Planck Institut, Bonn, 1988 (MPI/88-3).
- [28] E.J.N. Looijenga: *Isolated Singular Points on Complete Intersections*, London Math. Soc. Lect. Note Series **77**, Cambridge, 1984.
- [29] D.B. Massey and D. Siersma: *Deformation of Polar Methods*, Preprint Utrecht no. 613, June 1990.
- [30] F. Michel and C. Weber: Sur le rôle de la monodromie entière dans la topologie des singularités, *Annales de l'Institut Fourier* **36**, 1(1986), pp. 183-218.
- [31] J. Milnor, *Singular Points of Complex Hypersurfaces*, Annals of Mathematics Study 61, Princeton U.P., 1968.
- [32] A. Némethi: *The Milnor fiber and the zeta-function of the singularities of type $f = P(h, g)$* , Preprint INCREST, Bucharest, 1989, to appear in *Compositio*.
- [33] W.D. Neumann: A Calculus for Plumbing, Applied to the Topology of Complex Surface Singularities and Degenerating Complex Curves, *Trans. A.M.S.* **268** (1981), pp. 299-344.
- [34] W.D. Neumann: Invariants of Plane Curve Singularities, *Noeuds, tresses et singularités*, Monograph de l'Enseign. Math. no. 31, 1983, pp. 223-232.
- [35] W.D. Neumann: Splicing Algebraic Links, in *Complex Analytic Singularities*, Advanced Studies in Pure Math. **8**, 1986, pp. 349-361.
- [36] R. Pellikaan: *Hypersurface Singularities and Resolutions of Jacobi Modules*, Thesis, Utrecht 1985.
- [37] R. Pellikaan: Finite Determinacy of Functions with Non-Isolated Singularities, *Proc. London Math. Soc.* (3) **57** (1988) pp. 357-382.
- [38] R. Pellikaan: Deformations of Hypersurfaces with a One-Dimensional Singular Locus, preprint Vrije Universiteit Amsterdam 1987, to appear in *Journal of Pure and Applied Algebra*.
- [39] R. Pellikaan: Series of Isolated Singularities, *Contemporary Mathematics* **90** (1989), Proceedings Iowa, ed. R. Randell.

- [40] F. Pham: *Singularités des courbes planes: Une introduction à la géométrie analytique complexe*, Cours de 3e cycle, Faculté des Sciences de Paris, année univ. 1969–1970.
- [41] D. Rolfsen: *Knots and Links*, Math. Lect. Series vol. 7, Publish or Perish, 1976.
- [42] M. Saito: *Vanishing Cycles and Mixed Hodge Modules*, preprint IHES, August 1988. See also: *On Steenbrink's Conjecture*, preprint RIMS 710, Kyoto, August 1990.
- [43] R. Schrauwen: *Topological Series of Isolated Plane Curve Singularities*, preprint Utrecht no. 544, February 1989.
- [44] R. Schrauwen: *Topological Series of Isolated Plane Curve Singularities*, *Enseignement Mathématique* **36** (1990), pp. 115–141.
- [45] R. Schrauwen: *Deformations and the Milnor Number of Non-Isolated Plane Curve Singularities*, preprint Utrecht no. 574, July 1989, to appear in the Proceedings of the Warwick Symposium on Singularities, 1989.
- [46] R. Schrauwen, J.H.M. Steenbrink and J. Stevens: *Spectral Pairs and the Topology of Curve Singularities*, preprint Utrecht no. 596, October 1989. To appear in the Proceedings of the Symposium on Complex Geometry and Lie Theory, Sundance, 1989, ed. J. Carlson.
- [47] Th. Schulze-Röbbecke: *Algorithmen zur Auflösung und Deformation von Singularitäten ebener Kurven*, Bonner Math. Schrift Nr. 96, Bonn 1977.
- [48] D. Siersma: *Isolated Line Singularities Proc. Symp. Pure Maths* **40** Vol. 2 (1983), pp. 485–496.
- [49] D. Siersma: *Singularities with Critical Locus a One-Dimensional Complete Intersection and Transversal Type A_1* , *Topology and its Applications* **27** (1987), pp. 51–73.
- [50] D. Siersma: *Hypersurfaces with Singular Locus a Plane Curve and Transversal Type A_1* , *Proc. Warsaw Semester on Singularities*, Banach Center Publ. **20**, PWN-Polish Scientific Publ., Warsaw 1988, pp. 397–410.
- [51] D. Siersma: *Variation Mappings on 1-Isolated Singularities*, preprint Utrecht no. 582, September 1989, to appear in *Topology*.
- [52] D. Siersma: *The Monodromy of a Series of Singularities*, *Comm. Math. Helv.* **65** (1990), pp. 181–197.
- [53] E.H. Spanier: *Algebraic Topology*, New York etc., McGraw-Hill, 1966.

- [54] J.H.M. Steenbrink: Mixed Hodge Structures on the Vanishing Cohomology, *Real and Complex Singularities*, ed. P. Holm, Sijthoff-Noordhoff, Alphen aan den Rijn, 1977, pp. 525–563 ('Oslo').
- [55] J.H.M. Steenbrink: Mixed Hodge Structures Associated With Isolated Singularities, *Proc. Symp. Pure Math.* **40** Vol. 2 (1983), pp. 513–536.
- [56] J.H.M. Steenbrink: The Spectrum of Hypersurface Singularities, *Théorie de Hodge*, Luminy Juin 1987, *Astérisque*, **179–180** (1989), pp. 163–184.
- [57] J.H.M. Steenbrink and S. Zucker: Polar curves, resolution of singularities, and the filtered mixed Hodge structure on the vanishing cohomology, in *Singularities, Representations of Algebras, and Vector Bundles (Proceedings Lambrecht 1985)*, Springer LNM **1273**, pp. 178–202, 1987.
- [58] J. Stevens: *Series*, private communication.
- [59] B. Teissier: Introduction to equisingularity problems, *Proc. Symp. Pure Maths* **29** (1975).
- [60] B. Teissier: Variétés Polaires I. Invariants polaires des singularités d'hypersurfaces, *Invent. Math.* **40** (1977), pp. 267–292.
- [61] C.T.C. Wall: Notes on the Classification of Singularities, *Proc. L.M.S.* **48** (1984), pp. 461–513.
- [62] C. Weber: *A Topological Interpretation for the Polar Quotients of an Algebraic Plane Curve Singularity*, preprint Genève, August 1987.
- [63] I.N. Yomdin, Complex surfaces with a 1-dimensional set of singularities, *Siberian Math. J.* **15** (5) (1974), pp. 1061–1082.
- [64] O. Zariski: *Le problème des modules pour les branches planes*, with an appendix by B. Teissier, Hermann, Paris, 1986.

Index

| | | | |
|--------------------------------|--------|--------------------------------|----------------|
| admissible | 75 | polar | |
| algebraicity condition | 12 | curve | 21, 74 |
| branches | 3 | ratio | 21, 75 |
| cable | 4 | Puiseux expansion | 6 |
| Cerf diagram | 21, 74 | quasi-homogeneous | 89 |
| codimension | 54 | resolution graph | 20 |
| $D[p, q]$ -point | 53 | rupture point | 20 |
| deformation | 57, 58 | Seifert form | 43, 45 |
| making p -parts smooth | 58 | series | 23, 26, 73 |
| network map | 57 | spectrum within | 50 |
| dot | 9 | polar | 77 |
| equivalence | | topological | 26 |
| analytical | 3 | Yomdin | 24, 78, 82, 89 |
| topological | 4 | zeta-function within | 31 |
| $j_I(f)$ | 54 | signature | 43 |
| link, algebraic | 4 | singularity, plane curve | 3 |
| linking number | 14 | spectral pairs | 40 |
| Milnor | | spectrum | 40 |
| fibration | 4 | within series | 50 |
| number | 4 | formula | 42 |
| monodromy | 4 | splice formula | 48 |
| horizontal | 5, 83 | splice condition | 12 |
| vertical | 5, 83 | splice decomposition | 13 |
| morsifications | 68 | splicing | 10 |
| splicing of | 69 | zeta-function | 17, 88 |
| multilink | 4 | and polar ratios | 83 |
| node | 9 | within series | 31, 88 |

Dankwoord

Op deze plaats wil ik enkelen bedanken die direct of indirect van invloed zijn geweest op dit proefschrift.

In de eerste plaats wil ik mijn promotor, Dirk Siersma, bedanken voor de bijzonder plezierige samenwerking en voor zijn ideeën en suggesties.

De inbreng van Jan Stevens mag niet vergeten worden. Met zijn opmerkingen wist hij altijd precies de kern van de zaak eruit te lichten en indien nodig had hij een opbeurend woord paraat. Ook Jozef Steenbrink wil ik bedanken voor de leerzame samenwerking, in het bijzonder tijdens de preparatie van [SSS].

Ik heb altijd uitermate graag mijn onderwijstaken vervuld. Vaak werkte ik met dezelfde collega's samen. Ik denk in het bijzonder aan Piet Lemmens; het was een groot genoegen drie jaar lang met hem de Topologie te verzorgen.

Met mijn voormalige kamergenoten van kamer 521, Arno Kuijlaars en Frans van Gool, had ik een aantal zeer gezellige jaren. Het was altijd leuk om met hen over diverse onderwerpen van gedachten te wisselen of samen iets uit te zoeken. De beschikbaarstelling van de *hop* door André de Meijer heb ik in hoge mate gewaardeerd.

Tenslotte wil ik mijn ouders bedanken, die mij altijd — niet in de laatste plaats financieel — gesteund hebben.

Samenvatting in het Nederlands

Series van singulariteiten zijn altijd een inspiratiebron geweest voor het onderzoek in de singulariteitentheorie. Niet dat er een definitie is van ‘series’, maar ze bestaan ontegenzeggelijk (Arnol’d schrijft: ‘series undoubtedly exist’). In dit proefschrift verhelderen we het begrip serie door voornamelijk naar de *topologische* aspecten te kijken.

We beschouwen kiemen van holomorfe functies $f : (\mathbb{C}^{n+1}, 0) \rightarrow (\mathbb{C}, 0)$. Dat wil zeggen: we bekijken holomorfe functies met $f(0) = 0$ en we beschouwen ze gelijk als ze overeenstemmen op een kleine omgeving van 0. Waar de gradiënt van zo’n functie verdwijnt, zit een singulier punt. Als alleen de oorsprong singulier is, dan spreken we over een geïsoleerde singulariteit.

Om te beginnen bekijken we het geval $n = 1$. In dat geval definieert f een vlakke kromme $X = f^{-1}(0)$. Als we X doorsnijden met een klein 3-sfeertje, dan ontstaat er een schakel K , waarvan de samenhangscomponenten precies overeenkomen met de priemfactoren van f . Het complement van de schakel is gevezeld (met de cirkel als basisruimte) door de afbeelding $f/|f|$. Deze vezeling heet de Milnorvezeling. Het is een van de belangrijkste invarianten van een singulariteit. In Hoofdstuk 1 wordt gememoreerd hoe men de schakel kan construeren en noteren door middel van een graaf, het zogenaamde EN-diagram (uitgevonden door Eisenbud en Neumann [14]). In Hoofdstuk 2 laten we zien hoe diverse topologische invarianten uit het EN-diagram zijn af te leiden.

In Hoofdstuk 3 bekijken we series van vlakke krommen. Een eenvoudig voorbeeld hiervan bestaat uit de functies $xy^2 + x^{p-1}$, door Arnol’d aangeduid met D_p . Intuïtief is duidelijk dat deze singulariteiten bij elkaar horen, en dat aan het ‘hoofd’ ervan de functie xy^2 staat (die de naam D_∞ heeft gekregen). Deze laatste functie heeft een niet-geïsoleerde singulariteit. We kunnen laten zien, dat de Milnorvezeling van een element van de serie ontstaat uit die van D_∞ door een omgeving van de singuliere locus weg te snijden en iets

terug te plakken op zo'n manier dat het resultaat de Milnorvezeling is van een geïsoleerde singulariteit. Met dit idee kunnen we *topologische series* definiëren. Zij voldoen aan de eigenschappen die we van de topologie van Arnol'ds series gewend zijn. Nadat we de definitie van topologische serie hebben gepresenteerd, laten we zien hoe verschillende bekende invarianten zich gedragen binnen de serie. Dit geeft ook een verband tussen het niet-geïsoleerde 'hoofd' van de serie en de rest: in het algemeen zijn geïsoleerde singulariteiten namelijk goed beschreven en niet-geïsoleerde niet.

Vele topologische invarianten hebben te maken met de monodromie van de Milnorvezeling. In Hoofdstuk 3 wordt bijvoorbeeld de zêta-functie van de monodromie berekend. Een stap verder is het spectrum, gedefinieerd door Arnol'd en Steenbrink. In Hoofdstuk 4 kijken we naar het spectrum binnen een serie, maar hiervoor moeten we eerst enkele algemene resultaten afleiden. Interessant is dat deze stellingen te maken hebben met voormalige vermoedens over het spectrum en over signaturen en Seifertvormen. Dit was aanleiding deze resultaten op te nemen in gezamenlijk werk met J. Steenbrink en J. Stevens [46].

Een van de mooiste artikelen over vlakke krommen is wel het artikel van A'Campo [1], dat een methode geeft om het Dynkin-diagram van de intersectievorm op de Milnorvezel uit te rekenen. Helaas is deze methode alleen voor geïsoleerde singulariteiten van toepassing. Om het voor niet-geïsoleerde singulariteiten en series geschikt te maken, is in ieder geval een goede deformatietheorie nodig. In Hoofdstuk 5 wordt de deformatietheorie van vlakke krommen volledig beschreven. Dit bouwt voort op werk van Pellikaan. Aan het eind wordt aangestipt wat men hiermee kan bereiken op het gebied van de Dynkin-diagrammen.

In Hoofdstuk 6 tenslotte verlaten we het terrein van de vlakke krommen en bestuderen series van hyperoppervlakken ($n \geq 1$). We nemen aan dat de niet-geïsoleerde singulariteit nog steeds een één-dimensionale singuliere locus bezit. De zaak ligt hier direct veel ingewikkelder. Een resultaat om naar te streven is een generalisatie van de formules voor de zêta-functie. We bieden twee methoden aan. De eerste is vooralsnog alleen geldig op het niveau van de Euler-karakteristiek. De tweede werkt goed, maar voor ons gevoel voldoen niet genoeg functies aan de voorwaarden. Het idee is, dat een preciese beschrijving van de functies waarvoor de eerste methode werkt, de weg kan openen naar een definitie van series van hyperoppervlakken.

Curriculum Vitae

De auteur is geboren op 20 mei 1964 te Rotterdam. Vanaf 1976 doorliep hij het Atheneum aan de Rijksscholengemeenschap F.A. Minkema te Woerden, waar hij in 1982 het VWO-diploma behaalde. In 1982 begon hij met de studie Wiskunde aan de Rijksuniversiteit te Utrecht. Zijn keuzevak was de Informatica. In oktober 1983 legde hij het propaedeutisch examen en in november 1986 het doctoraal examen wiskunde af. Sinds maart 1987 is hij als AIO werkzaam aan het Mathematisch Instituut te Utrecht. Naast het geven van onderwijs bestond zijn werk uit het verrichten van onderzoek in de theorie van singulariteiten, hetgeen zijn neerslag gevonden heeft in dit proefschrift. Vanaf 1989 was hij bovendien lid van de Faculteitsraad Wiskunde en Informatica.

The cover shows front views of London Underground rolling stock. The front cover features '*tube-stock*', running on the deep tube lines. We chose from the large number of such series the ones called 1938-stock and 1983-stock. The back cover shows examples of stock running on the 'surface lines', where series (like singularities) are denoted by letters (in this case *A-stock* and *D-stock*). See also page 71.

